

Introduction to radio astronomy

Lectures 7 & 8

Miroslav Bárta

barta@asu.cas.cz



EUROPEAN ARC
ALMA Regional Centre || Czech



**Astronomical
Institute**
of the Czech Academy
of Sciences

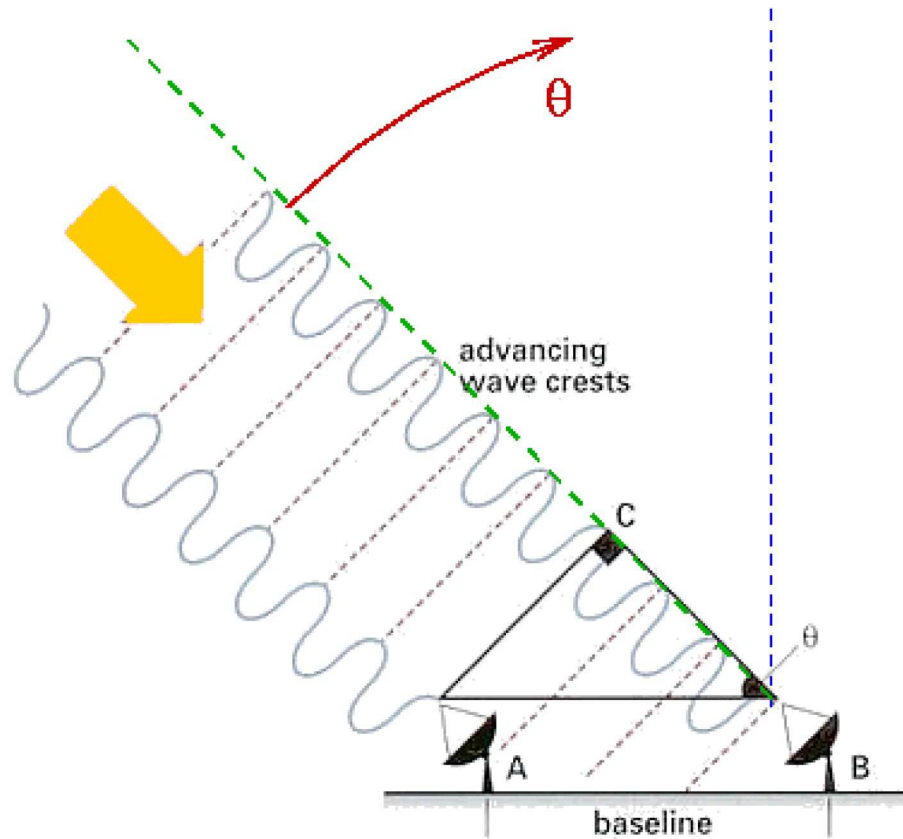
- ▶ Interferometric imaging – aperture synthesis
 - Difference to phased arrays
 - Mathematical foundations: Van Cittert-Zernike theorem
 - Geometrical considerations and coordinate systems
 - From complex visibilities to image: Gridding, weighting, IFT & deconvolution
 - Dirty and clean images
 - Cleaning algorithms

- ▶ Calibration of interferometric spectral data
 - „System“ imperfectness: Atmosphere, pointing, antenna...
 - Total flux
 - Bandpass – spectral flattening
 - Amplitude & phase variations
 - Applying the calibration tables

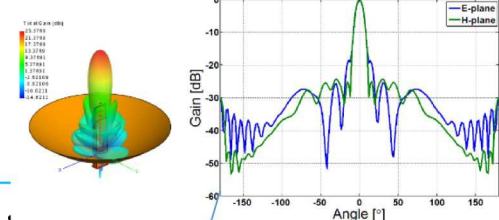
- ▶ Modern frequency-agile interferometric arrays
 - LOFAR, SKA, MUSER
 - ALMA
 - ARCs: The ALMA user-support infrastructure

Interferometry: Basic approaches

Phased arrays



$$|I_{AB}(\theta)| = 1 + \cos \frac{2\pi D}{\lambda} \theta$$

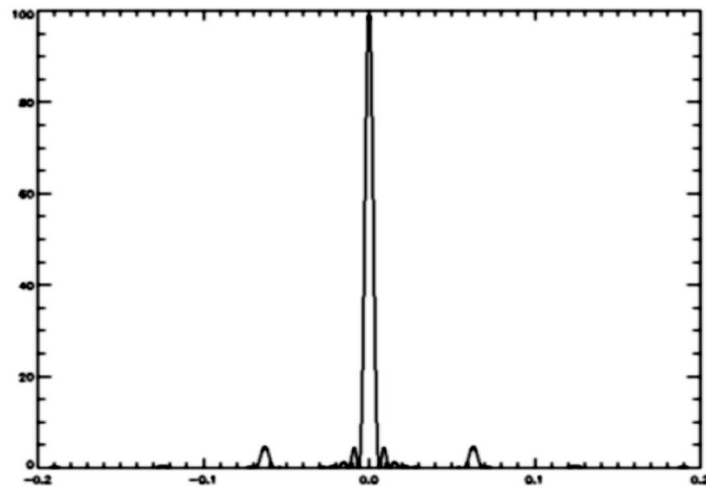
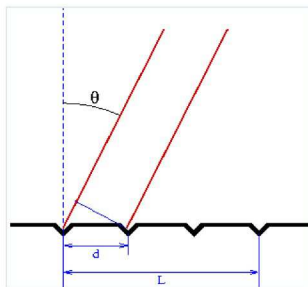
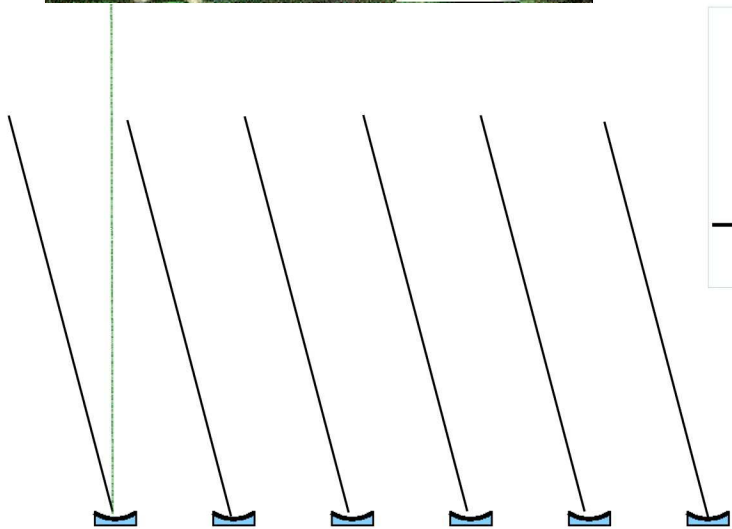
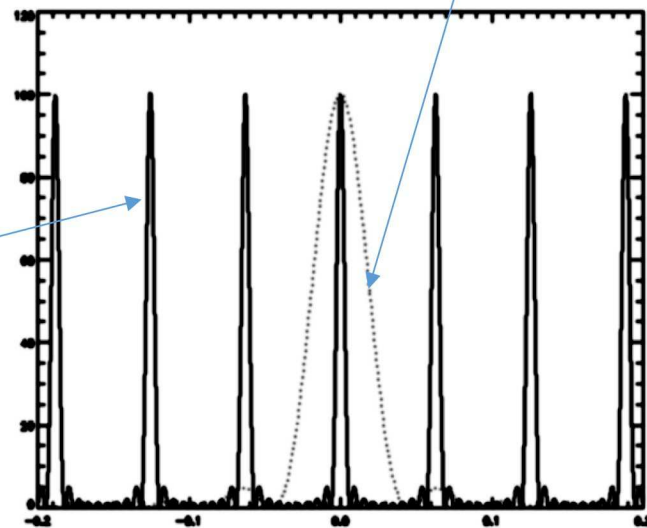


Old good times – sparse antenna rows / phased arrays (beam forming)

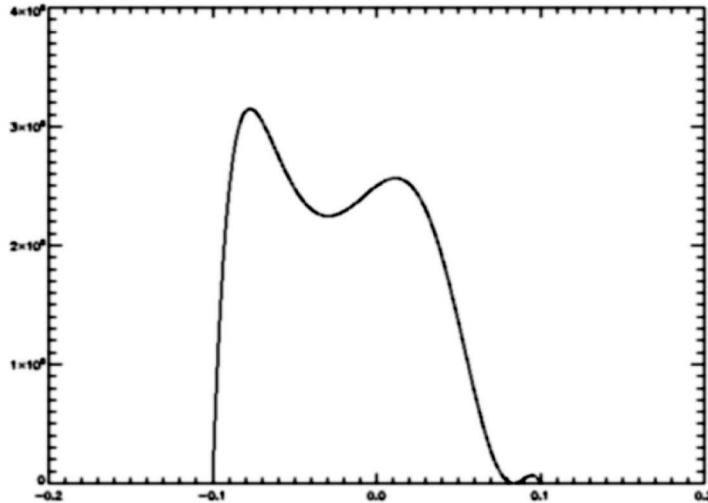


Analogy with optical gratings used in spectrographs

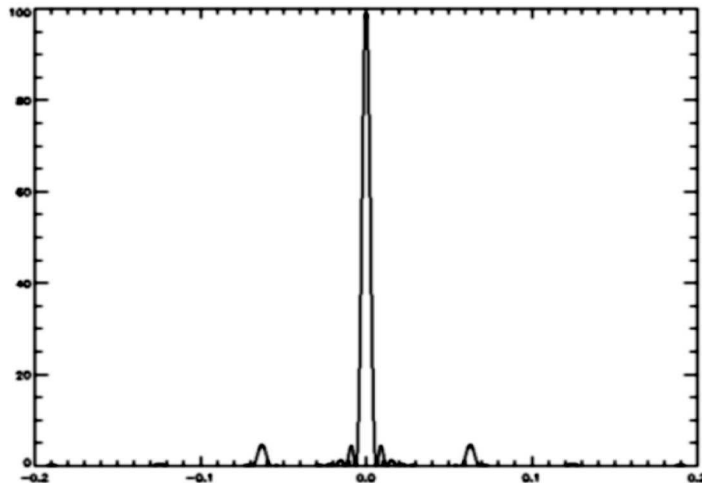
$$|I_{\Sigma}(\theta)| = \frac{1 - \cos N \frac{2\pi D}{\lambda} \theta}{1 - \cos \frac{2\pi D}{\lambda} \theta}$$



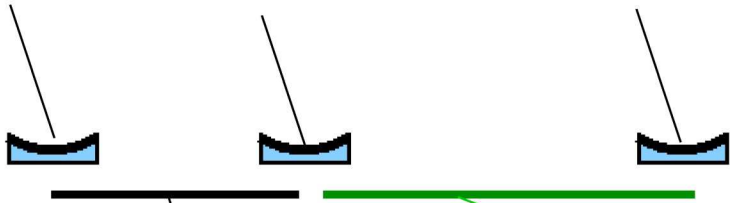
Old good times – sparse antenna rows/ phased arrays



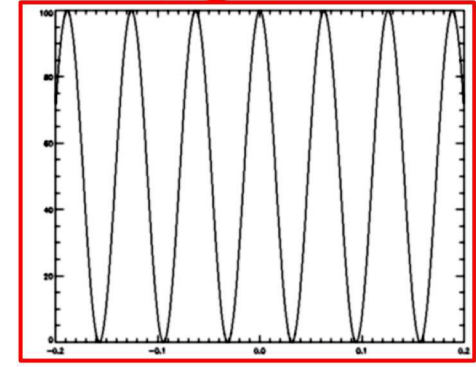
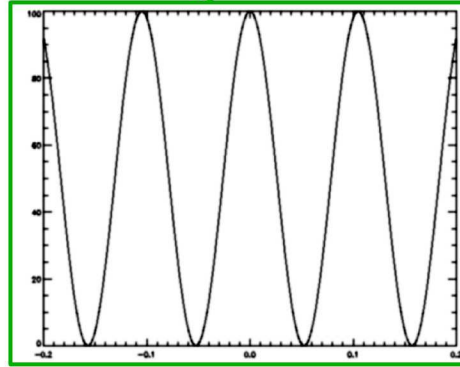
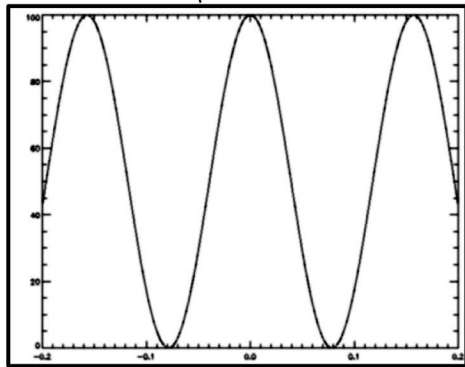
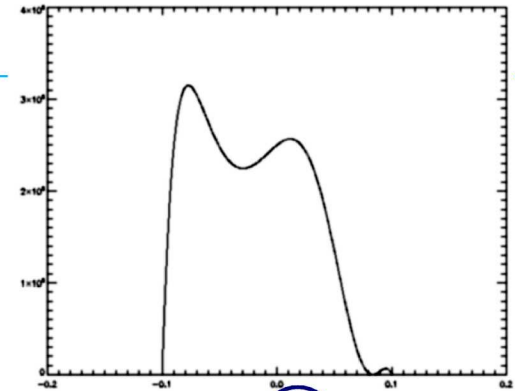
- Scanning with the beam
- Frequently supplied by MFI



Interferometry: Basic approaches



Aperture synthesis



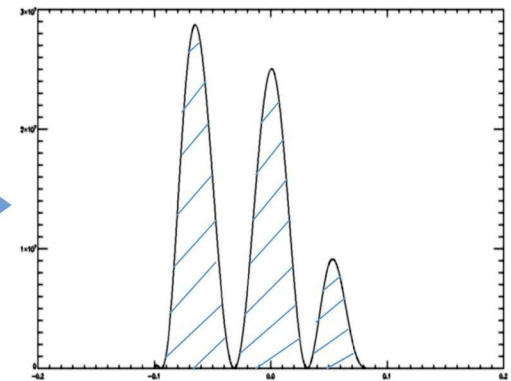
(X)

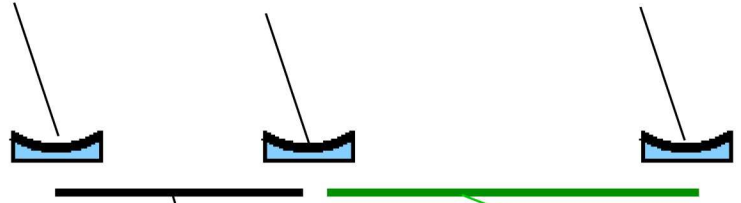
(Σ)

Nowadays: Aperture synthesis – decomposition of image to harmonics = Fourier transform

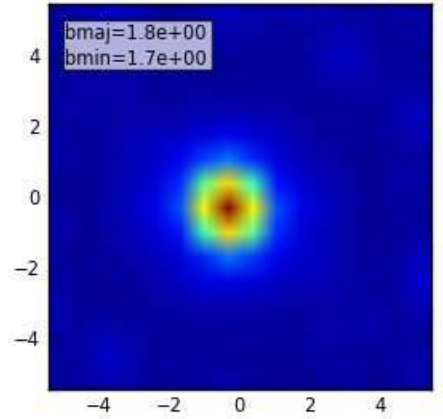
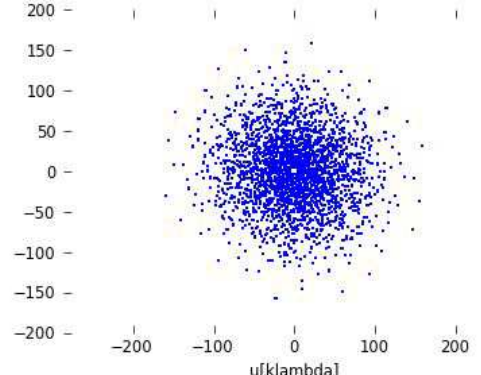
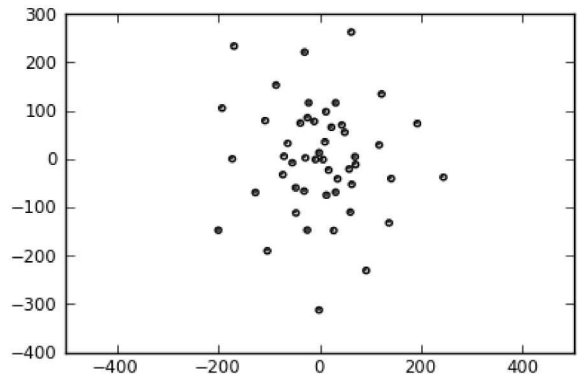
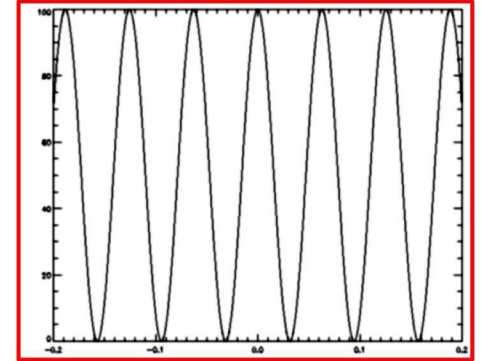
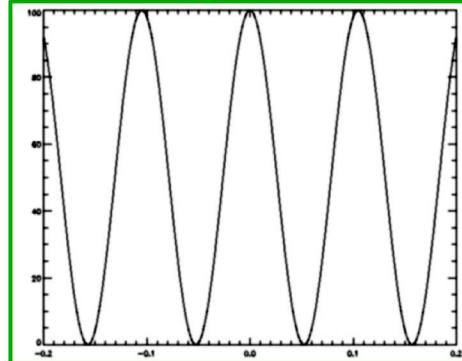
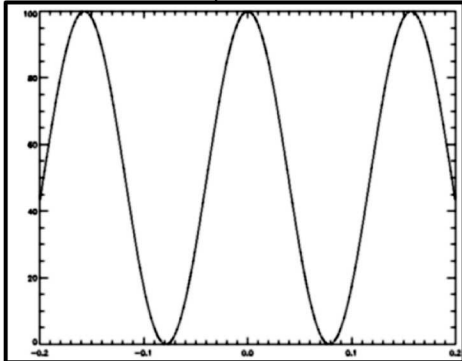
$$\langle I_{AB}(\theta) \rangle = \langle E_A \rangle \cdot \overline{\langle E_B \rangle} = \int_{-\infty}^{+\infty} B(\theta) \exp\left(i \frac{2\pi D}{\lambda} \theta\right) d\theta$$

Cross-correlations – interferometric visibilities

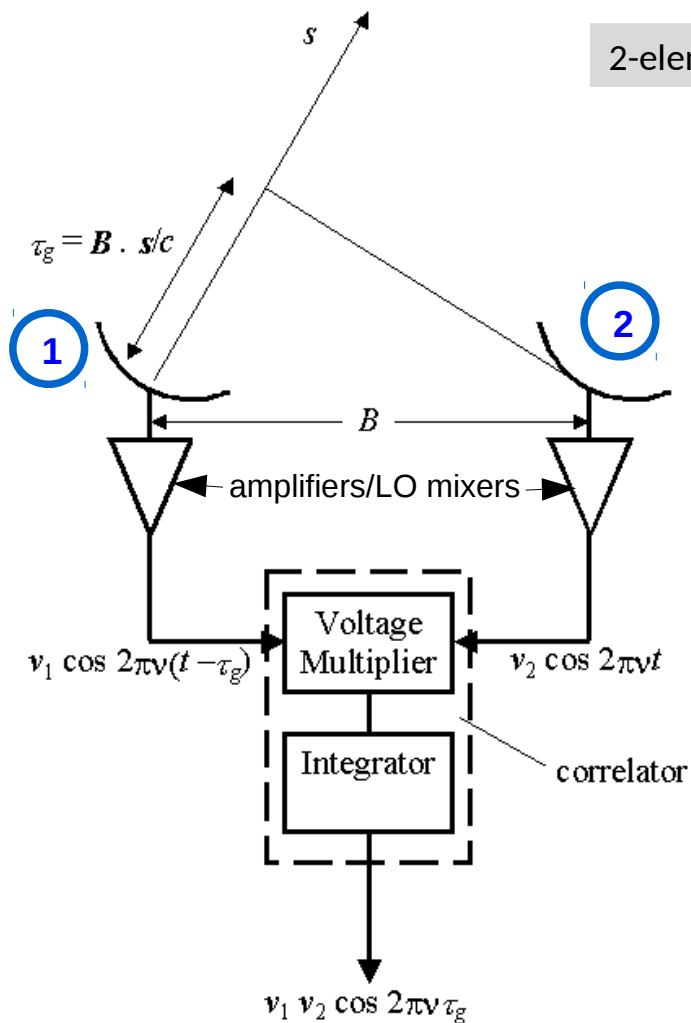




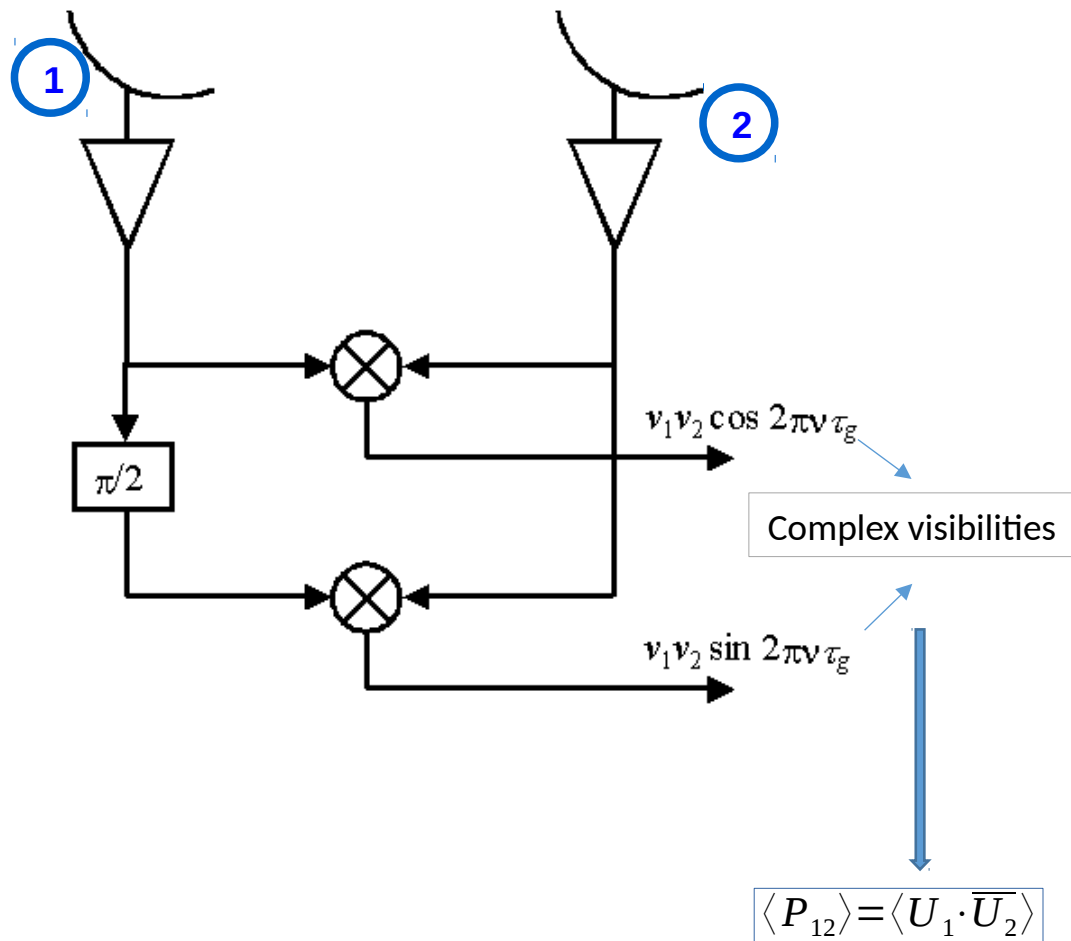
$$\langle I_{AB} \rangle(\theta) = \int_{-\infty}^{+\infty} B(\theta) \exp\left(i \frac{2\pi D}{\lambda} \theta\right) d\theta$$



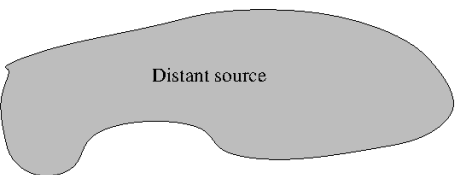
Aperture synthesis: Mathematical foundations



2-element interferometric correlator

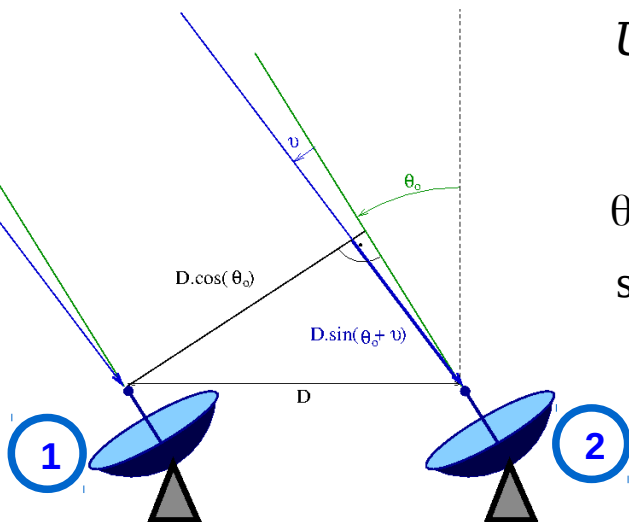


Aperture synthesis: Mathematical foundations



2-element interferometric correlator

1-D Geometry



$$\langle P_{12} \rangle = \langle U_1 \cdot \bar{U}_2 \rangle$$

$$U_1 = G_1 \cdot \int_{-\infty}^{+\infty} E(\theta) \cdot e^{i\varphi(\theta)} \cdot e^{-i\omega t} d\theta$$

$$U_2 = G_2 \cdot \int_{-\infty}^{+\infty} E(\theta) \cdot e^{i\varphi(\theta)} \cdot e^{-i\omega t} \cdot \exp\left(i \frac{2\pi D \sin \theta}{\lambda}\right) d\theta$$

“compact”-source assumption

$$\theta = \theta_0 + \vartheta$$

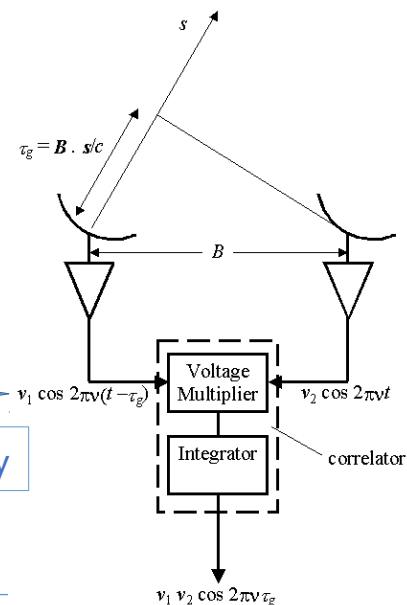
$$\sin(\theta_0 + \vartheta) = \sin \theta_0 \cos \vartheta + \cos \theta_0 \sin \vartheta \approx \sin \theta_0 + \cos \theta_0 \cdot \vartheta$$

$$U_1 = G_1 \cdot \int_{-\infty}^{+\infty} E(\vartheta) \cdot e^{i\varphi(\vartheta)} \cdot e^{-i\omega t} d\vartheta$$

$$U_2 = G_2 \cdot \int_{-\infty}^{+\infty} E(\vartheta) \cdot e^{i\varphi(\vartheta)} \cdot e^{-i\omega t} \cdot \exp\left(i \frac{2\pi D \sin \theta_0}{\lambda} + i \frac{2\pi D \vartheta \cdot \cos \theta_0}{\lambda}\right) d\vartheta$$

$$U_2 = G_2 \cdot \int_{-\infty}^{+\infty} E(\vartheta) \cdot e^{i\varphi(\vartheta)} \cdot e^{-i\omega t} \cdot \exp\left(i \frac{2\pi D \vartheta \cdot \cos \theta_0}{\lambda}\right) d\vartheta$$

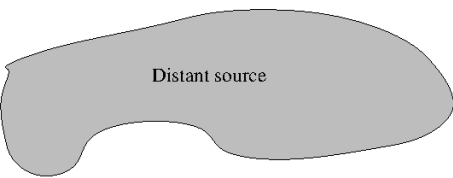
Pointing delay



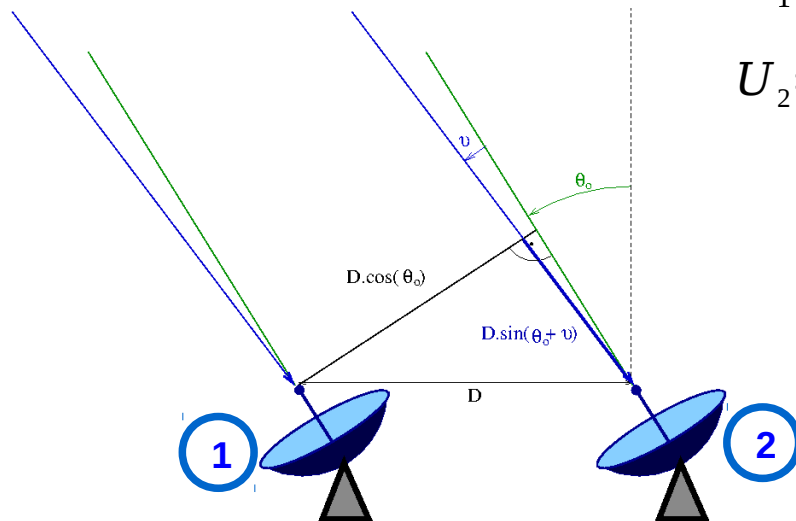
Aperture synthesis: Mathematical foundations

2-element interferometric correlator

1-D Geometry



Distant source



$$U_1 = G_1 \cdot \int_{-\infty}^{+\infty} E(\vartheta) \cdot e^{i\varphi(\vartheta)} \cdot e^{-i\omega t} d\vartheta$$

$$U_2 = G_2 \cdot \int_{-\infty}^{+\infty} E(\vartheta) \cdot e^{i\varphi(\vartheta)} \cdot e^{-i\omega t} \cdot \exp\left(i \frac{2\pi D \vartheta \cdot \cos \theta_0}{\lambda}\right) d\vartheta$$

$$\langle P_{12} \rangle = \langle U_1 \cdot \overline{U_2} \rangle = G_1 \overline{G_2} \cdot \left\langle \iint_{-\infty}^{+\infty} E(\vartheta) e^{i\varphi(\vartheta)} e^{-i\omega t} \cdot E(\vartheta') e^{-i\varphi(\vartheta')} e^{i\omega t} \cdot \exp\left(-i \frac{2\pi D \cos \theta_0 \cdot \vartheta'}{\lambda}\right) d\vartheta d\vartheta' \right\rangle$$

$$\langle P_{12} \rangle = G_1 \overline{G_2} \cdot \left\langle \iint_{-\infty}^{+\infty} E(\vartheta) \cdot E(\vartheta') e^{i\varphi(\vartheta) - i\varphi(\vartheta')} \cdot \exp\left(-i \frac{2\pi D \cos \theta_0 \cdot \vartheta'}{\lambda}\right) d\vartheta d\vartheta' \right\rangle$$

$$\langle P_{12} \rangle = G_1 \overline{G_2} \cdot \left\langle \iint_{-\infty}^{+\infty} E(\vartheta) \cdot E(\vartheta') e^{i\varphi(\vartheta) - i\varphi(\vartheta')} \cdot \exp\left(-i \frac{2\pi D \cos \theta_0 \cdot \vartheta'}{\lambda}\right) d\vartheta d\vartheta' \right\rangle$$

$$U = U_a + U_b$$

random-phase assumption

and the mutual coherence function (G.1) is

$$\begin{aligned} \langle U(P_1, t_1) U^*(P_2, t_2) \rangle &= \langle \{U_a(P_1, t_1) + U_b(P_1, t_1)\} \{U_a(P_2, t_2) + U_b(P_2, t_2)\}^* \rangle \\ &= \langle U_a(P_1, t_1) U_a^*(P_2, t_2) \rangle + \langle U_b(P_1, t_1) U_b^*(P_2, t_2) \rangle \\ &\quad + \langle U_a(P_1, t_1) U_b^*(P_2, t_2) \rangle \\ &\quad + \langle U_b(P_1, t_1) U_a^*(P_2, t_2) \rangle. \end{aligned} \quad (\text{G.7})$$

If we assume the two wave fields U_a and U_b are *incoherent*, we require that the field strengths U_a and U_b are uncorrelated even when measured at the same point, so that

$$\langle U_a(P_1, t_1) U_b^*(P_2, t_2) \rangle = \langle U_b(P_1, t_1) U_a^*(P_2, t_2) \rangle \equiv 0. \quad (\text{G.8})$$

$$\langle P_{12} \rangle = G_1 \overline{G_2} \cdot \iint_{-\infty}^{+\infty} I(\vartheta) \cdot \exp\left(-i \frac{2\pi D \cos \theta_0 \cdot \vartheta'}{\lambda}\right) d\vartheta$$

$$\langle P_{12} \rangle = G_1 \overline{G_2} \cdot \int_{-\infty}^{+\infty} I(\vartheta) \cdot \exp(-2\pi i u \vartheta) d\vartheta$$

$$u = \frac{D \cos \theta_0}{\lambda}$$

Aperture synthesis: Mathematical foundations

$$\langle P_{12} \rangle = G_1 \overline{G_2} \cdot \int_{-\infty}^{+\infty} I(\vartheta) \cdot \exp(-2\pi i u \vartheta) d\vartheta$$

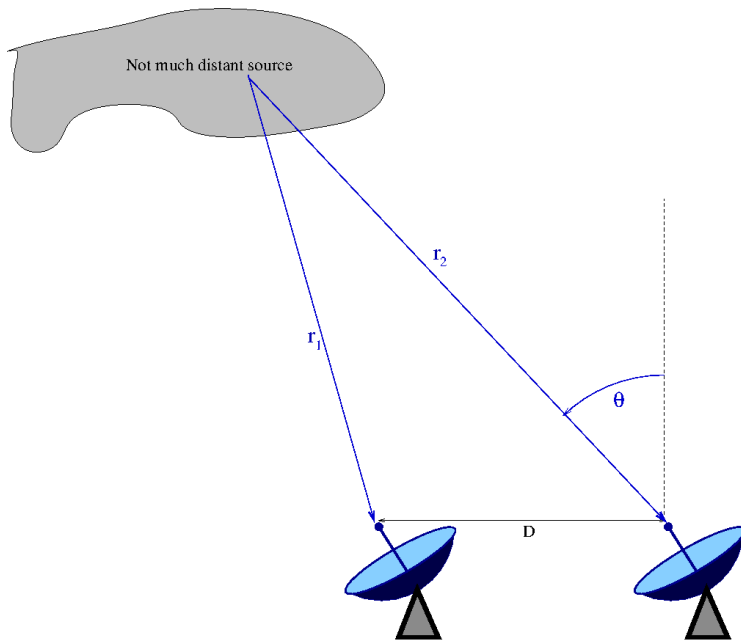
Generalisation for 2D

$$\langle P_{12} \rangle = G_1 \overline{G_2} \cdot \iint_{-\infty}^{+\infty} I(l, m) \cdot \exp(-2\pi i(u \cdot l + v \cdot m)) dl dm$$

2-element interferometric correlator

Van Cittert - Zernike theorem (1934)

distant-source assumption



$$r_1^2 = r_2^2 + D^2 - 2r_2 D \cos(\pi/2 - \theta)$$

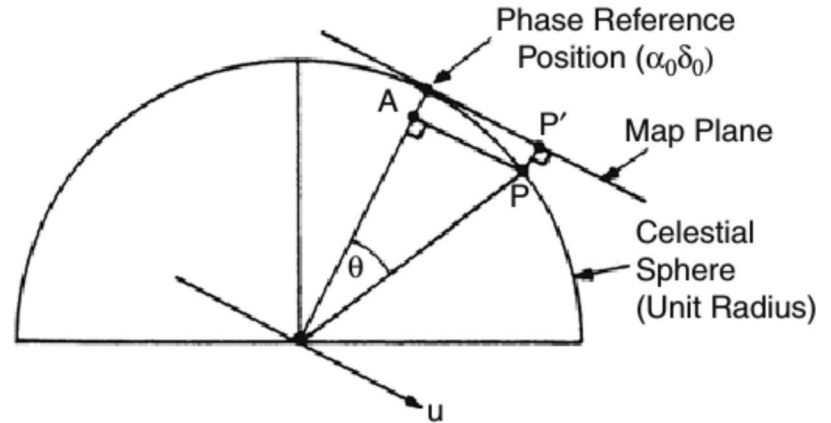
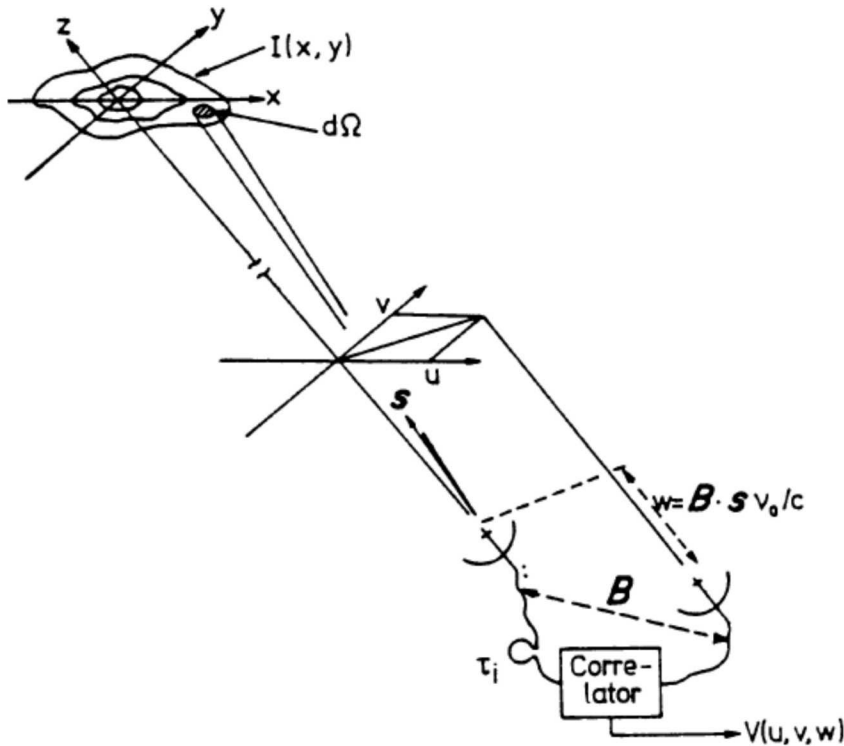
$$(r_2 - r_1)(r_2 + r_1) = -D^2 + 2r_2 D \sin \theta$$

$$r_2 - r_1 \approx D \sin \theta - \frac{D^2}{2r} \rightarrow \frac{D^2}{2r} \ll \lambda$$

considered phase delay

Aperture synthesis: Mathematical foundations

Van Cittert - Zernike theorem: 2-D geometry



$$\langle P_{12} \rangle = G_1 \overline{G_2} \cdot \iint_{-\infty}^{+\infty} I(\vartheta) \cdot \exp\left(-i \frac{2\pi D \cos \theta_0 \cdot \vartheta}{\lambda}\right) d\vartheta$$

$$R(\mathbf{B}) = \iint_{\Omega} A(s) I_v(s) \exp\left[i 2\pi v \left(\frac{1}{c} \mathbf{B} \cdot \mathbf{s} - \tau_i\right)\right] d\Omega dv$$

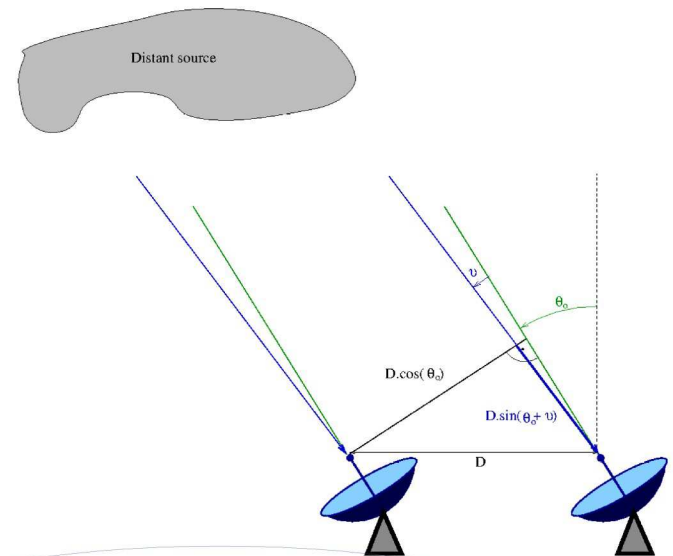
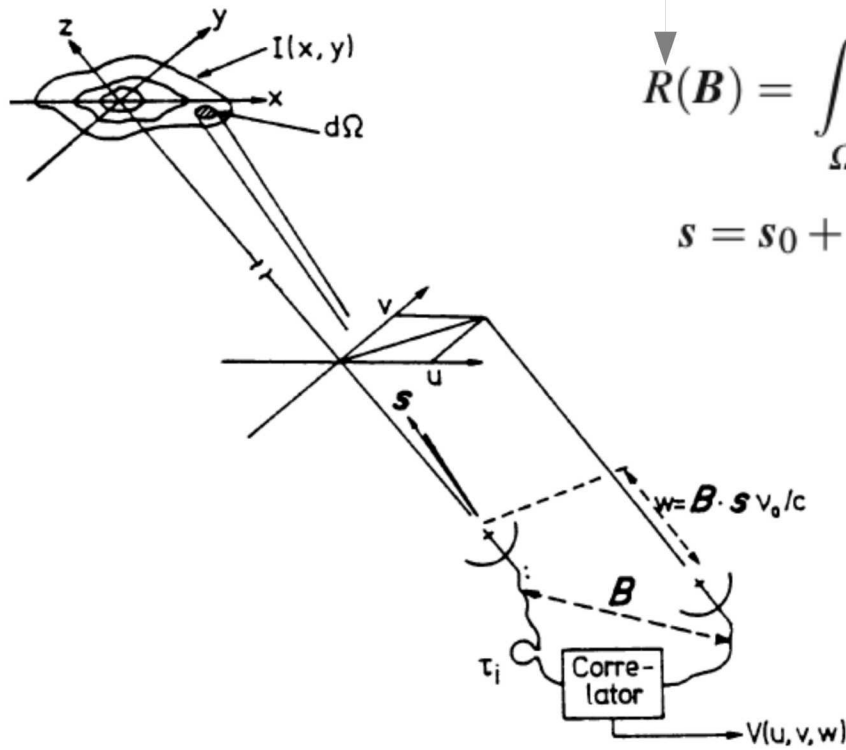
Aperture synthesis: Mathematical foundations

Van Cittert - Zernike theorem: 2-D geometry

Cross-correlation function

$$R(\mathbf{B}) = \iint_{\Omega} A(s) I_{\nu}(s) \exp \left[i 2 \pi \nu \left(\frac{1}{c} \mathbf{B} \cdot \mathbf{s} - \tau_i \right) \right] d\Omega d\nu$$

$$\mathbf{s} = \mathbf{s}_0 + \boldsymbol{\sigma}, \quad |\boldsymbol{\sigma}| = 1$$



$$R(\mathbf{B}) = \exp \left[i \omega \left(\frac{1}{c} \mathbf{B} \cdot \mathbf{s}_0 - \tau_i \right) \right] d\nu \iint_{\Omega} A(\boldsymbol{\sigma}) I(\boldsymbol{\sigma}) \exp \left(i \frac{\omega}{c} \mathbf{B} \cdot \boldsymbol{\sigma} \right) d\boldsymbol{\sigma}.$$

Aperture synthesis: Mathematical foundations

Van Cittert – Zernike theorem: 2-D geometry

$$V(\mathbf{B}) = \iint_S A(\boldsymbol{\sigma}) I(\boldsymbol{\sigma}) \exp\left(i \frac{\omega}{c} \mathbf{B} \cdot \boldsymbol{\sigma}\right) d\boldsymbol{\sigma}$$

$$\frac{\omega}{2\pi c} \mathbf{B} = (u, v, w)$$

“Visibilities”

$$V(u, v, w) = \int_{-\infty}^{\infty} \int_{-\infty}^{\infty} A(x, y) I(x, y) \times \exp[i2\pi(ux + vy + w\sqrt{1 - x^2 - y^2})] \frac{dx dy}{\sqrt{1 - x^2 - y^2}}$$

“compact”-source assumption

$$\sqrt{1 - x^2 - y^2} \cong \text{const} \cong 1$$

$$V(u, v, w) e^{-i2\pi w} = \int_{-\infty}^{\infty} \int_{-\infty}^{\infty} A(x, y) I(x, y) e^{i2\pi(ux + vy)} dx dy$$

Aperture synthesis: Mathematical foundations

Van Cittert - Zernike theorem: 2-D geometry

$$V(u, v, w) e^{-i2\pi w} = \int_{-\infty}^{\infty} \int_{-\infty}^{\infty} A(x, y) I(x, y) e^{i2\pi(ux+vy)} dx dy$$

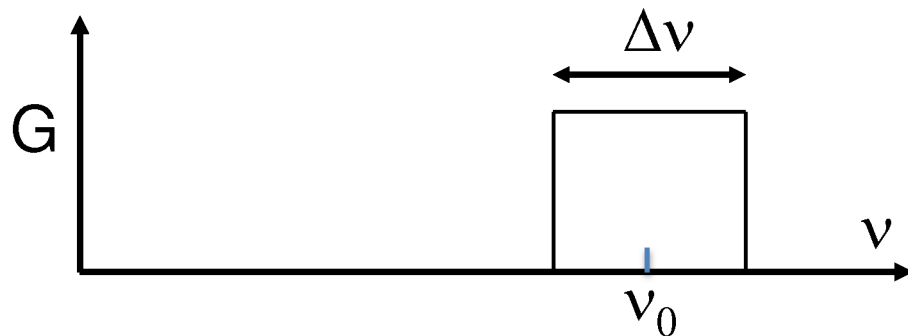
$$V(u, v, w) e^{-i2\pi w} \cong V(u, v, 0)$$

$$I'(x, y) = A(x, y) I(x, y) = \int_{-\infty}^{\infty} V(u, v, 0) e^{-i2\pi(ux+vy)} du dv$$

Primary beam (pbcorr)

The Effect of Bandwidth.

- Real interferometers must accept a range of frequencies. So we now consider the response of our interferometer over frequency.
- Define the frequency response function, $G(\nu)$, as the amplitude and phase variation of the signal over frequency.



- The function $G(\nu)$ is primarily due to the gain and phase characteristics of the electronics, but can also contain propagation path effects.
- In general, $G(\nu)$ is a complex function.

The Effect of Bandwidth.

- To find the finite-bandwidth response, we integrate our fundamental response over a frequency width $\Delta\nu$, centered at ν_0 :

$$V = \int \left(\frac{1}{\Delta\nu} \int_{\nu_0 - \Delta\nu/2}^{\nu_0 + \Delta\nu/2} I(\mathbf{s}, \nu) G_1(\nu) G_2^*(\nu) e^{-i2\pi\nu\tau_g} d\nu \right) d\Omega$$

- If the source intensity does not vary over the bandwidth, and the instrumental gain parameters G_1 and G_2 are square and identical, then

$$V = \iint I_\nu(\mathbf{s}) \frac{\sin(\pi\tau_g\Delta\nu)}{\pi\tau_g\Delta\nu} e^{-2i\pi\nu_0\tau_g} d\Omega = \iint I_\nu(\mathbf{s}) \text{sinc}(\tau_g\Delta\nu) e^{-2i\pi\nu_0\tau_g} d\Omega$$

where the **fringe attenuation function**, $\text{sinc}(x)$, is defined as:

$$\text{sinc}(x) = \frac{\sin(\pi x)}{\pi x}$$

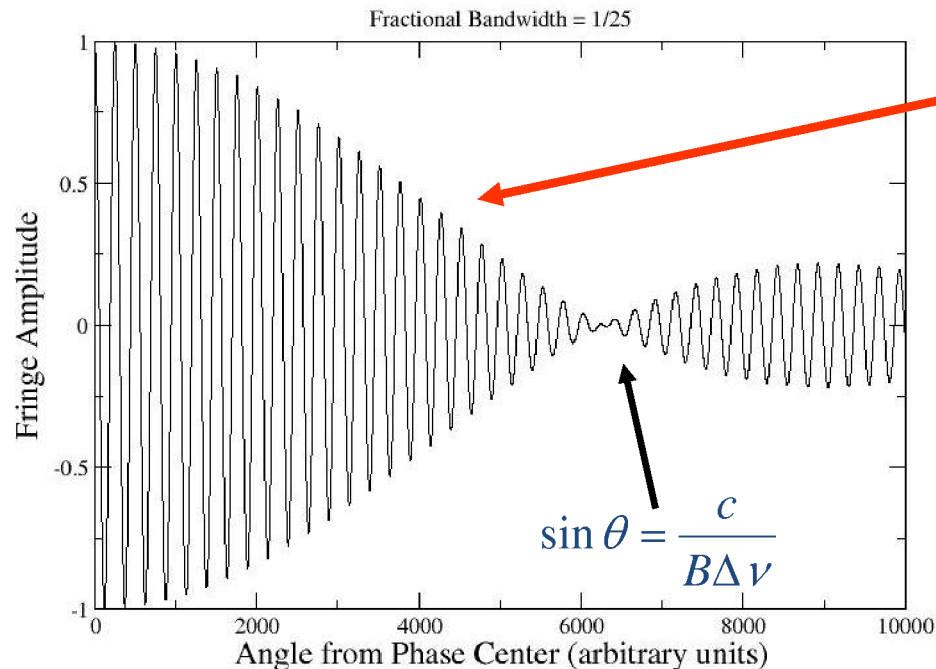


Bandwidth Effect Example

- For a square bandpass, the bandwidth attenuation reaches a null when $\tau_g \Delta\nu = 1$, or

$$\sin \theta = \frac{c}{B\Delta\nu} = \left(\frac{\lambda}{B}\right)\left(\frac{\nu_0}{\Delta\nu}\right)$$
- For the old VLA, and its 50 MHz bandwidth, and for the 'A' configuration, ($B = 35$ km), the null was ~ 1.3 degrees away.
- For the upgraded VLA, $\Delta\nu = 2$ MHz, and $B = 35$ km, then the null occurs at about 27 degrees off the meridian.

The Effect of Finite Bandwidth



Fringe Attenuation function:

$$\text{sinc}\left(\frac{B \Delta\nu}{\lambda \nu} \sin \theta\right) = \text{sinc}\left(\frac{B\Delta\nu}{c} \sin \theta\right)$$

Note: The fringe-attenuation function depends only on bandwidth and baseline length – not on frequency.

Observations off the Baseline Meridian

- In our basic scenario -- stationary source, stationary interferometer -- the effect of finite bandwidth will strongly attenuate the visibility from sources far from the meridional plane.
- Since each baseline has its own fringe pattern, the only point on the sky free of attenuation for all baselines is a small angle around the zenith (presuming all baselines are coplanar).
- Suppose we wish to observe an object far from the zenith?
- One solution is to use a very narrow bandwidth – this loses sensitivity, which can only be made up by utilizing many channels – feasible, but computationally expensive.
- Better answer: Shift the fringe-attenuation function to the center of the source of interest.

How? By adding time delay.

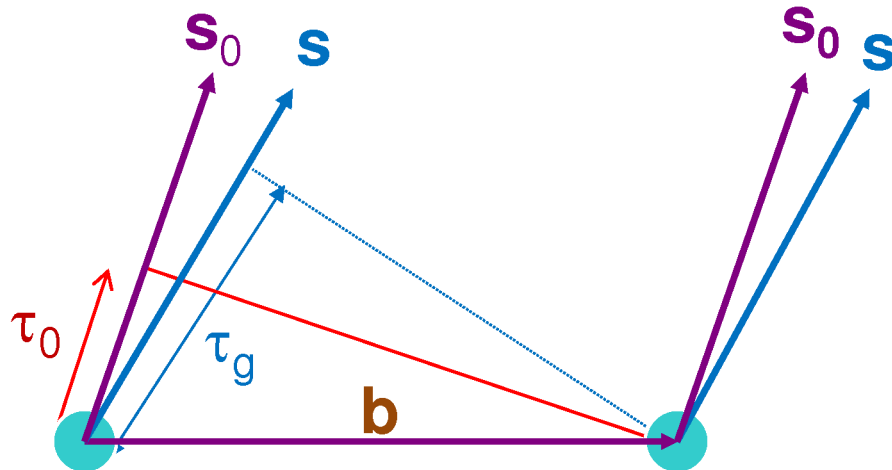


Adding Time Delay

$$\tau_g = \mathbf{b} \cdot \mathbf{s} / c$$

$$\tau_0 = \mathbf{b} \cdot \mathbf{s}_0 / c$$

\mathbf{S}_0 = reference (delay) direction
 \mathbf{S} = general direction



$$V_1 = E e^{-i\omega(t-\tau_g)}$$

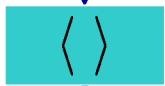
$$V_2 = E e^{-i\omega t}$$

The entire fringe pattern has been shifted over by angle

$$\sin \theta = c\tau_0/b$$



$$V_2 = E e^{-i\omega(t-\tau_0)}$$



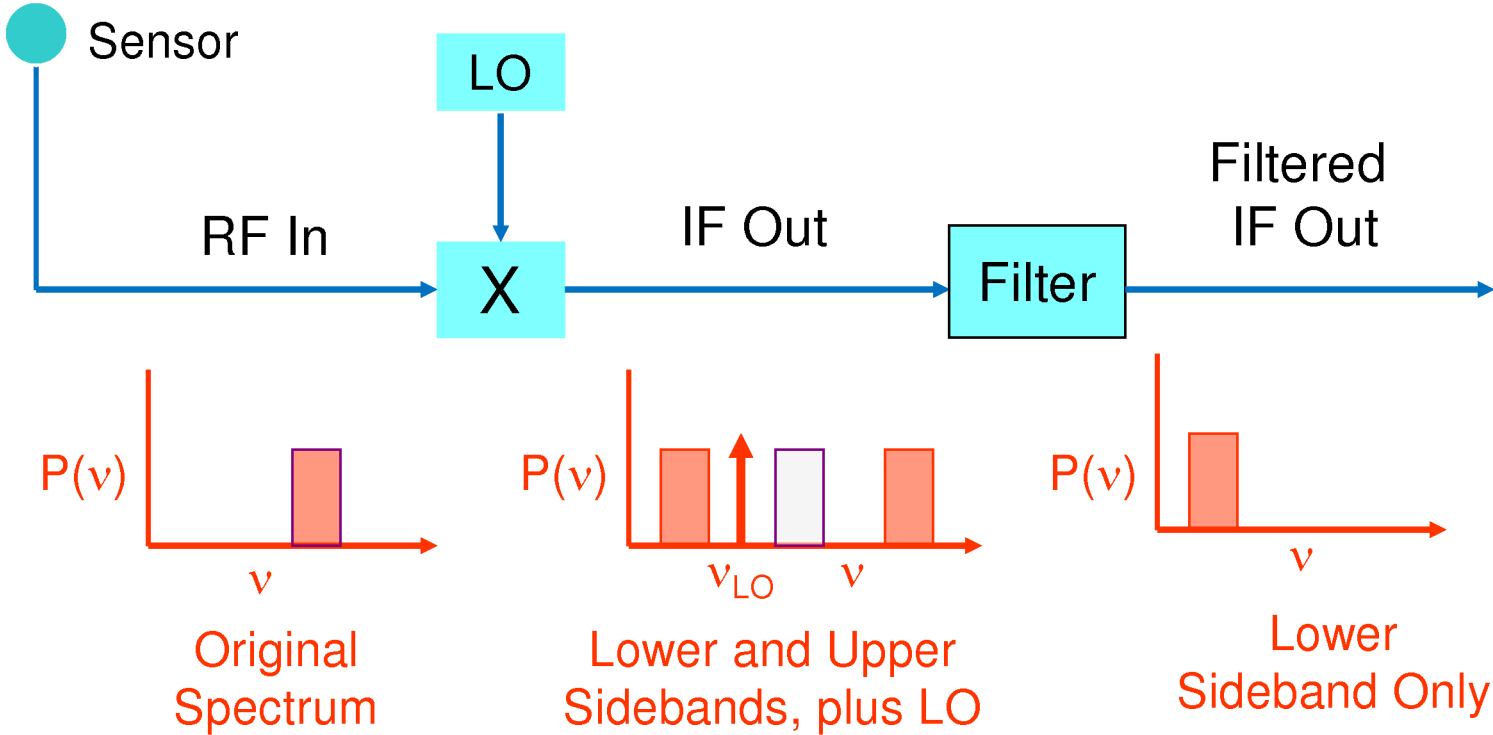
$$V = \langle V_1 V_2^* \rangle = E^2 e^{-i[\omega(\tau_0 - \tau_g)]}$$

$$= E^2 e^{i2\pi[\nu \mathbf{b} \cdot (\mathbf{s} - \mathbf{s}_0) / c]}$$



Downconversion

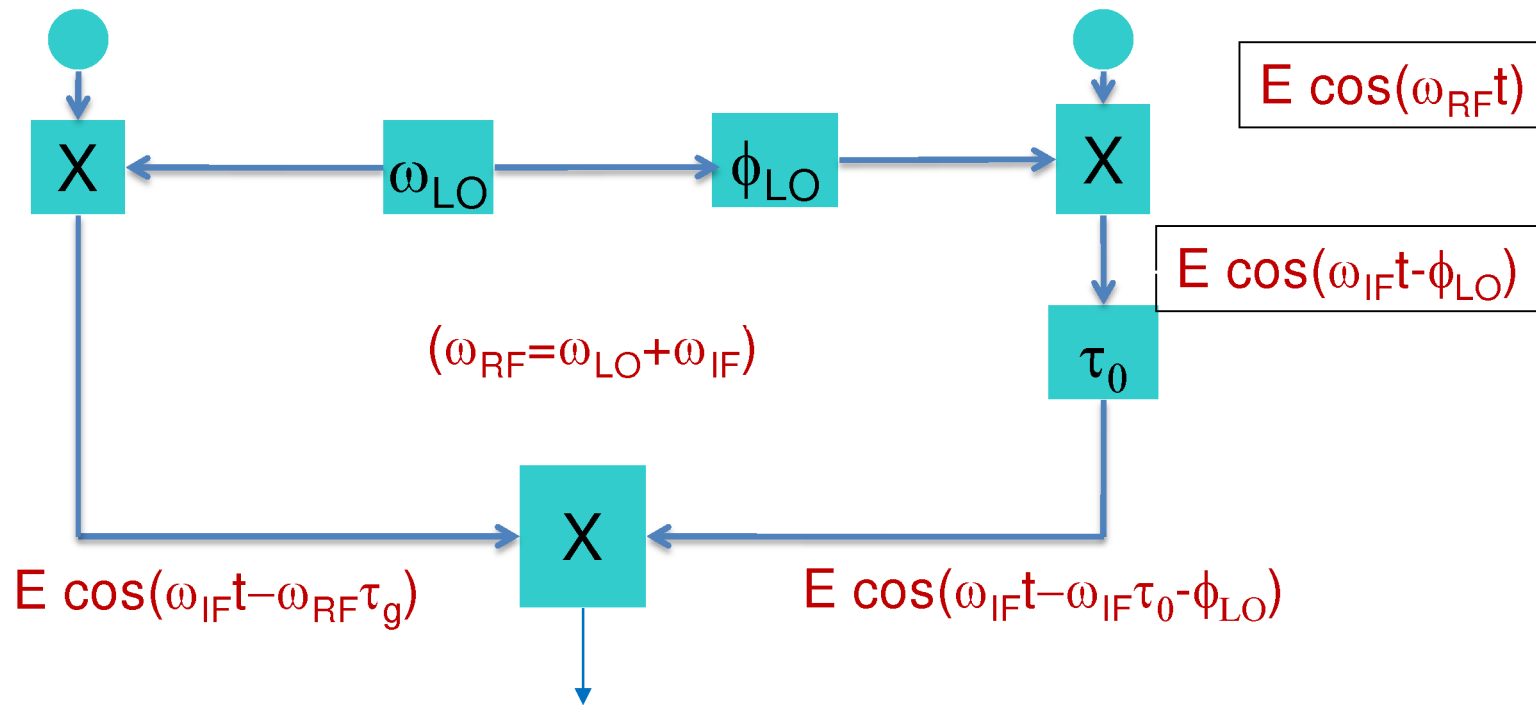
At radio frequencies, the spectral content within a passband can be shifted – with almost no loss in information, to a lower frequency through multiplication by a ‘LO’ signal.



This operation preserves the amplitude and phase relations

Signal Relations, with LO Downconversion

- The RF signals are multiplied by a pure sinusoid, at frequency ν_{LO}
- We can add arbitrary phase ϕ_{LO} on one side.



$$V = E^2 e^{-i(\omega_{RF}\tau_g - \omega_{IF}\tau_0 - \phi_{LO})}$$

Recovering the Correct Visibility Phase

- The correct phase (RF interferometer) is: $\omega_{RF} (\tau_g - \tau_0)$

- The observed phase (with frequency downconversion) is:

$$\omega_{RF} \tau_g - \omega_{IF} \tau_0 - \phi_{LO}$$

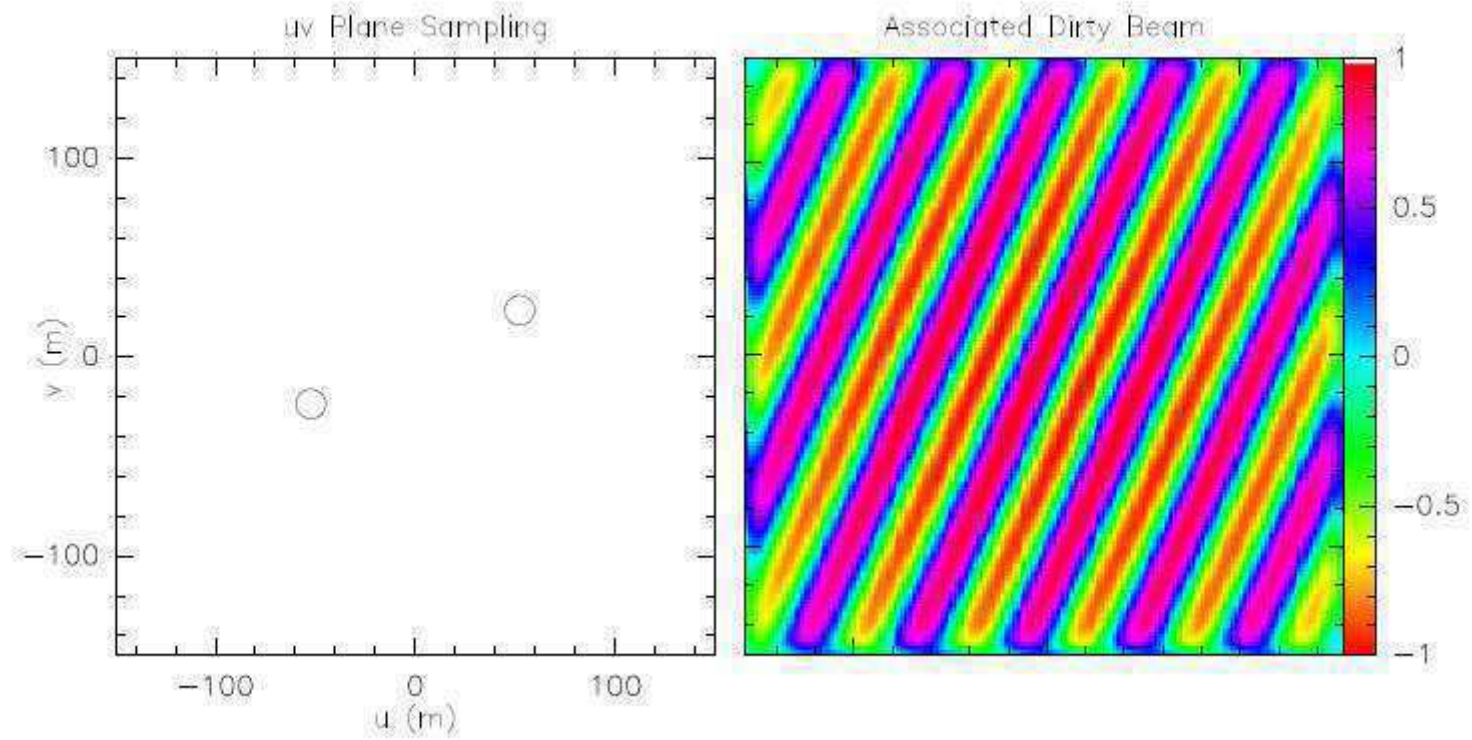
- These will be the same when the LO phase is set to:

$$\phi_{LO} = \omega_{LO} \tau_0$$

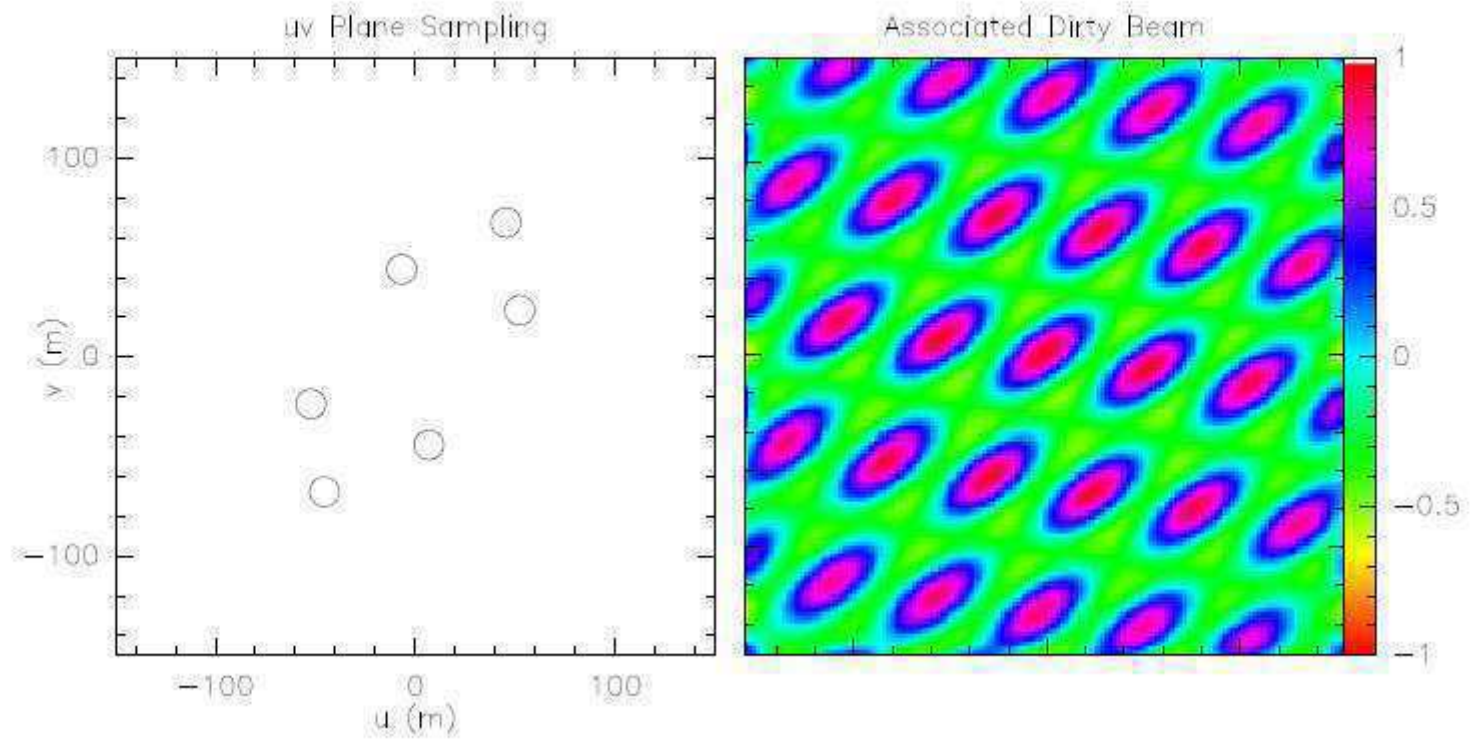
- This is necessary because the delay, τ_0 , has been added in the IF portion of the signal path, rather than at the frequency at which the delay actually occurs.
- The phase adjustment of the LO compensates for the delay having been inserted at the IF, rather than at the RF.



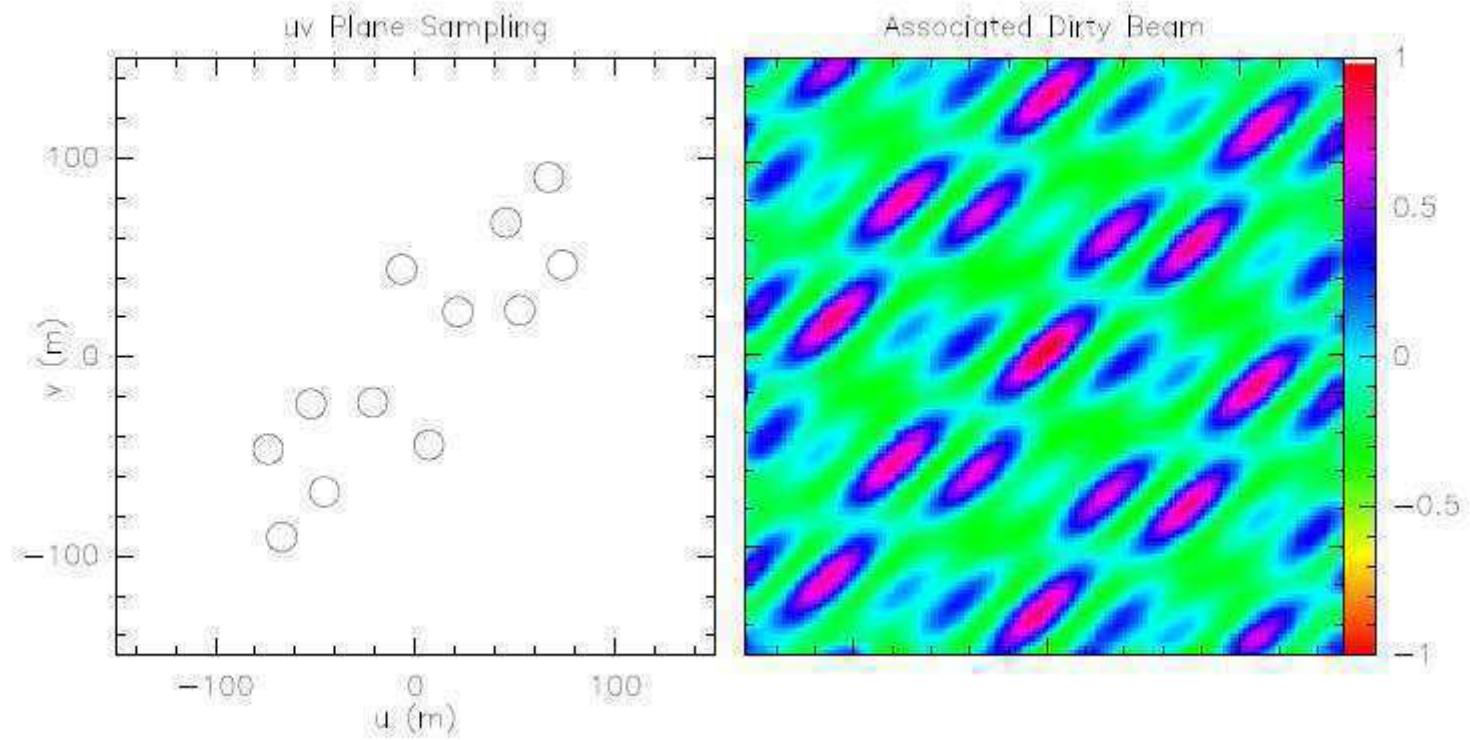
2 antennas



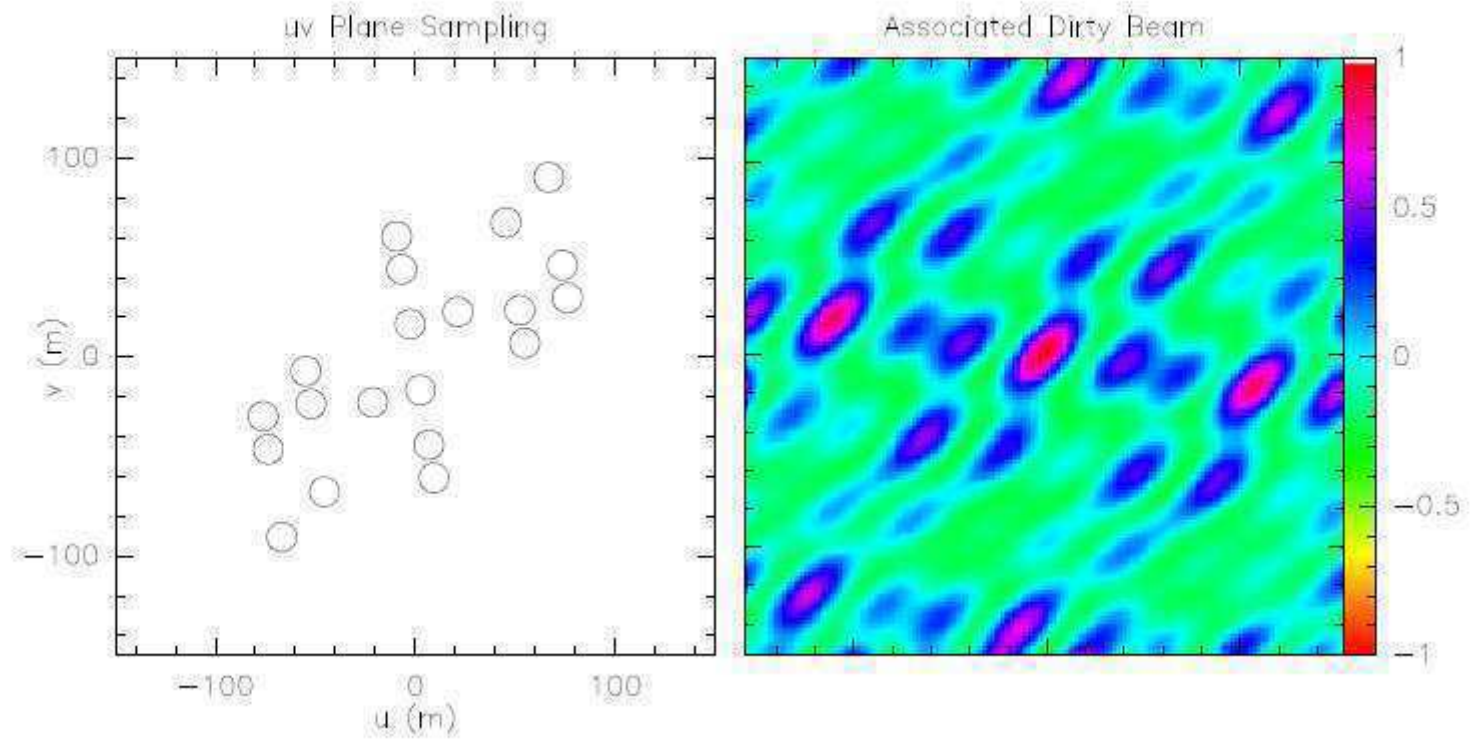
3 antennas



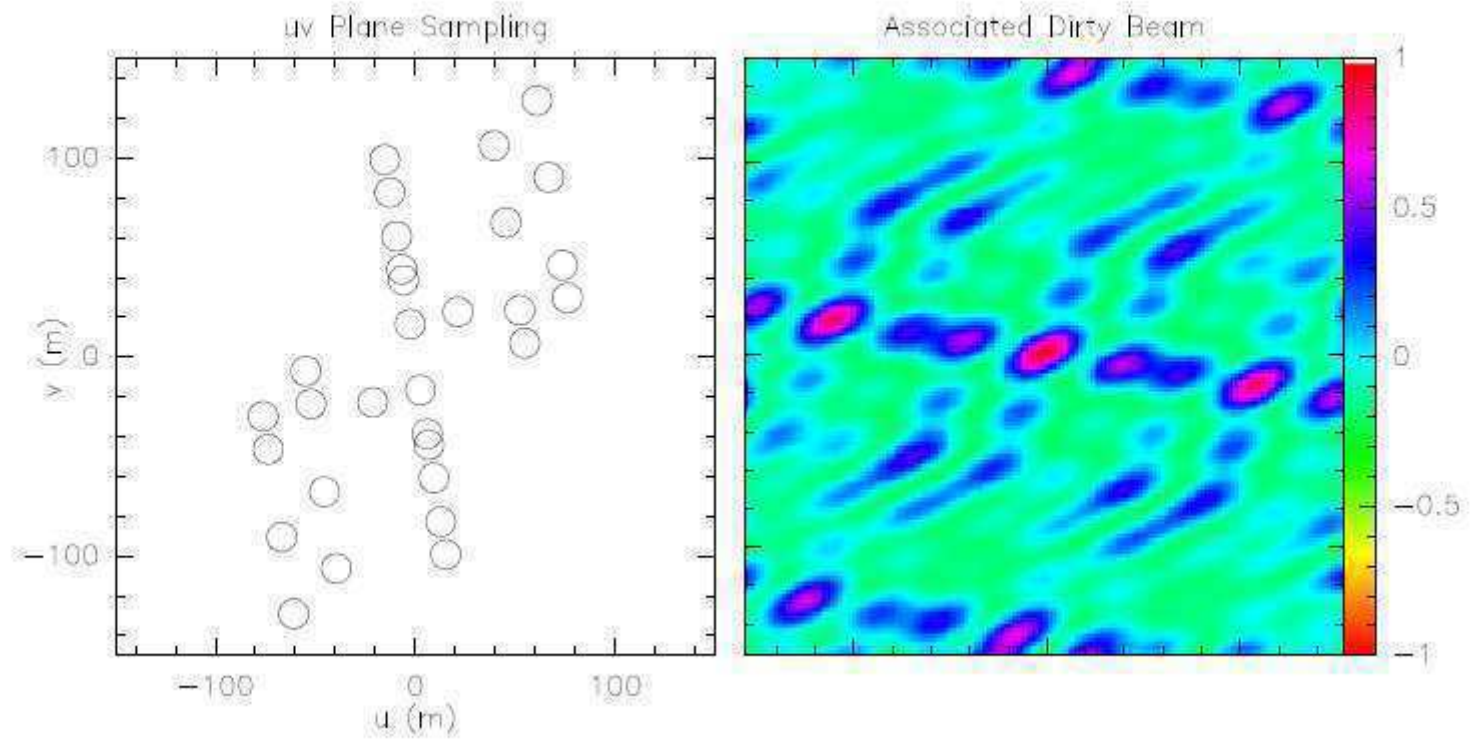
4 antennas



5 antennas



6 antennas

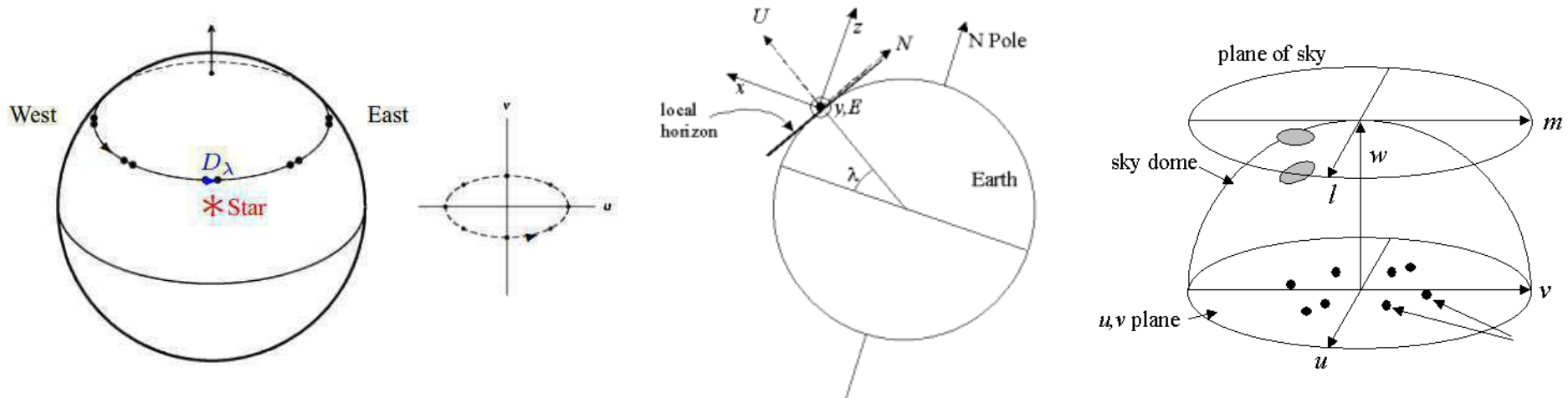


Earth-rotation aperture synthesis

- Geometric delay varies slowly with time due to earth rotation
- Natural fringe rate

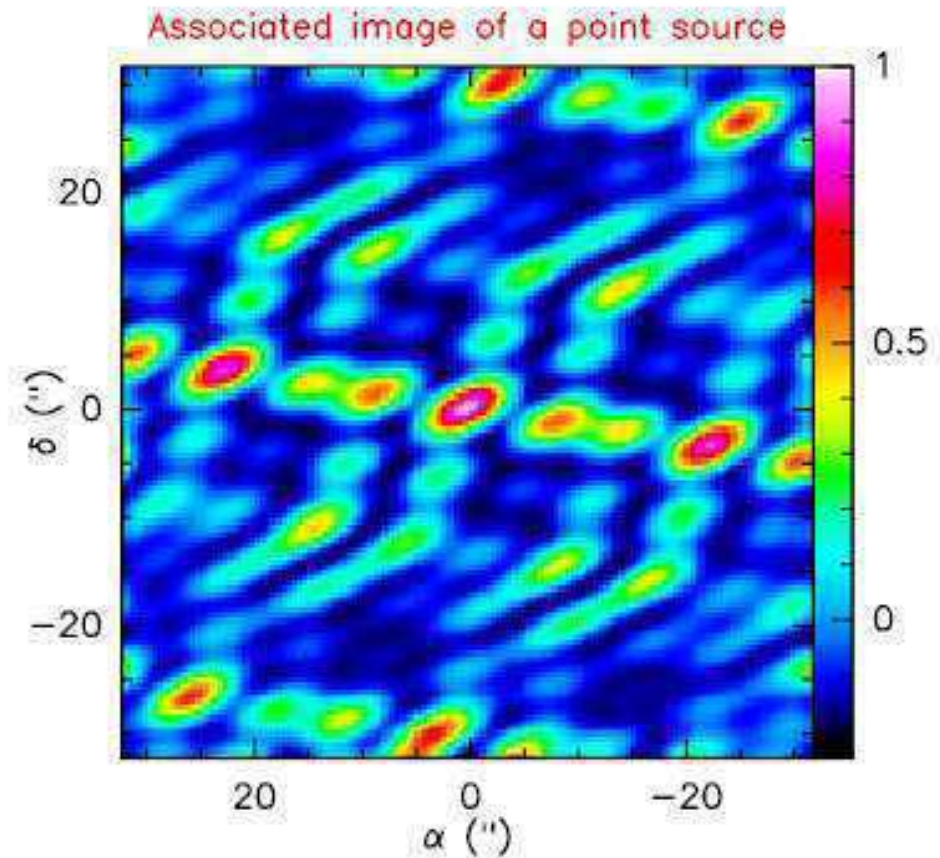
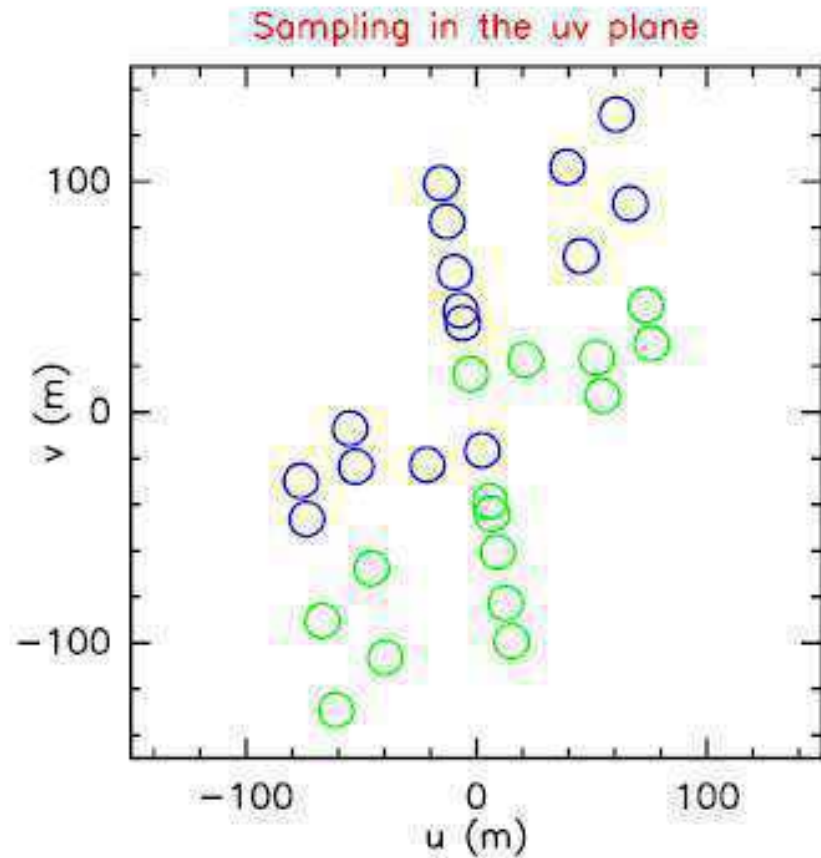
$$\tau_g = \frac{\vec{b} \cdot \hat{s}}{c} \quad v \frac{d\tau_g}{dt} \cong \Omega_{\text{earth}} \frac{bv}{c}$$

- τ_g is known from the antenna position, source direction, time → could be corrected
- u, v depends on the hour angle – as the earth rotates and the source appears to move across the sky, the array samples different u, v at different times

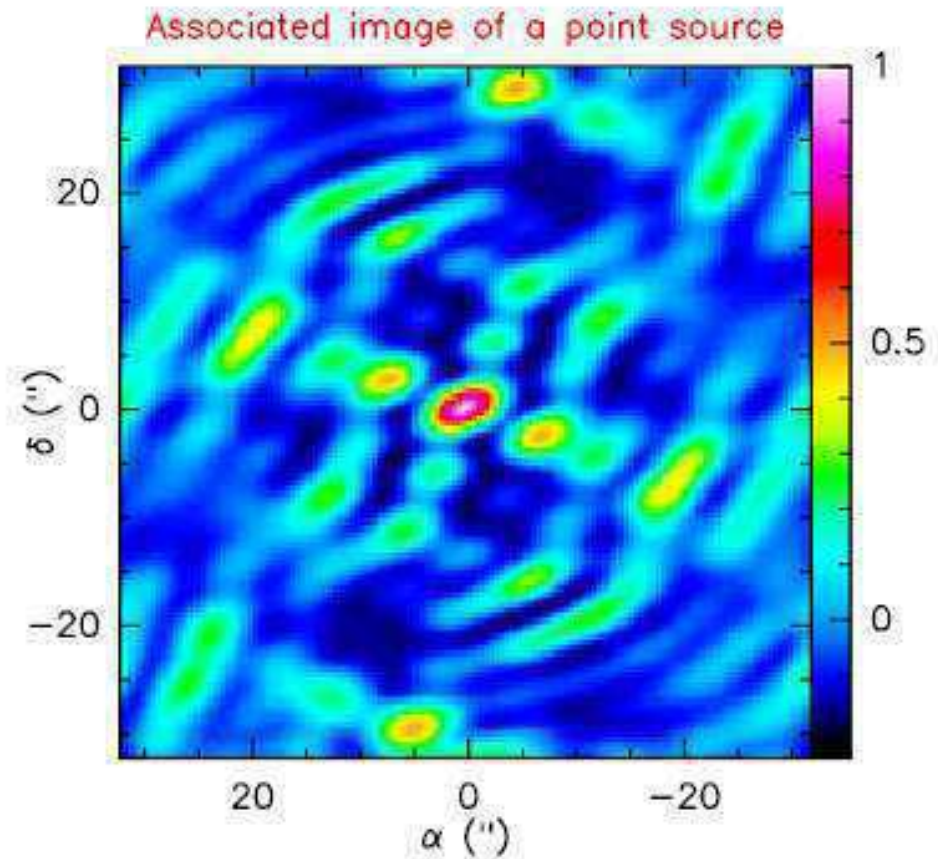
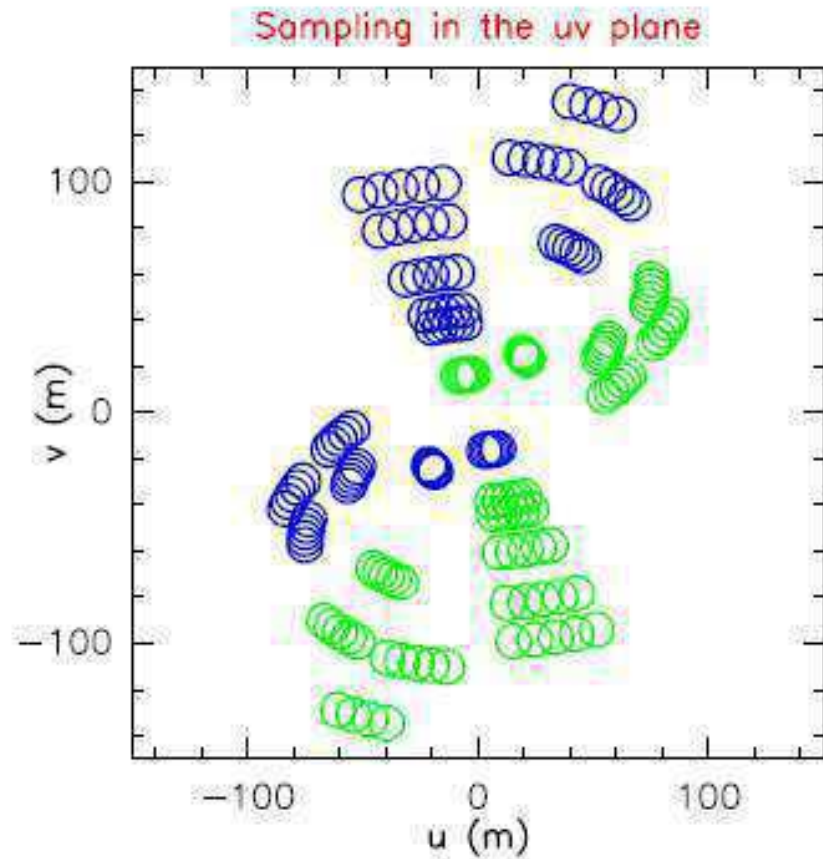


Earth-rotation aperture synthesis

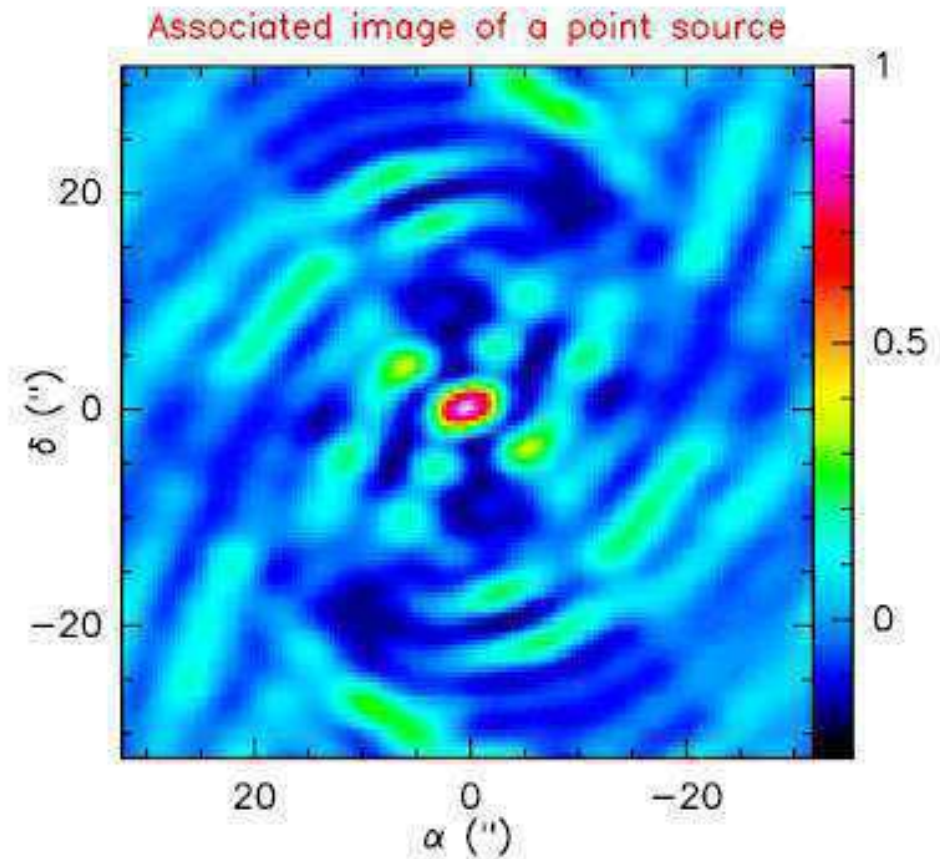
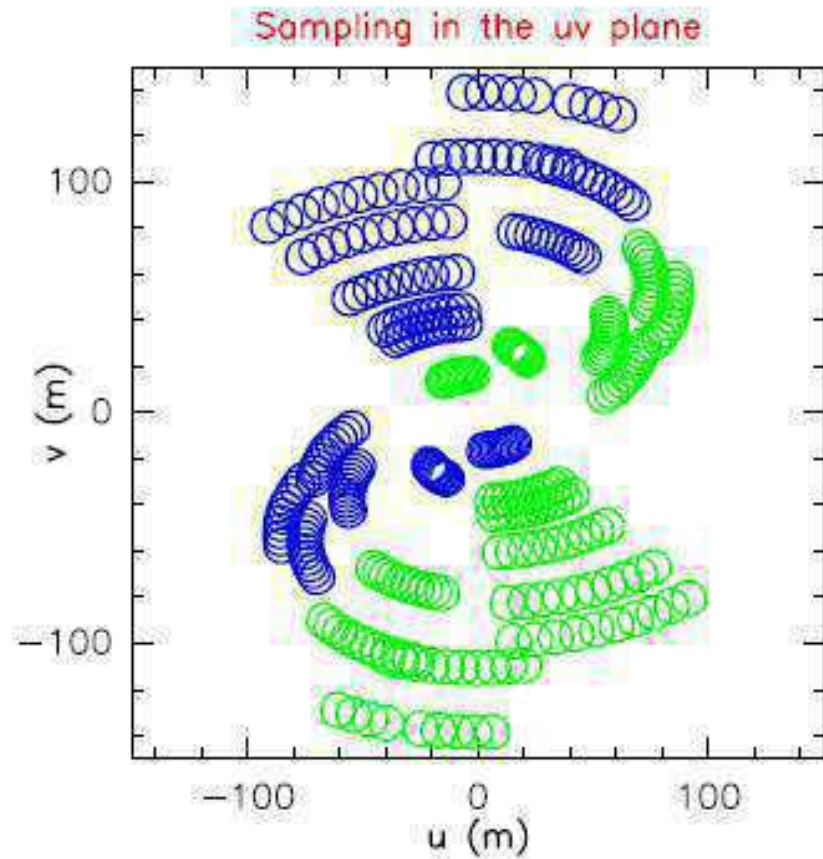
- Incomplete uv plane coverage



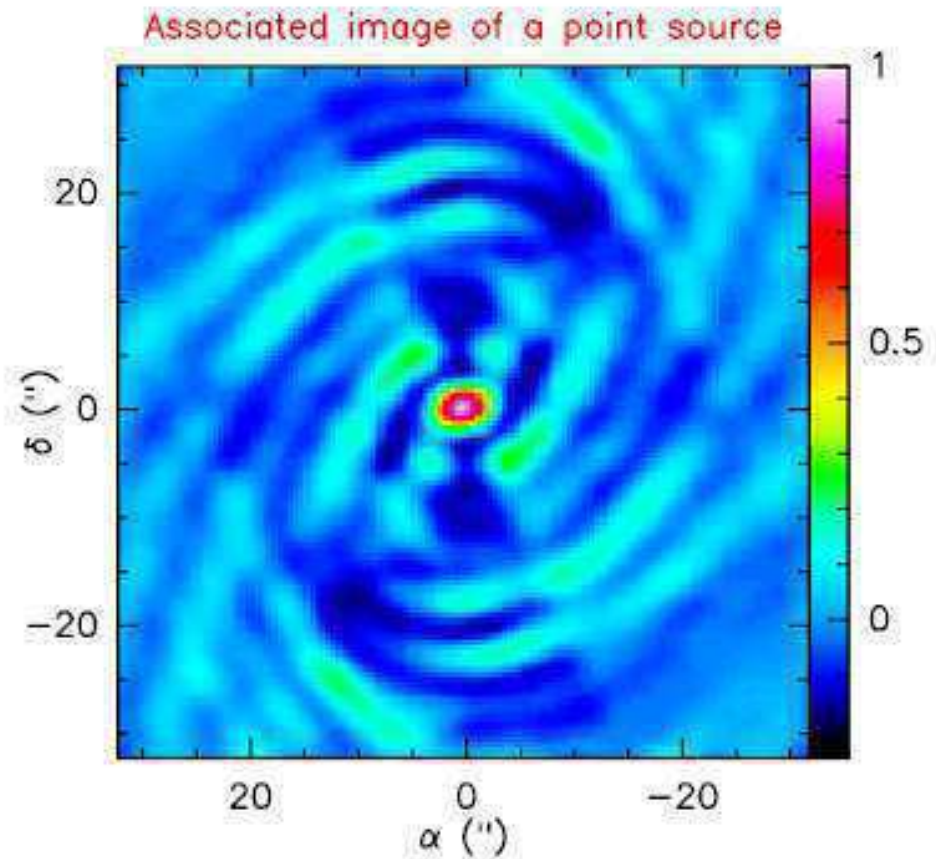
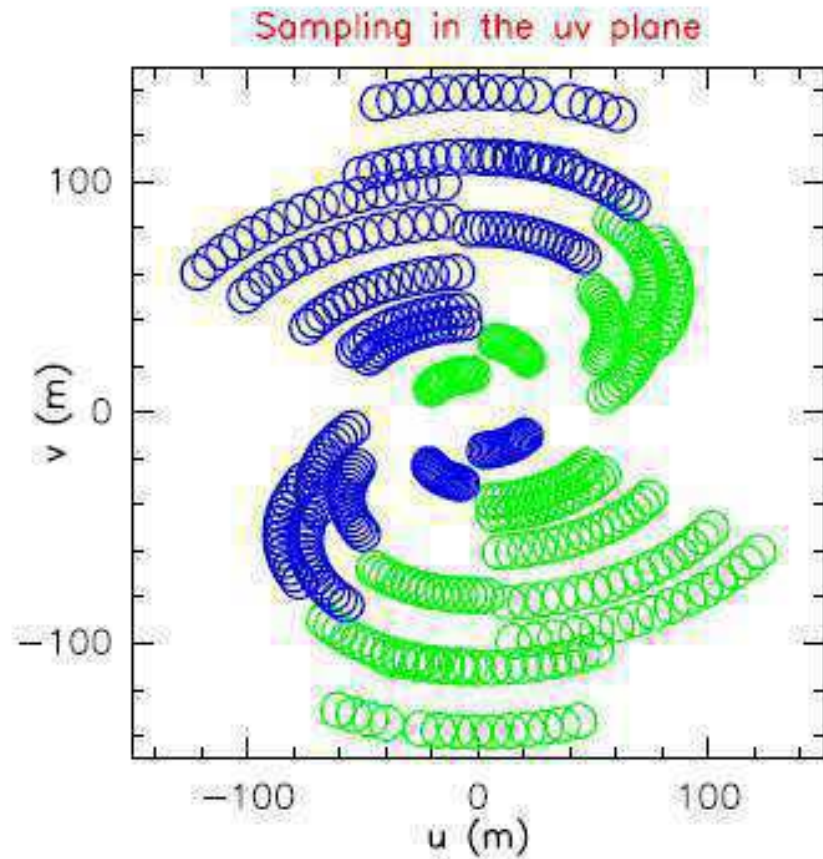
Earth-rotation aperture synthesis



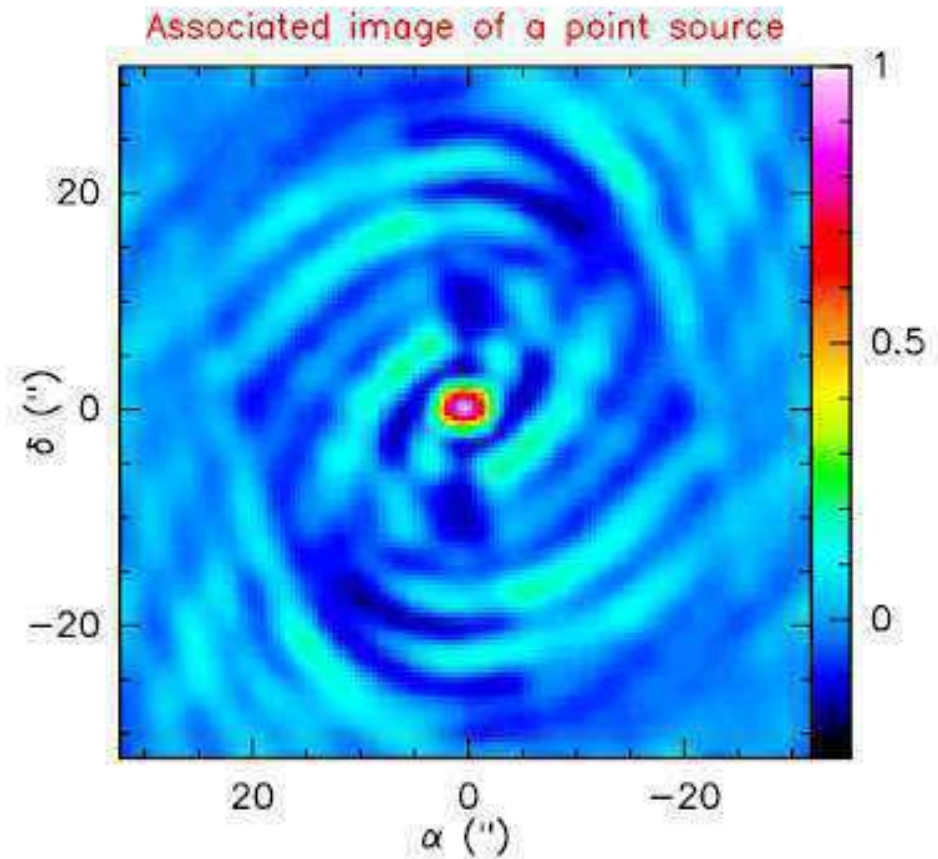
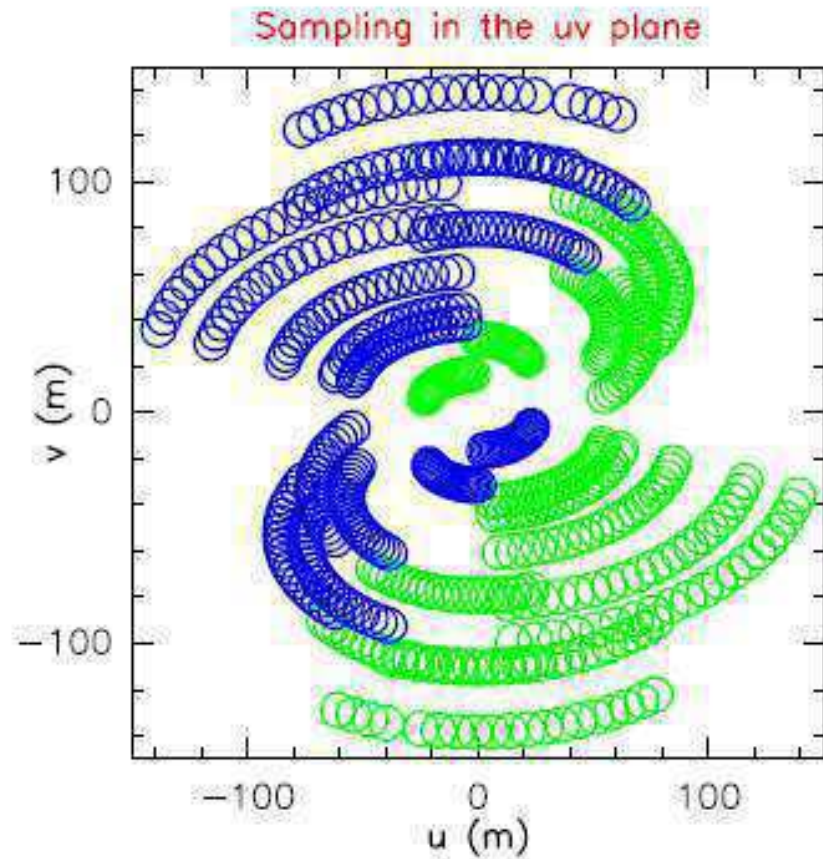
Earth-rotation aperture synthesis



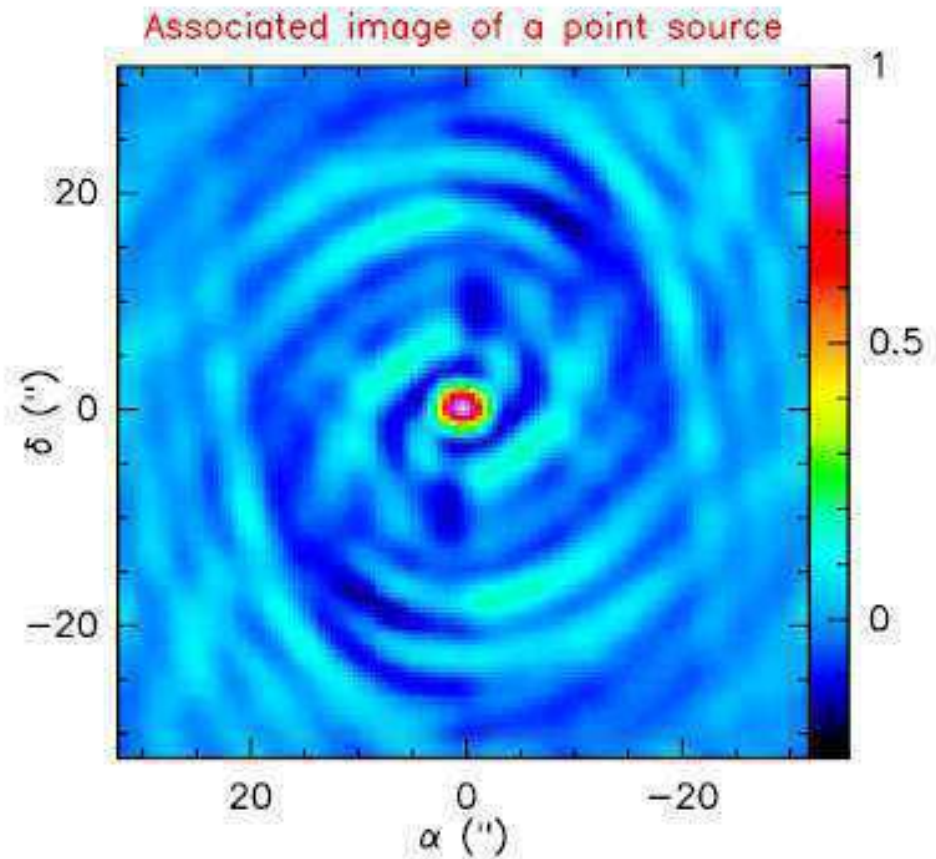
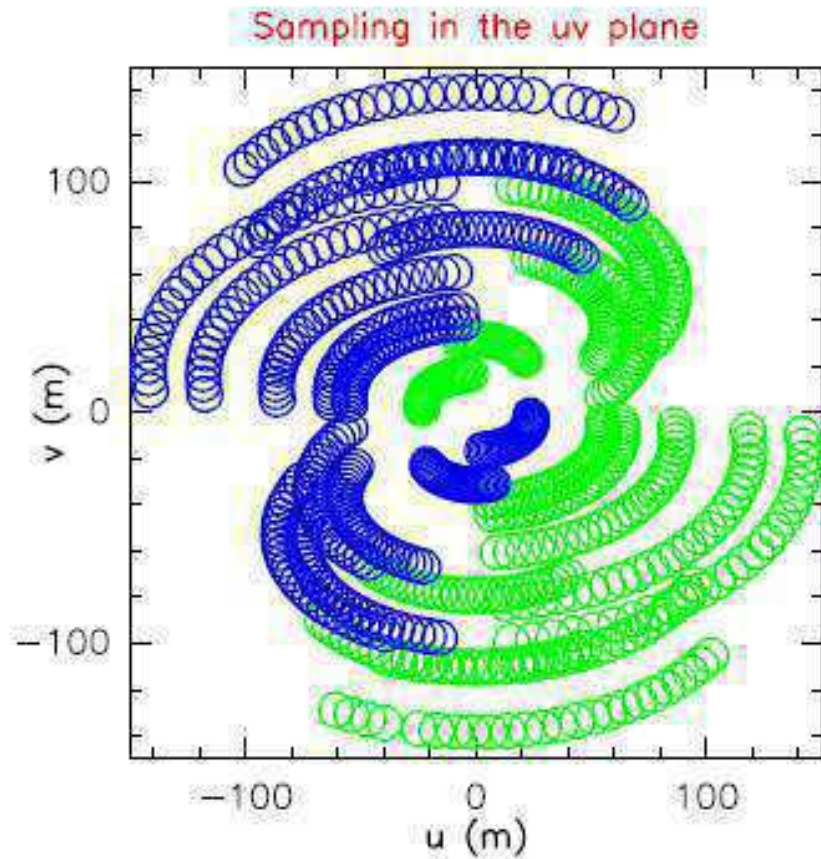
Earth-rotation aperture synthesis



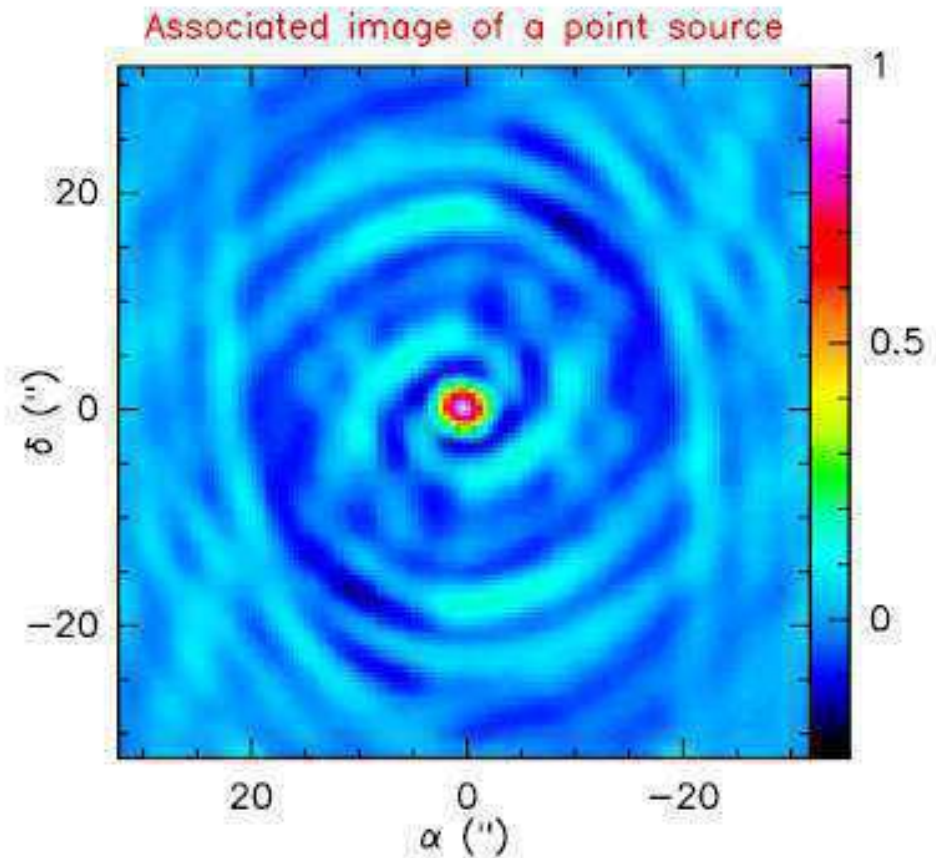
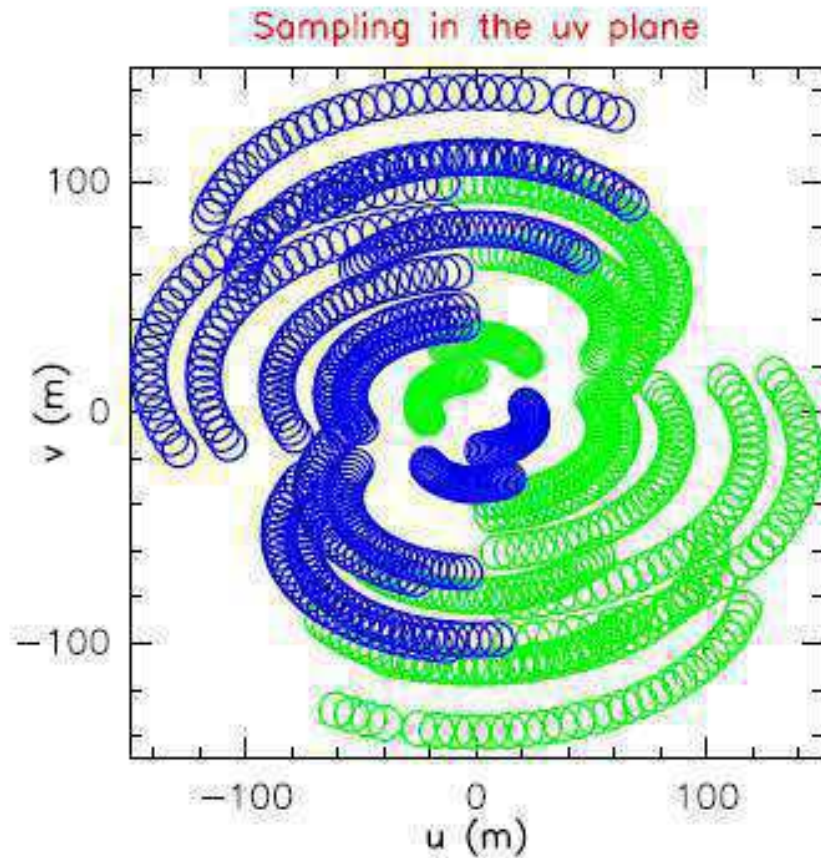
Earth-rotation aperture synthesis



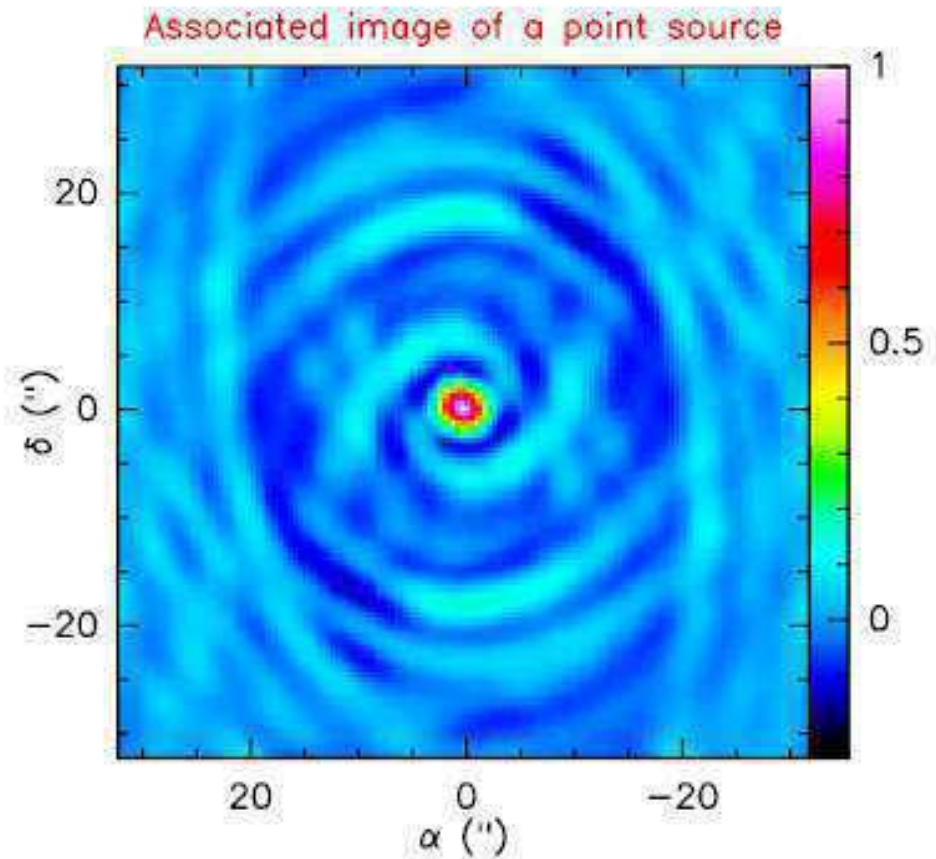
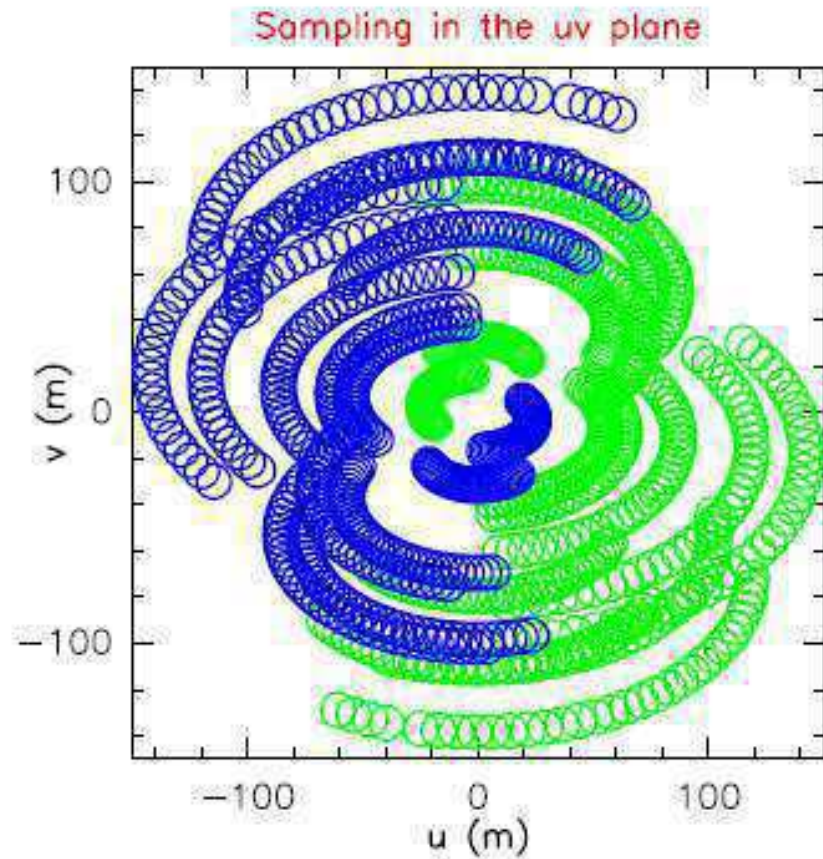
Earth-rotation aperture synthesis



Earth-rotation aperture synthesis



Earth-rotation aperture synthesis



Formal Description

- sample Fourier domain at discrete points

$$B(u, v) = \sum_k (u_k, v_k)$$

- the inverse Fourier transform is

$$T^D(x, y) = FT^{-1}\{B(u, v) \times V(u, v)\}$$

- the convolution theorem tells us

$$T^D(x, y) = b(x, y) \otimes T(x, y) \quad \text{(the point spread function)}$$

where

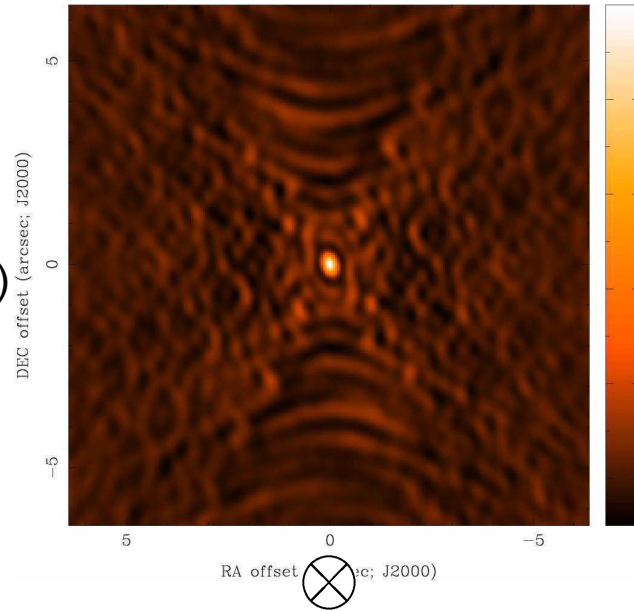
$$b(x, y) = FT^{-1}\{B(u, v)\}$$

Fourier transform of sampled visibilities yields the true sky brightness convolved with the point spread function

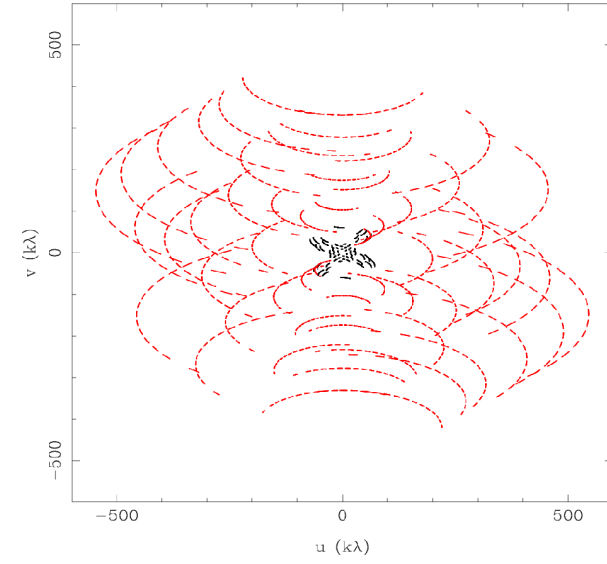
(the “dirty image” is the true image convolved with the “dirty beam”)

Dirty Beam and Dirty Image

$b(x,y)$
(dirty beam)

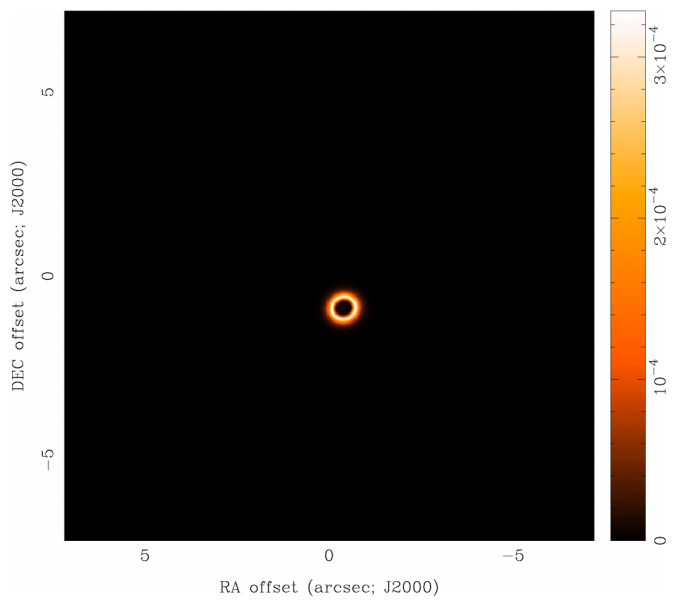


\Downarrow

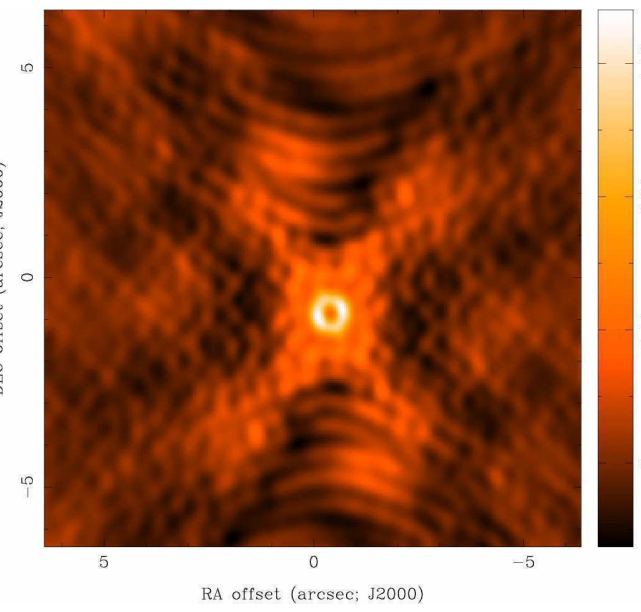


$B(u,v)$

$T(x,y)$



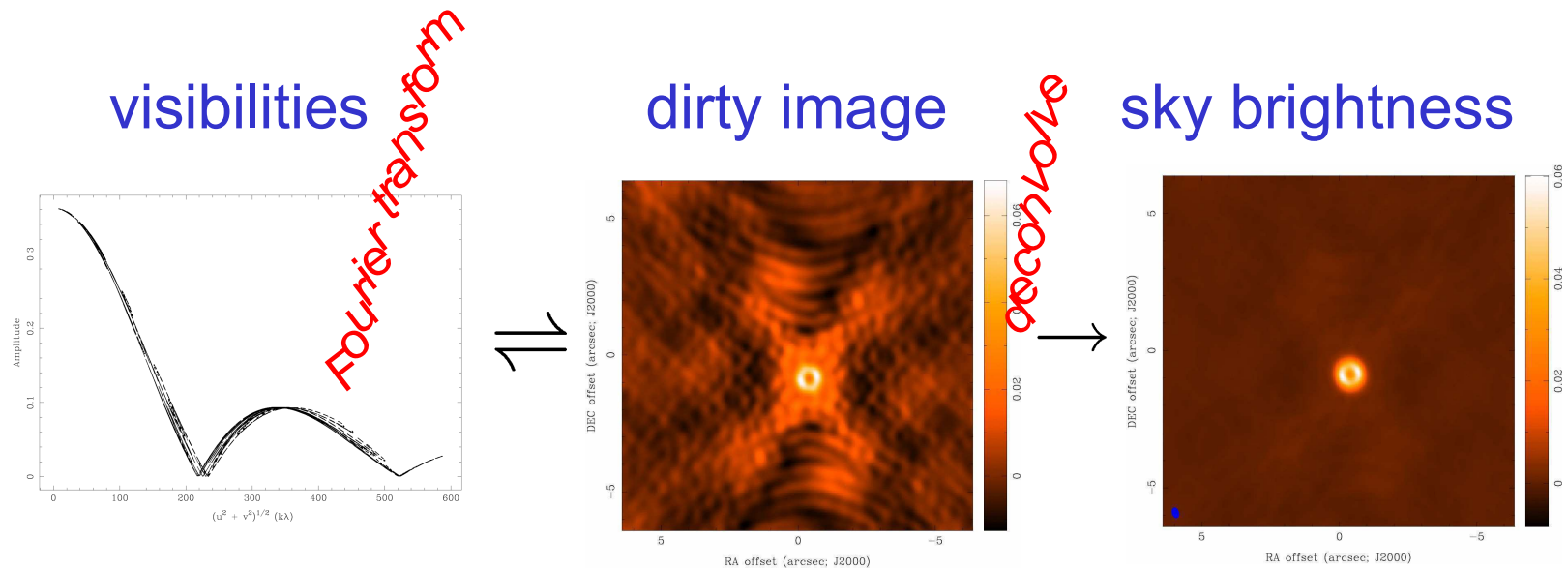
\Downarrow



$T^D(x,y)$
(dirty image)

How to analyze interferometer data?

- uv plane analysis
 - best for “simple” sources, e.g. point sources, disks
- image plane analysis
 - Fourier transform $V(u,v)$ samples to image plane, get $T^D(x,y)$
 - but difficult to do science on dirty image
 - deconvolve $b(x,y)$ from $T^D(x,y)$ to determine (model of) $T(x,y)$



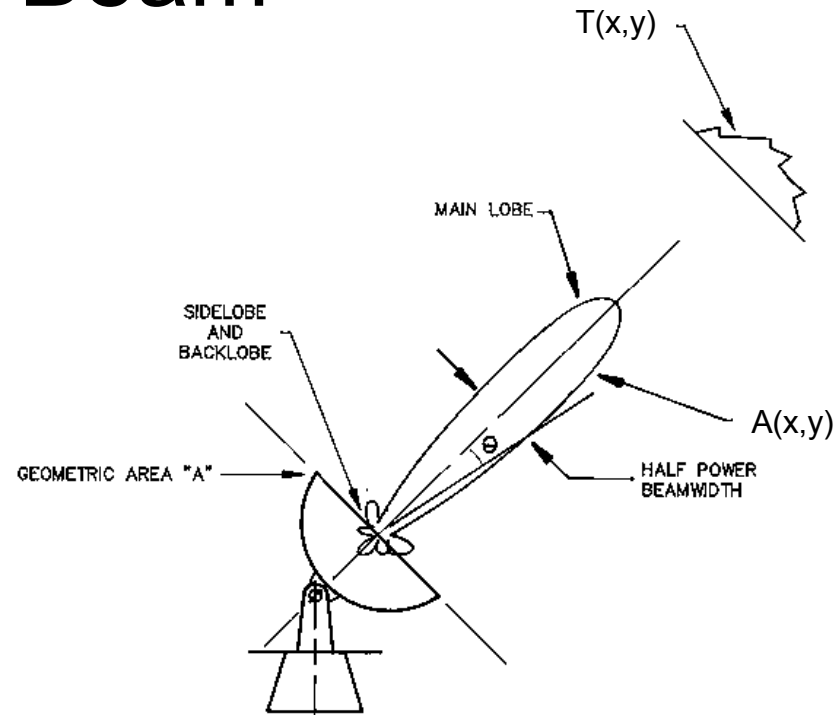
Details of the Dirty Image

- Fourier Transform
 - Fast Fourier Transform (FFT) much faster than simple Fourier summation, $O(N \log N)$ for $2^N \times 2^N$ image
 - FFT requires data on regularly spaced grid
 - aperture synthesis observations not on a regular grid...
- “Gridding” is used to resample $V(u,v)$ for FFT
 - customary to use a convolution technique
 - visibilities are noisy samples of a smooth function
 - nearby visibilities not independent
 - use special (“Spheroidal”) functions with nice properties
 - fall off quickly in (u,v) plane (not too much smoothing)
 - fall off quickly in image plane (avoid aliasing)

$$V^G(u, v) = V(u, v)B(u, v) \otimes G(u, v) \rightleftharpoons T^D(x, y)g(x, y)$$

Primary Beam

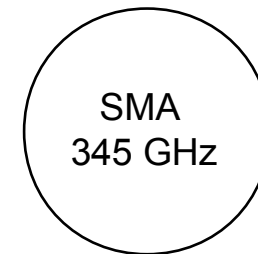
- A telescope does not have uniform response across the entire sky
 - main lobe approximately Gaussian, $\text{fwhm} \sim 1.2\lambda/D$, where D is ant diameter = “primary beam”
 - limited field of view
 - sidelobes, error beam (sometimes important)



- primary beam response modifies sky brightness: $T(x,y) \rightarrow A(x,y)T(x,y)$
 - correct with division by $A(x,y)$ in image plane



$T(x,y)$



large $A(x,y)$



ALMA
690 GHz

small $A(x,y)$

Pixel Size and Image Size

- pixel size
 - should satisfy sampling theorem for the longest baselines, $\Delta x < 1/2 u_{\max}$, $\Delta y < 1/2 v_{\max}$
 - in practice, 3 to 5 pixels across the main lobe of the dirty beam (to aid deconvolution)
 - e.g., SMA: 870 μm , 500 m baselines $\rightarrow 600 \text{ k}\lambda \rightarrow < 0.1 \text{ arcsec}$
- image size
 - natural resolution in (u,v) plane samples $\text{FT}\{A(x,y)\}$, implies image size 2x primary beam
 - e.g., SMA: 870 μm , 6 m telescope $\rightarrow 2x 35 \text{ arcsec}$
 - if there are bright sources in the sidelobes of $A(x,y)$, then they will be aliased into the image (need to make a larger image)

Dirty Beam Shape and Weighting

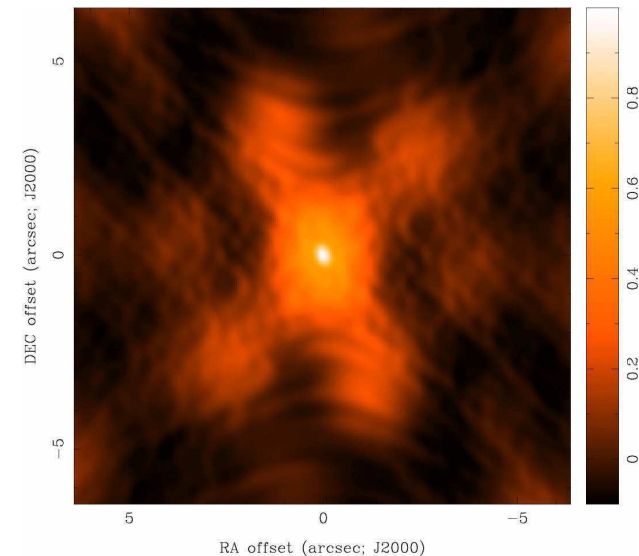
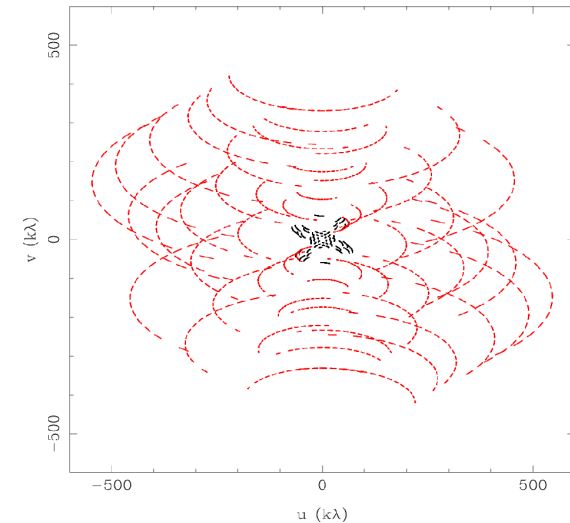
- introduce weighting function $W(u,v)$

$$b(x, y) = FT^{-1}\{W(u, v)B(u, v)\}$$

- W modifies sidelobes of dirty beam
(W is also gridded for FFT)

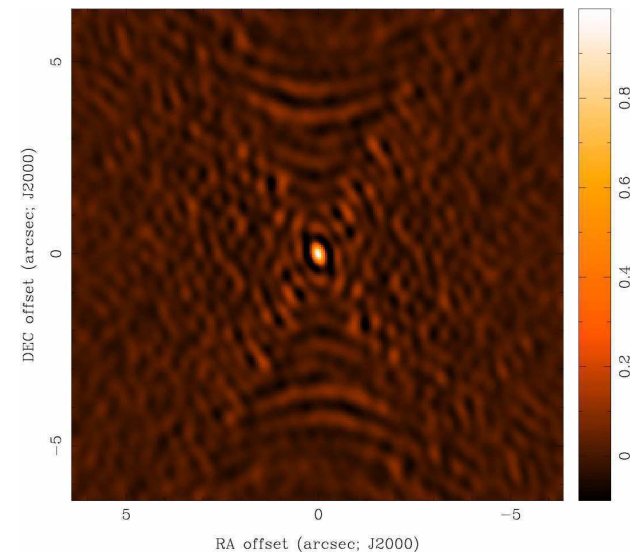
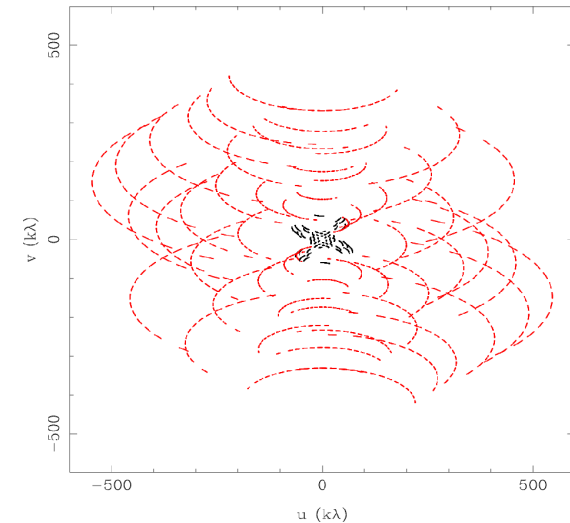
- “Natural” weighting

- $W(u,v) = 1/\sigma^2(u,v)$ at points with data and zero elsewhere, where $\sigma^2(u,v)$ is the noise variance of the (u,v) sample
- maximizes point source sensitivity (lowest rms in image)
- generally more weight to short baselines (large spatial scales), degrades resolution



Dirty Beam Shape and Weighting

- “Uniform” weighting
 - $W(u,v)$ is inversely proportional to local density of (u,v) points, so sum of weights in a (u,v) cell is a constant (or zero)
 - fills (u,v) plane more uniformly, so (outer) sidelobes are lower
 - gives more weight to long baselines and therefore higher angular resolution
 - degrades point source sensitivity (higher rms in image)
 - can be trouble with sparse sampling: cells with few data points have same weight as cells with many data points

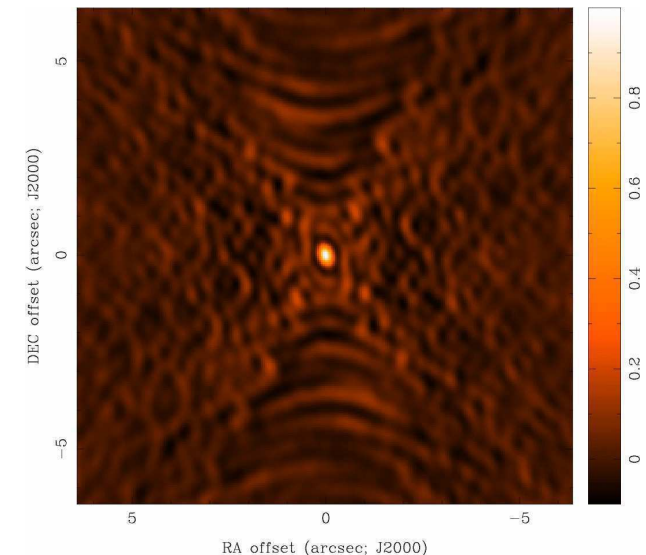
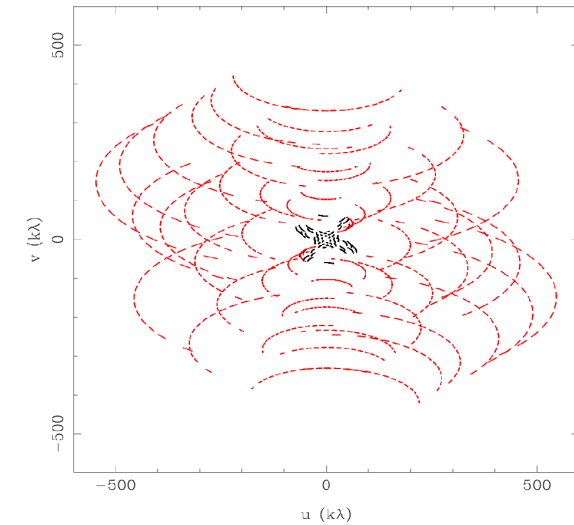


Dirty Beam Shape and Weighting

- “Robust” (Briggs) weighting
 - variant of “uniform” that avoids giving too much weight to cell with low natural weight
 - implementations differ, e.g. S_N is natural weight of a cell, S_t is a threshold

$$W(u, v) = \frac{1}{\sqrt{1 + S_N^2 / S_t^2}}$$

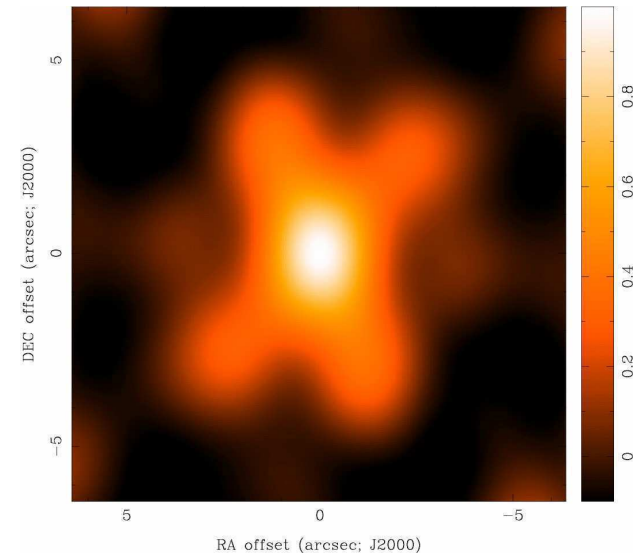
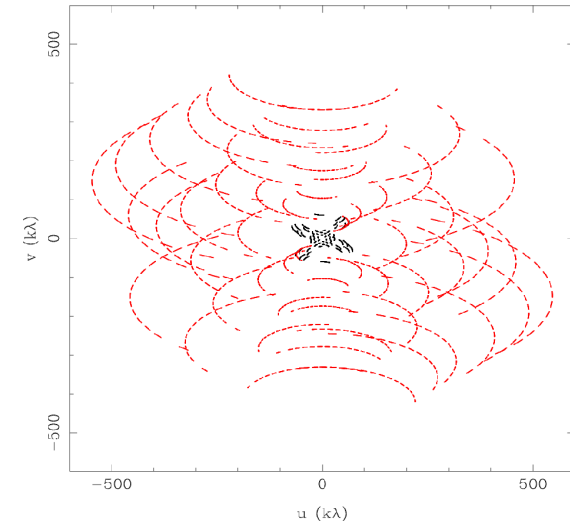
- large threshold \rightarrow natural weighting
- small threshold \rightarrow uniform weighting
- an adjustable parameter that allows for continuous variation between highest angular resolution and optimal point source sensitivity



Dirty Beam Shape and Weighting

- “Tapering”
 - apodize the (u,v) sampling by a Gaussian
$$W(u, v) = \exp \left\{ -\frac{(u^2 + v^2)}{t^2} \right\}$$

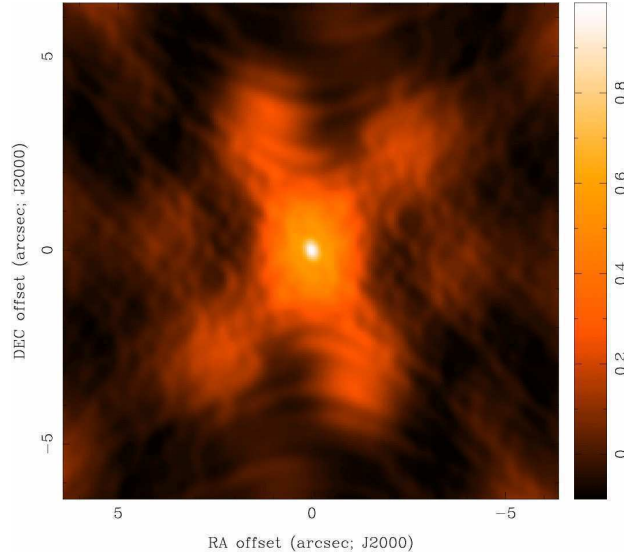
t = tapering parameter (in $k\lambda$; arcsec)
 - like smoothing in the image plane (convolution by a Gaussian)
 - gives more weight to short baselines, degrades angular resolution
 - degrades point source sensitivity but can improve sensitivity to extended structure
 - could use elliptical Gaussian, other function
 - limits to usefulness



Weighting and Tapering: Noise

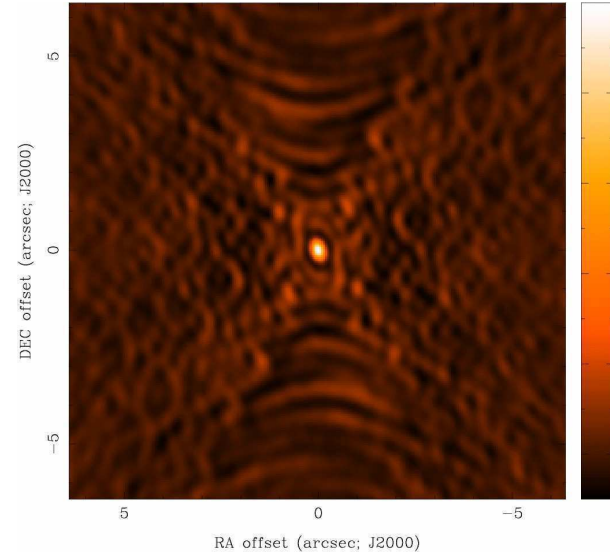
Natural
0.77x0.62

$\sigma=1.0$



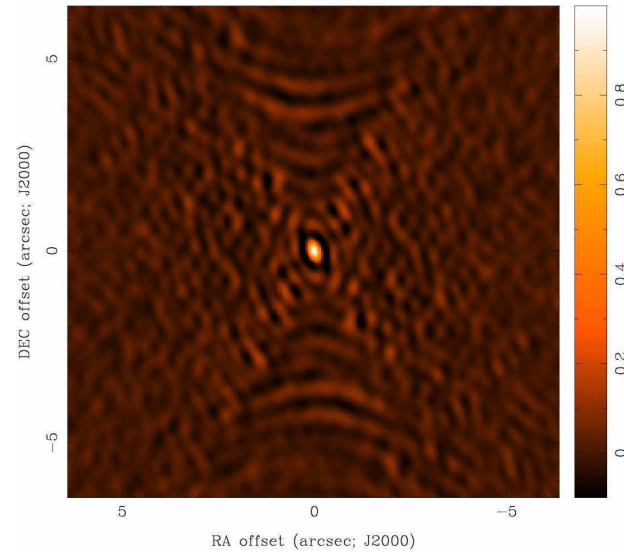
Robust 0
0.41x0.36

$\sigma=1.6$



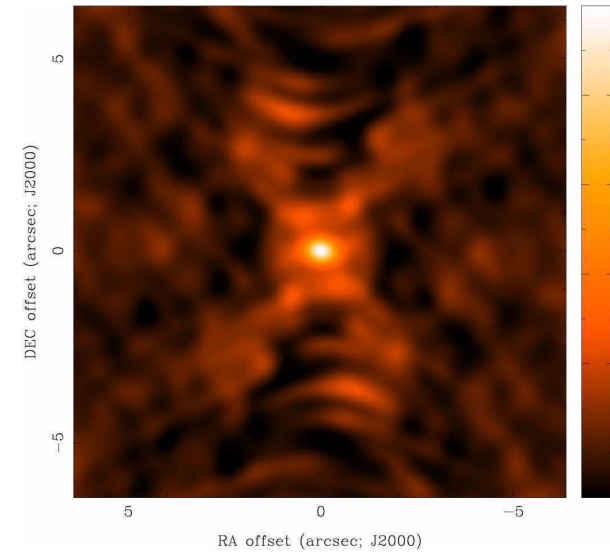
Uniform
0.39x0.31

$\sigma=3.7$



Robust 0
+ Taper
0.77x0.62

$\sigma=1.7$



Weighting and Tapering: Summary

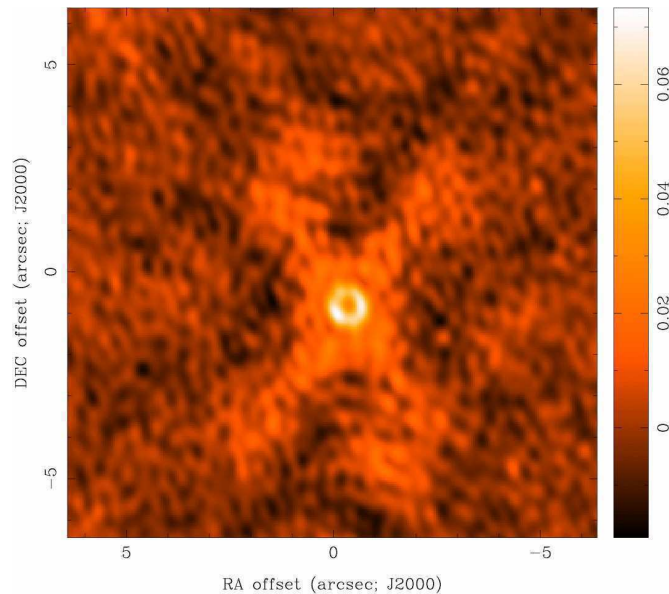
- imaging parameters provide a lot of freedom
- appropriate choice depends on science goals
-

	Robust/Uniform	Natural	Taper
Resolution	higher	medium	lower
Sidelobes	lower	higher	depends
Point Source Sensitivity	lower	maximum	lower
Extended Source Sensitivity	lower	medium	higher

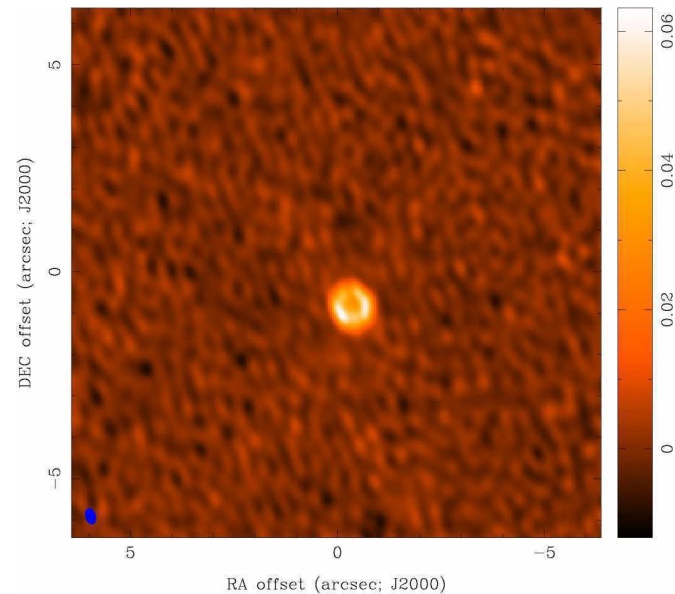
Deconvolution

- difficult to do science on dirty image
- deconvolve $b(x,y)$ from $T^D(x,y)$ to recover $T(x,y)$
- information is missing, so be careful!
(there's noise, too)

dirty image



“CLEAN” image



Deconvolution Philosophy

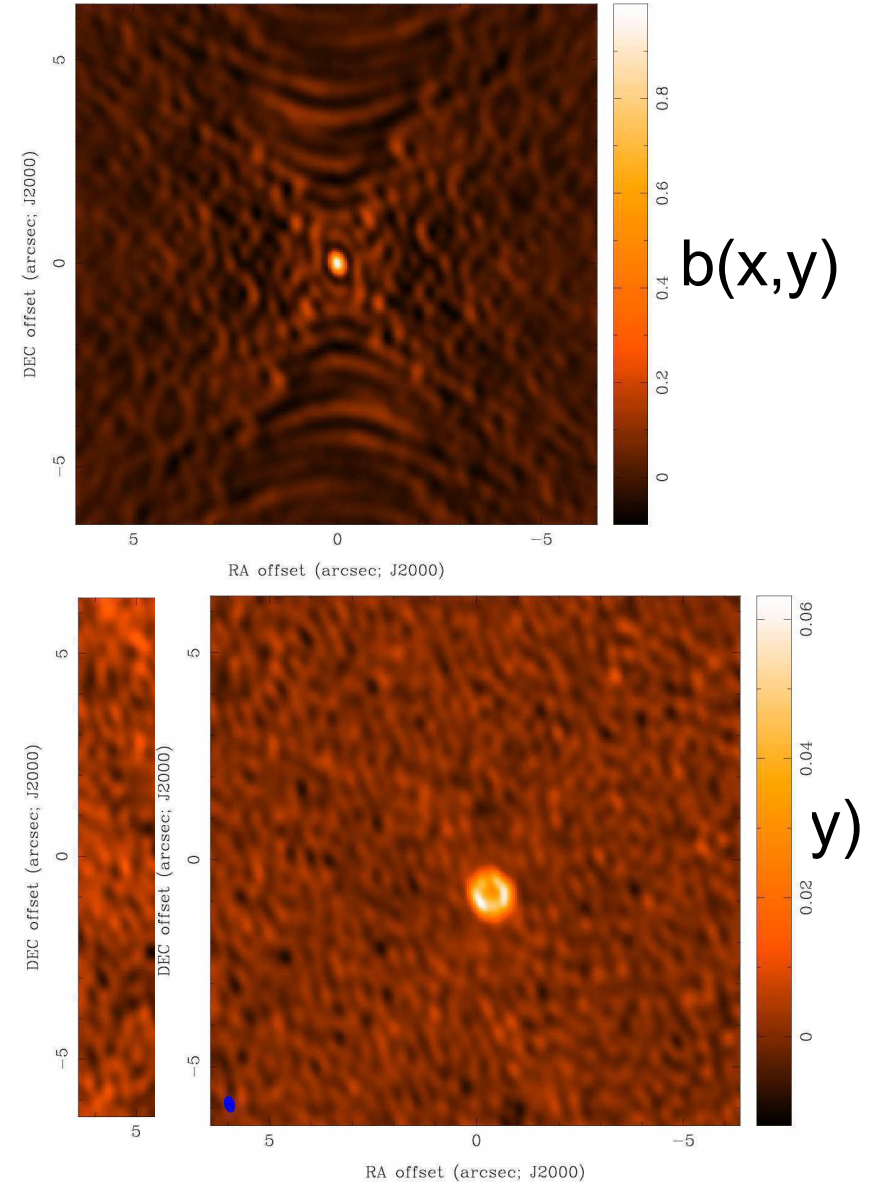
- to keep you awake at night
 - \exists an infinite number of $T(x,y)$ compatible with sampled $V(u,v)$, i.e. “invisible” distributions $R(x,y)$ where $b(x,y) \otimes R(x,y) = 0$
 - no data beyond $u_{\max}, v_{\max} \rightarrow$ unresolved structure
 - no data within $u_{\min}, v_{\min} \rightarrow$ limit on largest size scale
 - holes between u_{\min}, v_{\min} and $u_{\max}, v_{\max} \rightarrow$ sidelobes
 - noise \rightarrow undetected/corrupted structure in $T(x,y)$
 - no unique prescription for extracting optimum estimate of true sky brightness from visibility data
- deconvolution
 - uses non-linear techniques effectively interpolate/extrapolate samples of $V(u,v)$ into unsampled regions of the (u,v) plane
 - aims to find a **sensible** model of $T(x,y)$ compatible with data
 - requires *a priori* assumptions about $T(x,y)$

Deconvolution Algorithms

- most common algorithms in radio astronomy
 - CLEAN (Högbom 1974)
 - *a priori* assumption: $T(x,y)$ is a collection of point sources
 - variants for computational efficiency, extended structure
 - Maximum Entropy (Gull and Skilling 1983)
 - *a priori* assumption: $T(x,y)$ is smooth and positive
 - vast literature about the deep meaning of entropy (Bayesian)
 - hybrid approaches of these can be effective
- deconvolution requires knowledge of beam shape and image noise properties (usually OK for aperture synthesis)
 - atmospheric seeing can modify effective beam shape
 - deconvolution process can modify image noise properties

Basic CLEAN Algorithm

1. Initialize
 - a *residual* map to the dirty map
 - a *Clean component* list to empty
- Identify strongest feature in *residual* map as a point source
- Add a fraction g (the loop gain) of this point source to the clean component list
- Subtract the fraction g times $b(x,y)$ from *residual* map
- If stopping criteria not reached, goto step 2 (an iteration)
- Convolve *Clean component* (cc) list by an estimate of the main lobe of the dirty beam (the “Clean beam”) and add *residual* map to make the final “restored” image

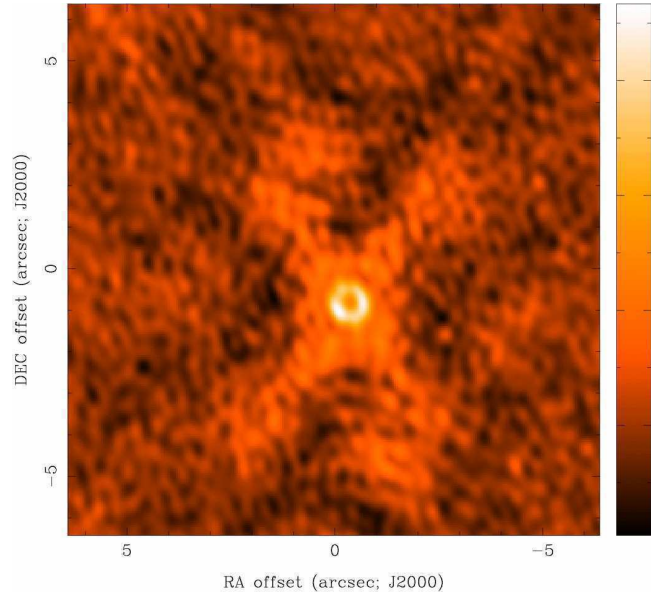


Basic CLEAN Algorithm (cont)

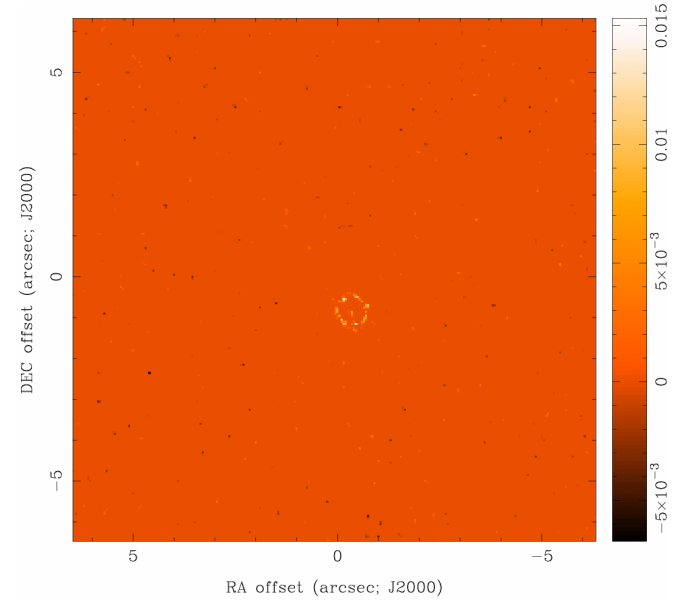
- stopping criteria
 - *residual* map max < multiple of rms (when noise limited)
 - *residual* map max < fraction of dirty map max (dynamic range limited)
 - max number of clean components reached (no justification)
- loop gain
 - good results for $g \sim 0.1$ to 0.3
 - lower values can work better for smoother emission, $g \sim 0.05$
- easy to include *a priori* information about where to search for clean components (“clean boxes”)
 - very useful but potentially dangerous!
- Schwarz (1978): CLEAN is equivalent to a least squares fit of sinusoids, in the absence of noise

CLEAN

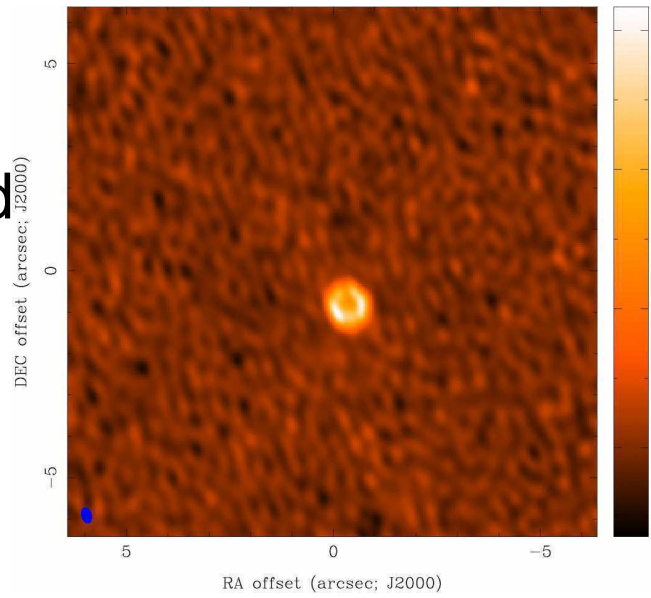
$T^D(x,y)$



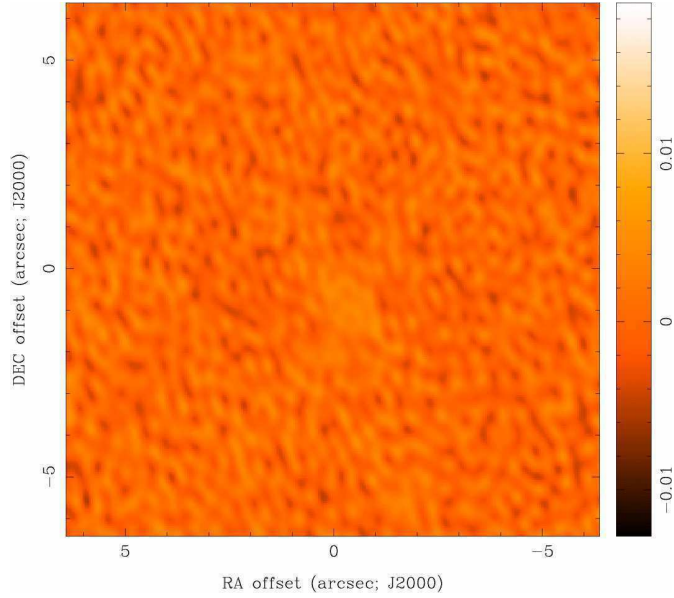
CLEAN
model



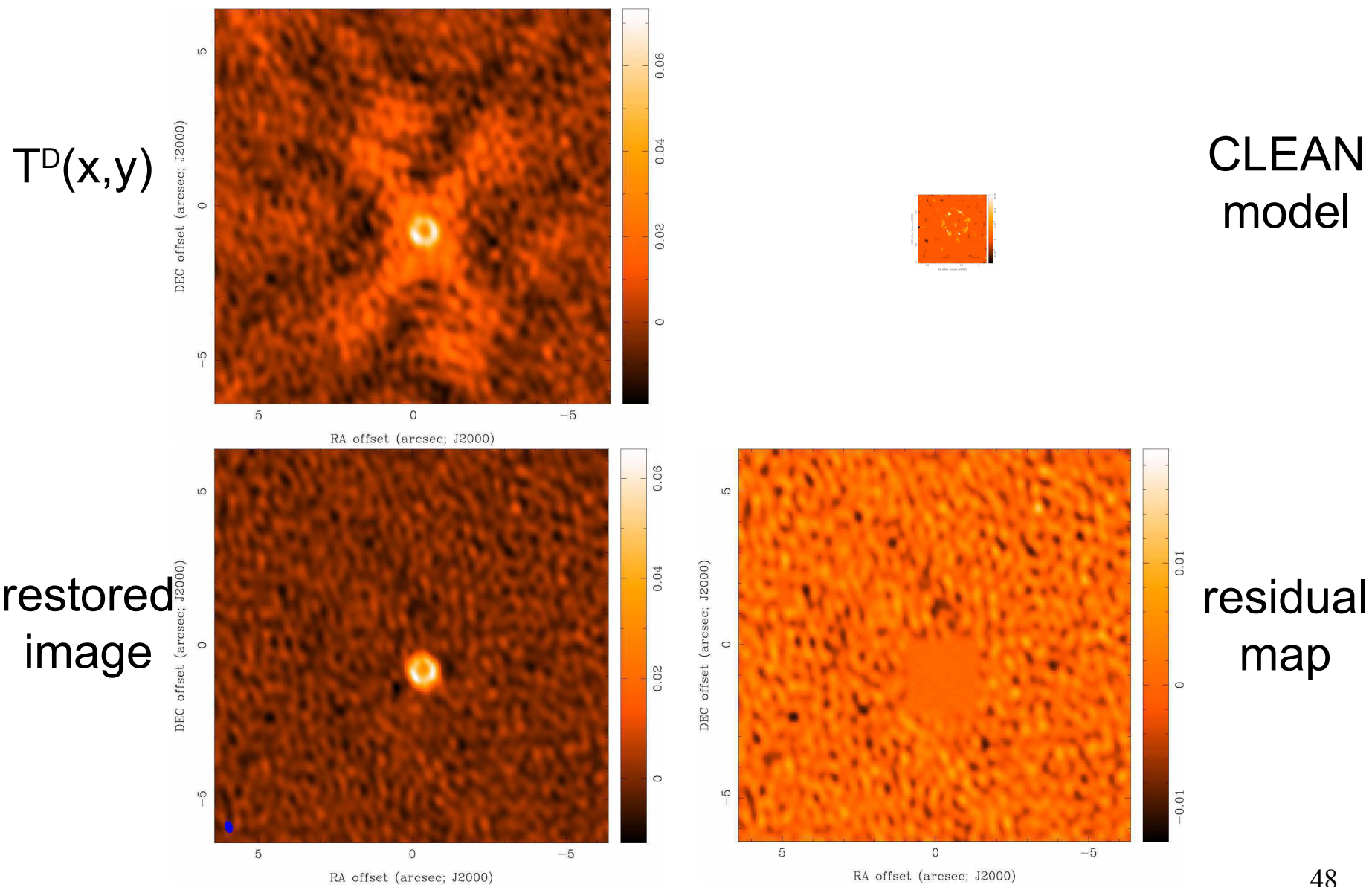
restored
image



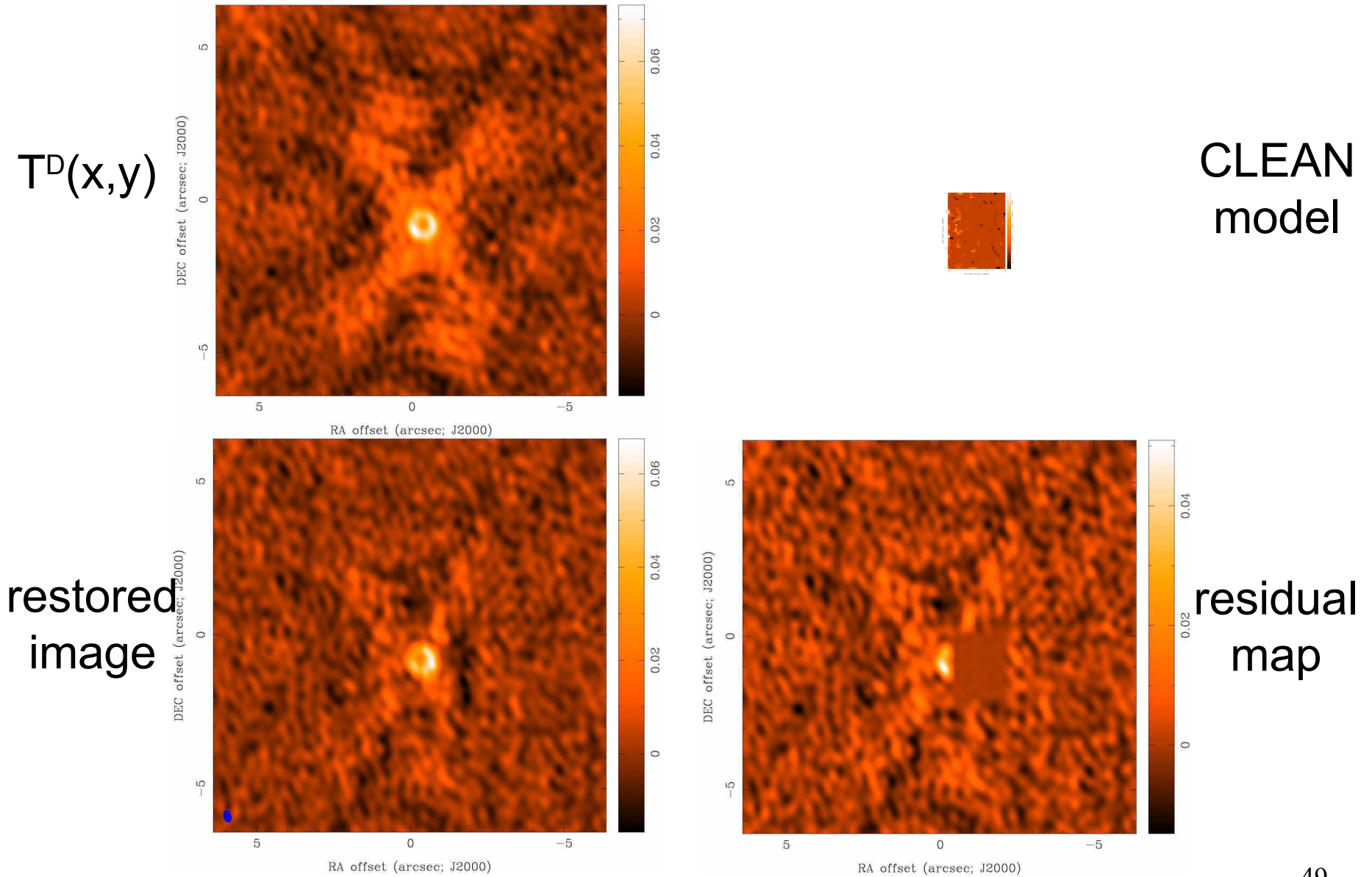
residual
map



CLEAN with Box



CLEAN with Poor Choice of Box



CLEAN Variants

- **Clark CLEAN**
 - aims at faster speed for large images
 - Högbom-like “minor” cycle w/ truncated dirty beam, subset of largest residuals
 - in “major” cycle, cc’s are FFT’d and subtracted from the FFT of the residual image from the previous “major” cycle
- **Cotton-Schwab CLEAN (MX)**
 - in “major” cycle, cc’s are FFT’d and subtracted from ungridded visibilities
 - more accurate but slower (gridding steps repeated)
- **Steer, Dewdney, Ito (SDI) CLEAN**
 - aims to suppress CLEAN “stripes” in smooth, extended emission
 - in “minor” cycles, any point in the residual map greater than a fraction (<1) of the maximum is taken as a cc
- **Multi-Resolution CLEAN**
 - aims to account for coupling between pixels by extended structure
 - independently CLEAN a smooth map and a difference map, fewer cc’s

“Restored” Images

- CLEAN beam size:
 - natural choice is to fit the central peak of the dirty beam with elliptical Gaussian
 - unit of deconvolved map is Jy per CLEAN beam area
(= intensity, can convert to brightness temperature)
 - minimize unit problems when adding dirty map residuals
 - modest super resolution often OK, but be careful
- photometry should be done with caution
 - CLEAN does not conserve flux (extrapolates)
 - extended structure missed, attenuated, distorted
 - phase errors (e.g. seeing) can spread signal around

Noise in Images

- point source sensitivity: straightforward
 - telescope area, bandwidth, integration time, weighting
 - in image, modify noise by primary beam response
- extended source sensitivity: problematic
 - not quite right to divide noise by \sqrt{n} beams covered by source: smoothing = tapering, omitting data \rightarrow lower limit
 - Interferometers always missing flux at some spatial scale
- be careful with low signal-to-noise images
 - if position known, 3σ OK for point source detection
 - if position unknown, then 5σ required (flux biased by $\sim 1\sigma$)
 - if $< 6\sigma$, cannot measure the source size (require $\sim 3\sigma$ difference between “long” and “short” baselines)
 - spectral lines may have unknown position, velocity, width

Maximum Entropy Algorithm

- Maximize a measure of smoothness (the entropy)

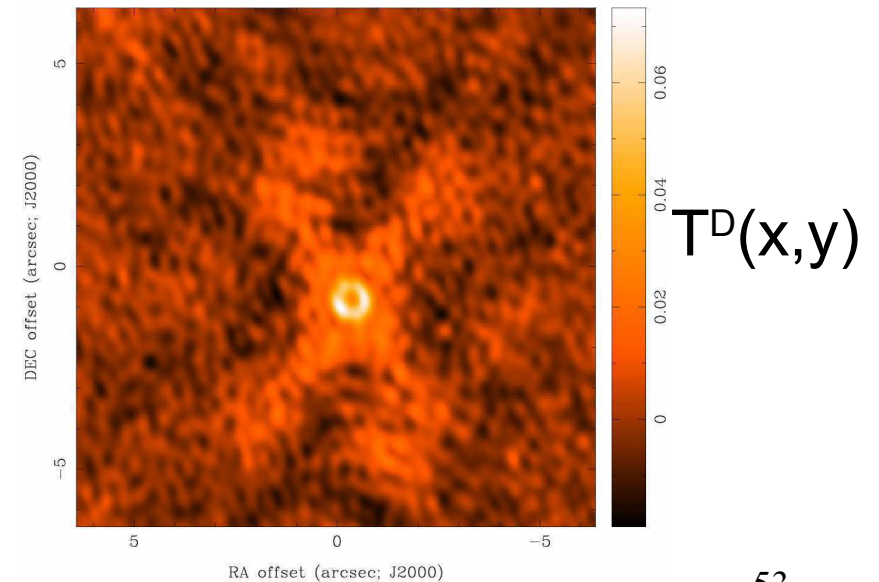
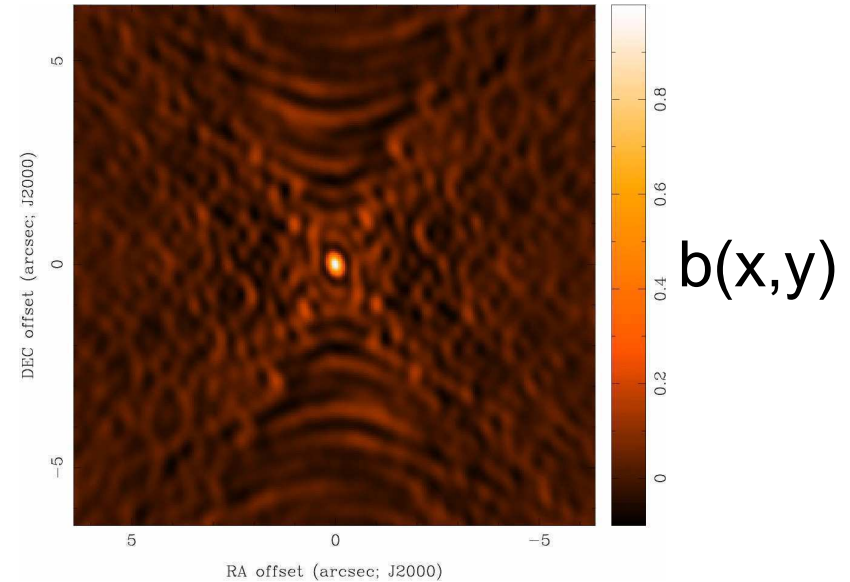
$$H = - \sum_k T_k \log \left(\frac{T_k}{M_k} \right)$$

subject to the constraints

$$\chi^2 = \sum_k \frac{|V(u_k, v_k) - \text{FT}\{T\}|^2}{\sigma_k^2}$$

$$F = \sum_k T_k$$

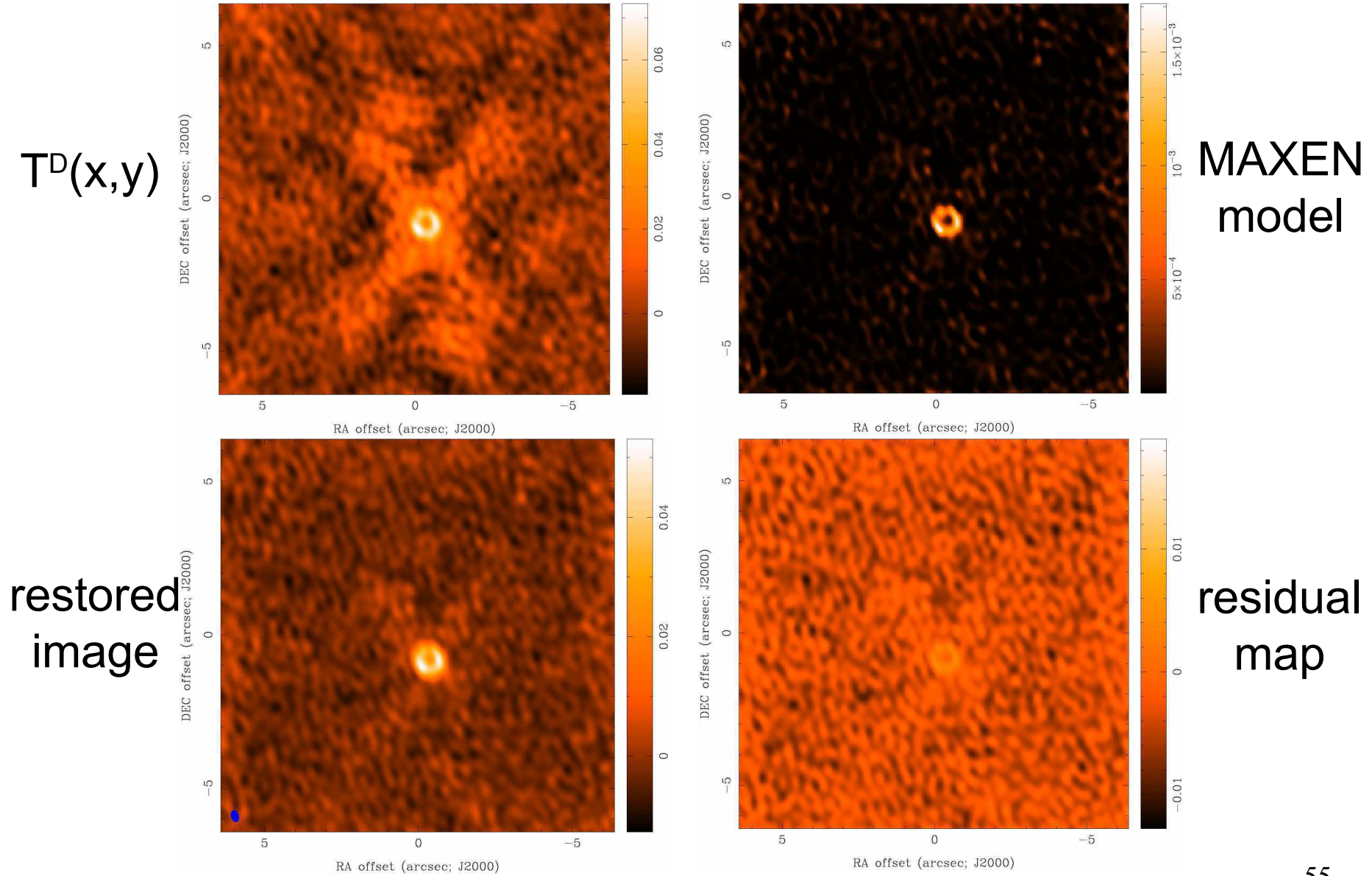
- M is the “default image”
- fast (NlogN) non-linear optimization solver due to Cornwell and Evans (1983)
- optional: convolve with Gaussian beam and add residual map to make image



Maximum Entropy Algorithm (cont)

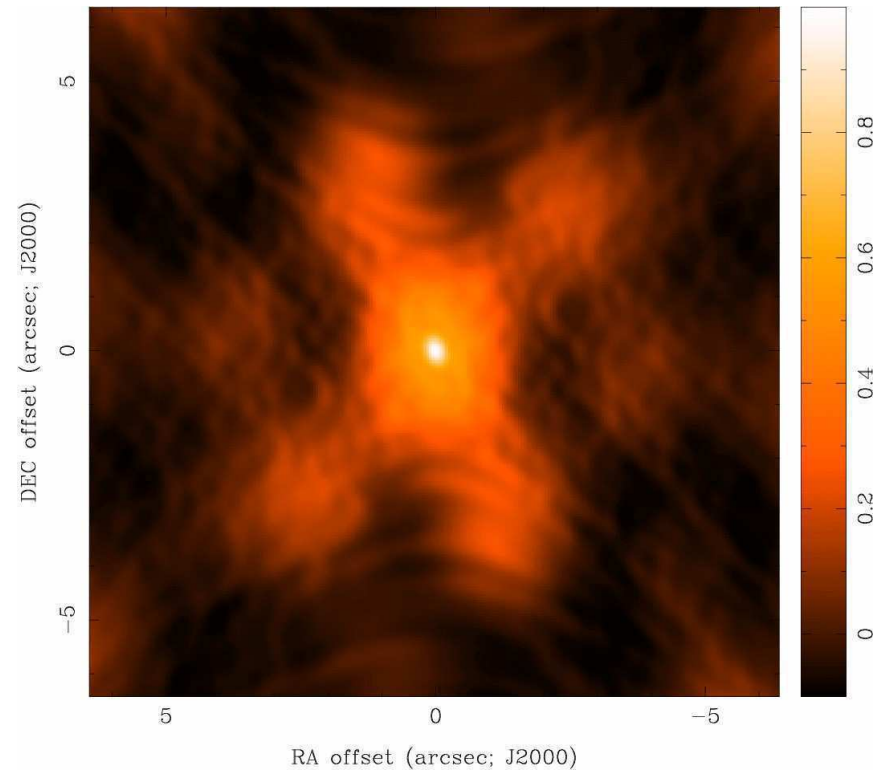
- easy to include *a priori* information with default image
 - flat default best only if nothing known (or nothing observed!)
- straightforward to generalize χ^2 to combine different observations/telescopes and obtain optimal image
- many measures of “entropy” available
 - replace log with cosh \rightarrow “emptiness” (does not enforce positivity)
- less robust and harder to drive than CLEAN
- works well on smooth, extended emission
- trouble with point source sidelobes
- no noise estimate possible from image

Maximum Entropy

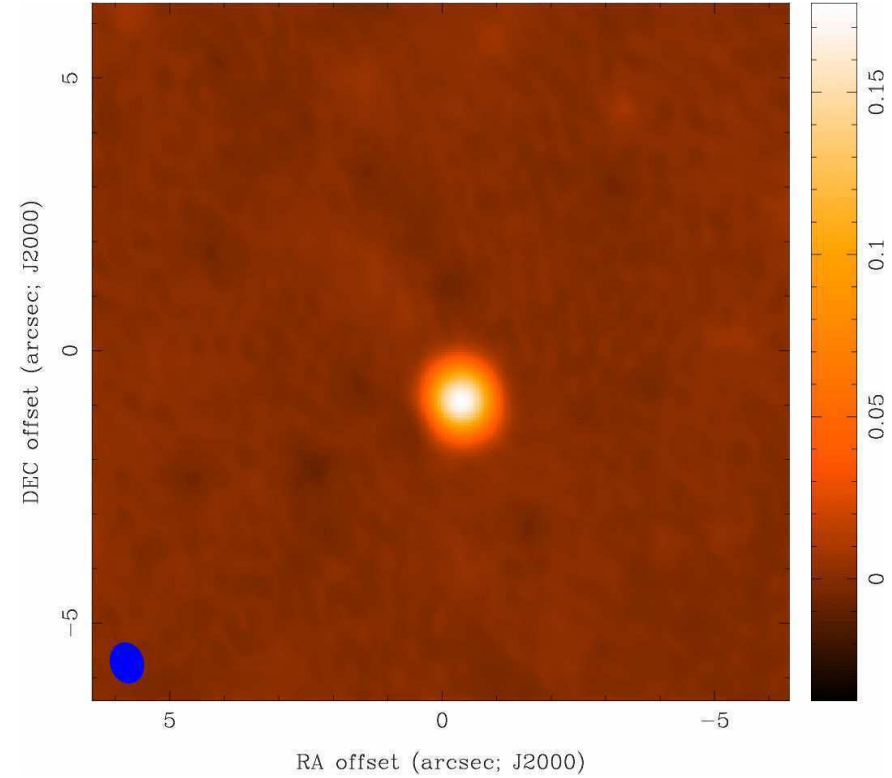


Imaging Results

Natural Weight Beam

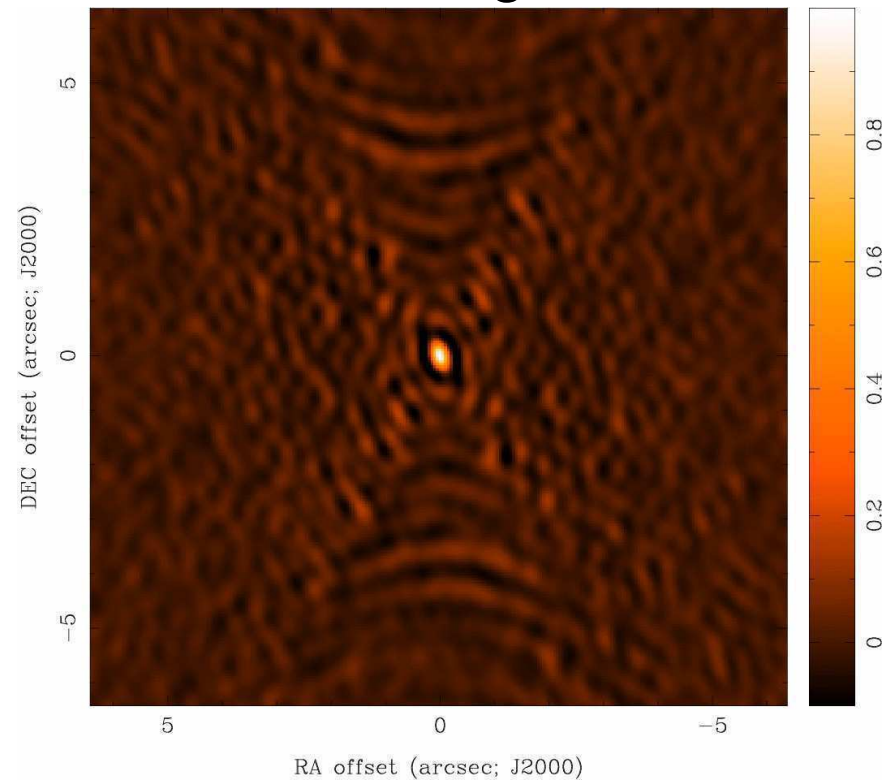


CLEAN image

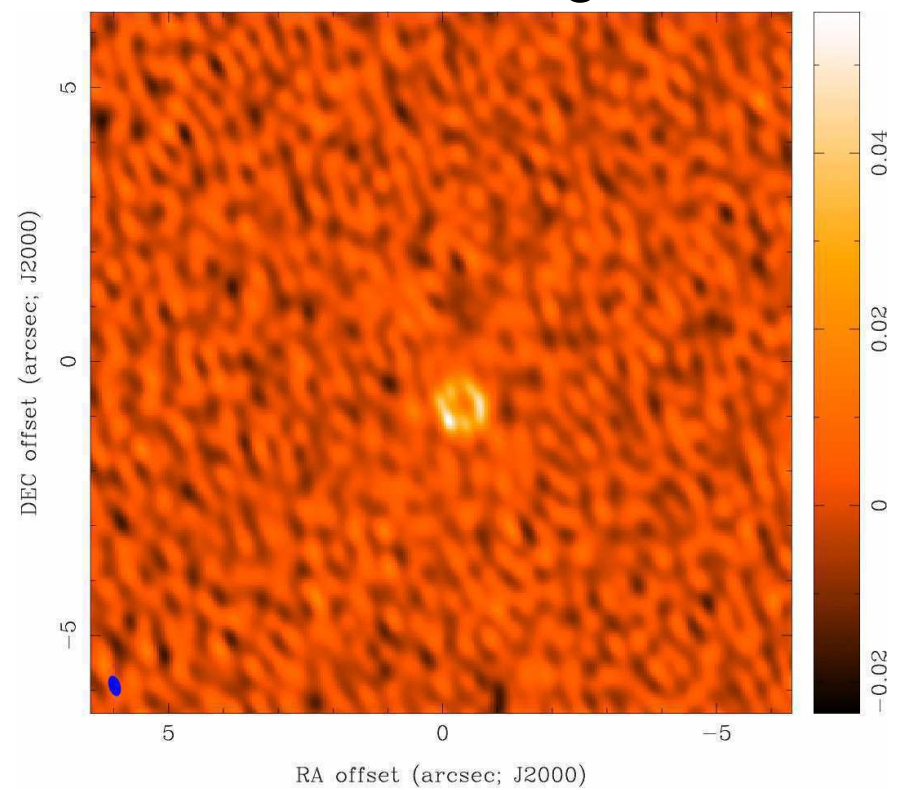


Imaging Results

Uniform Weight Beam

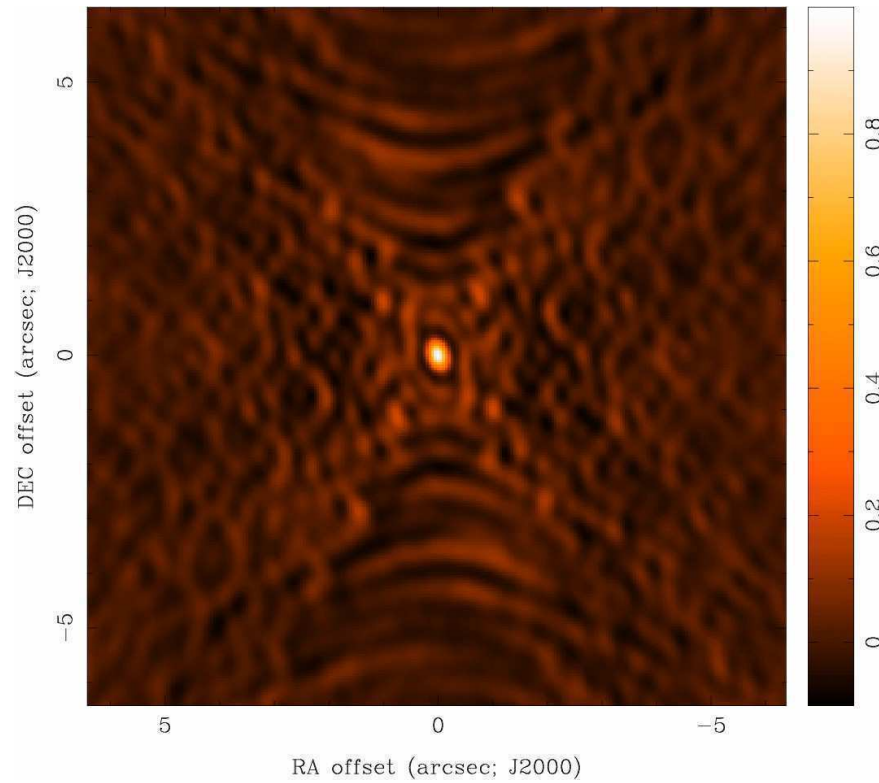


CLEAN image

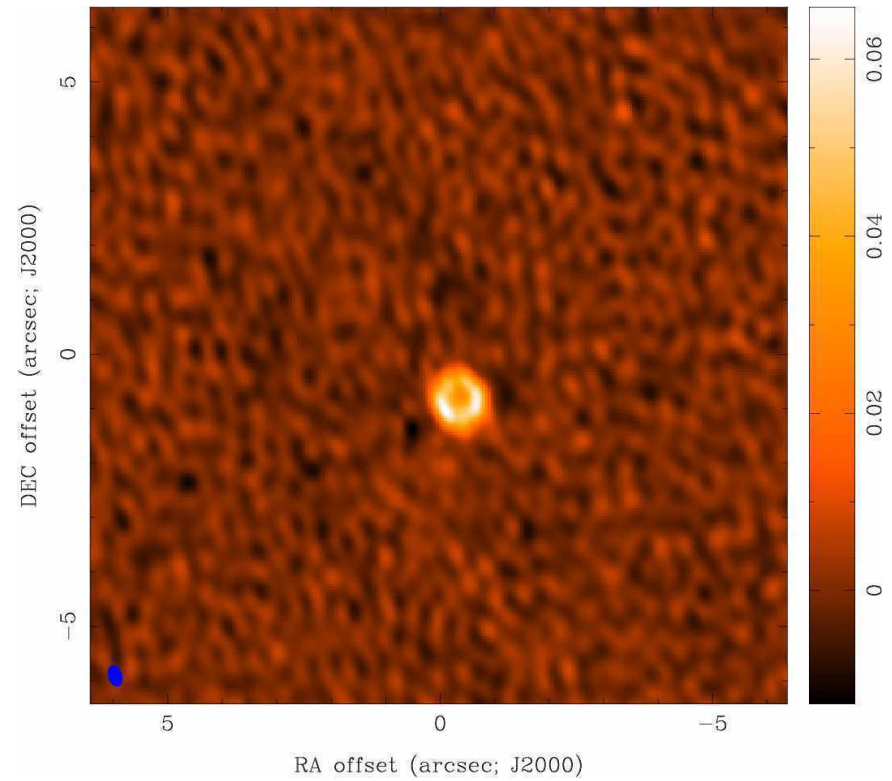


Imaging Results

Robust=0 Beam

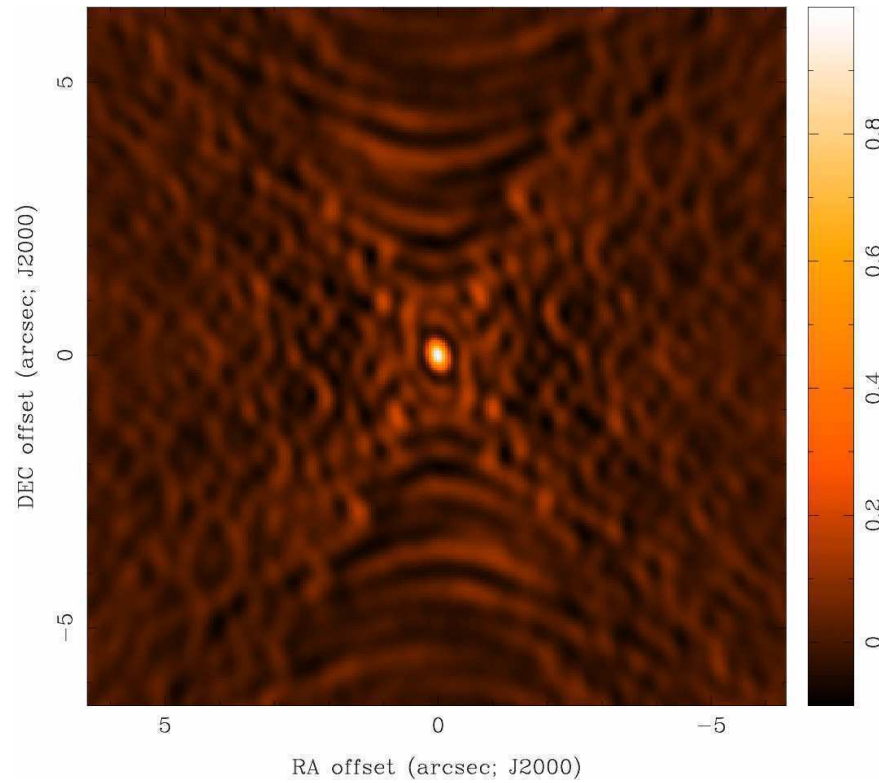


CLEAN image

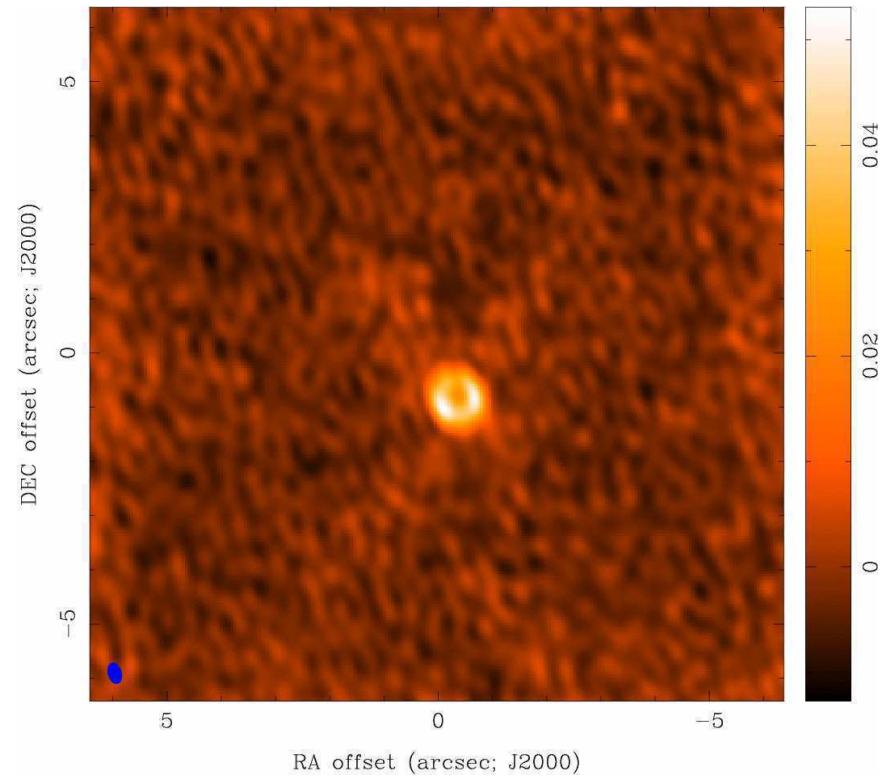


Imaging Results

Robust=0 Beam

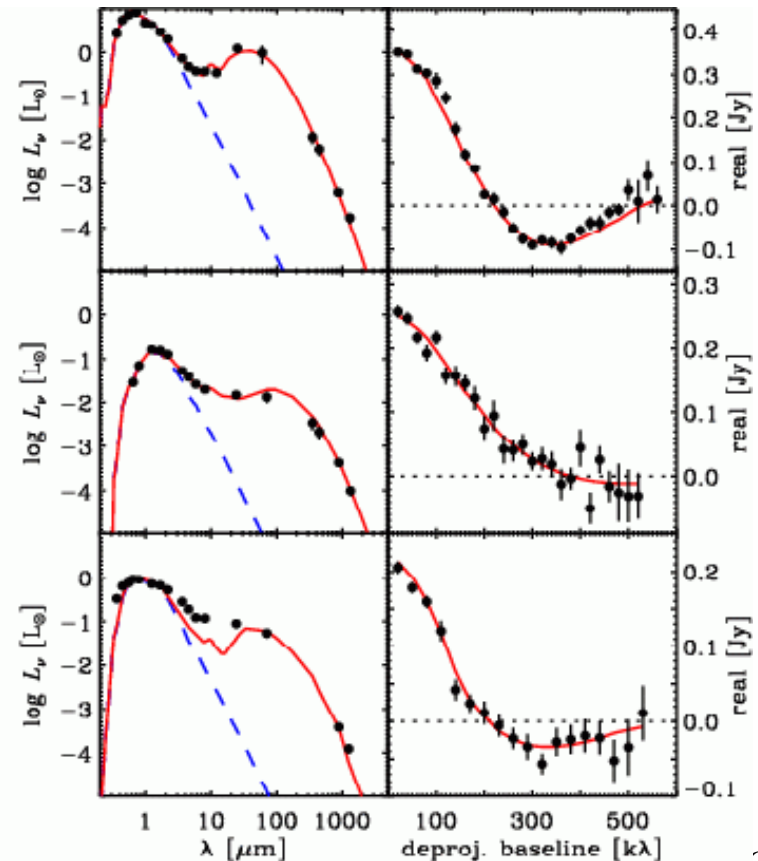
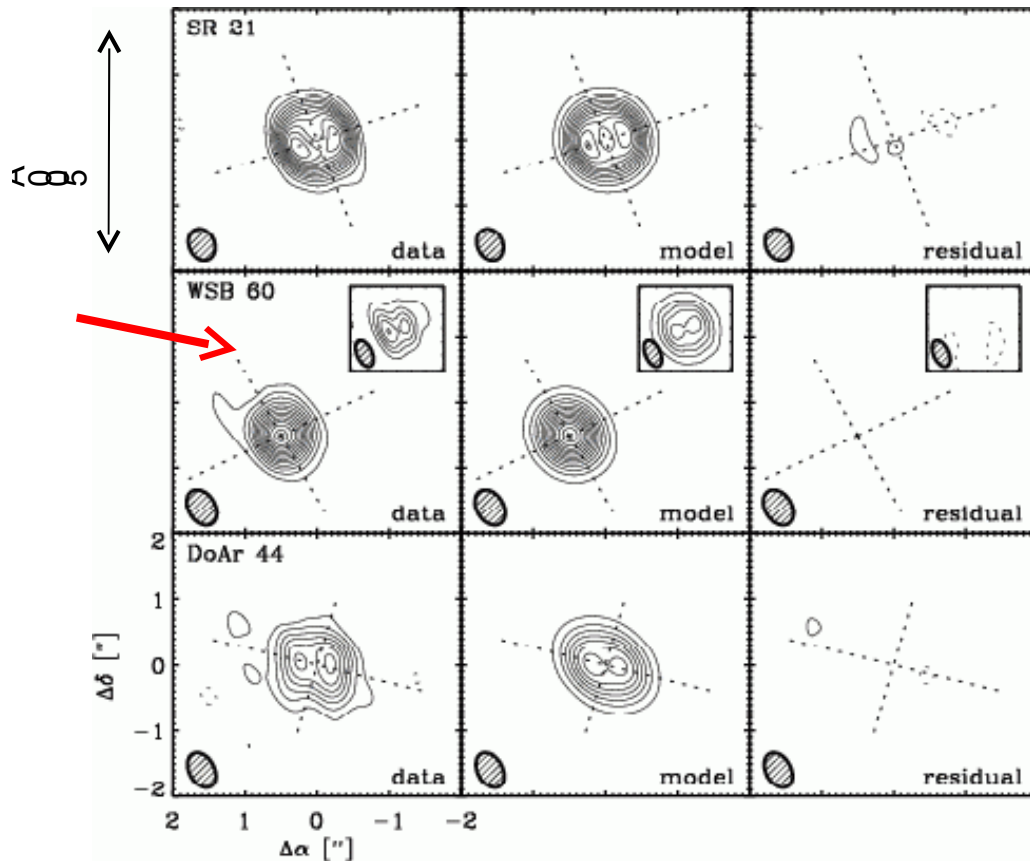


MAXEN image



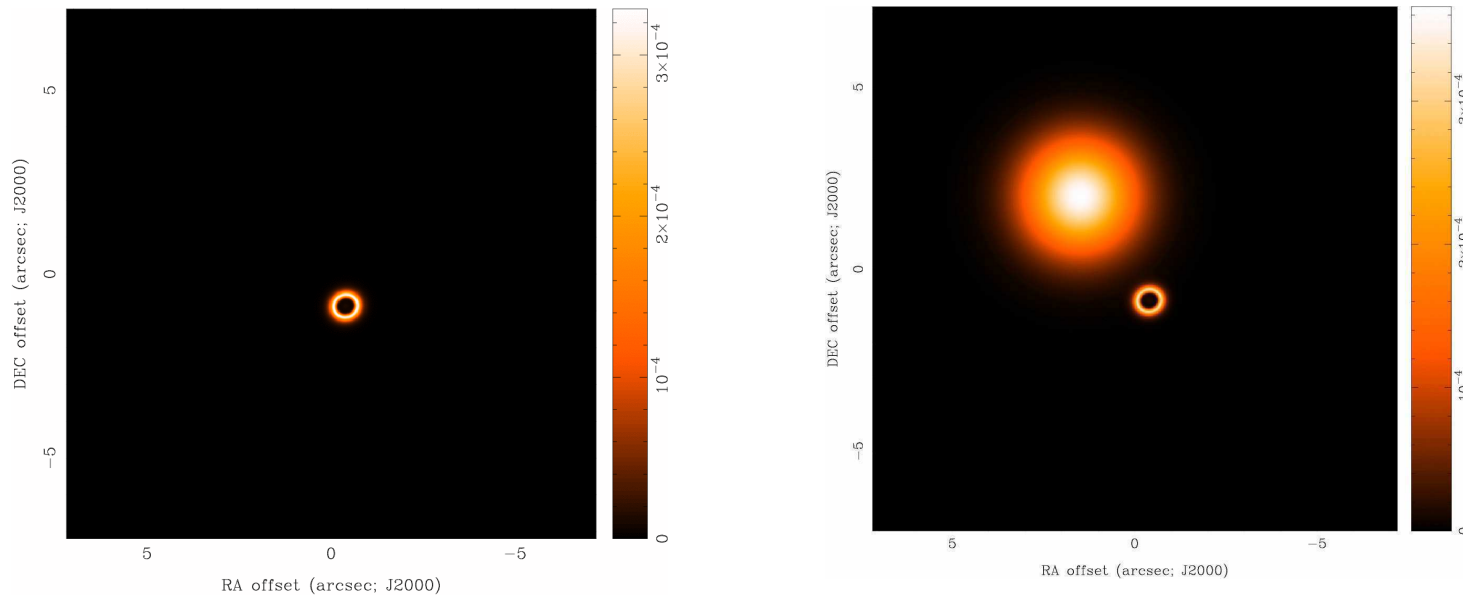
Tune Resolution/Sensitivity to suit Science

- e.g. Andrews, Wilner et al. 2009, ApJ, 700, 1502
 - SMA 870 μm images of “transitional” protoplanetary disks with resolved inner holes, note images of WSB 60



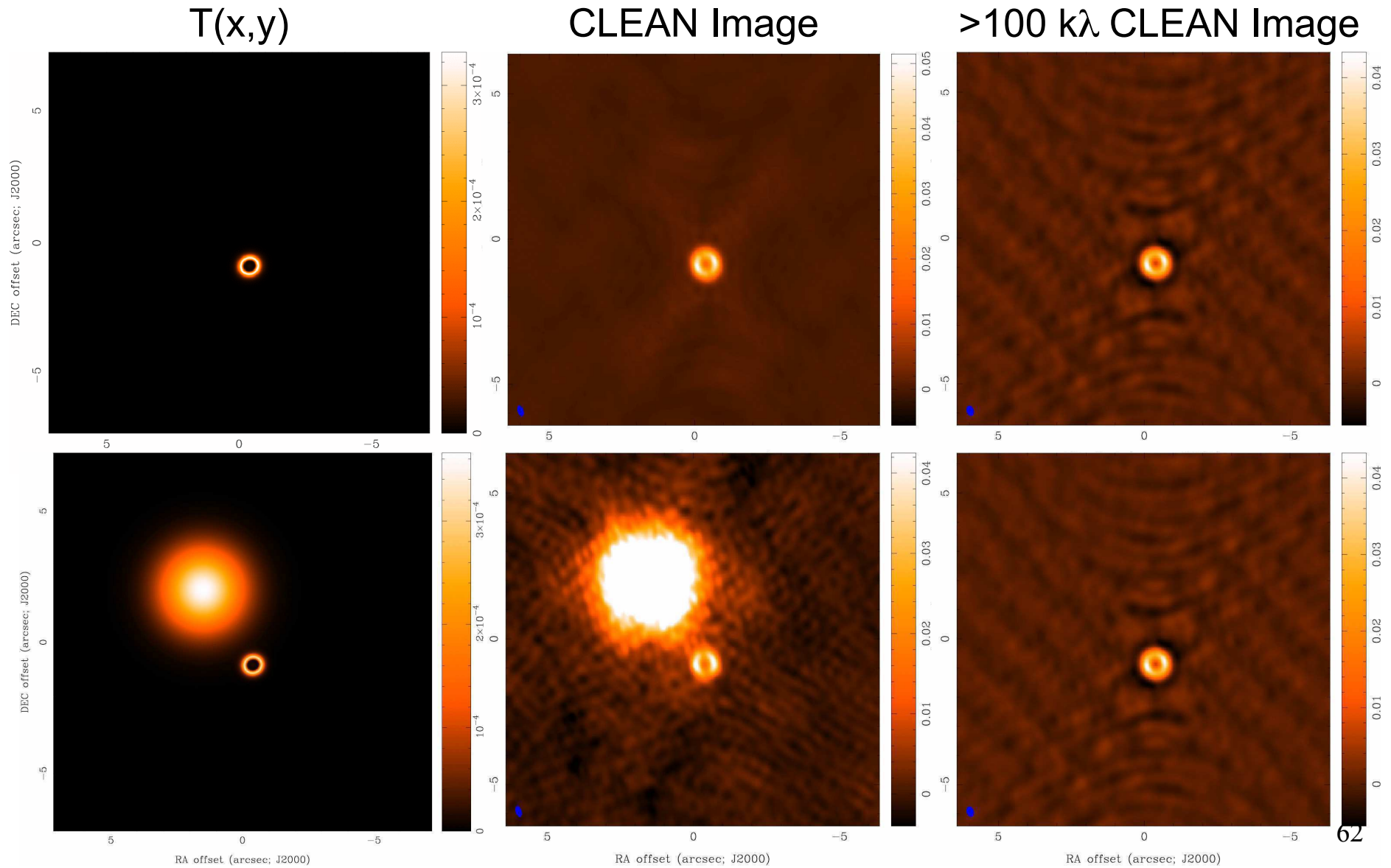
Missing Short Spacings

Do the visibilities in the example discriminate between these models of the sky brightness distribution, $T(x,y)$?



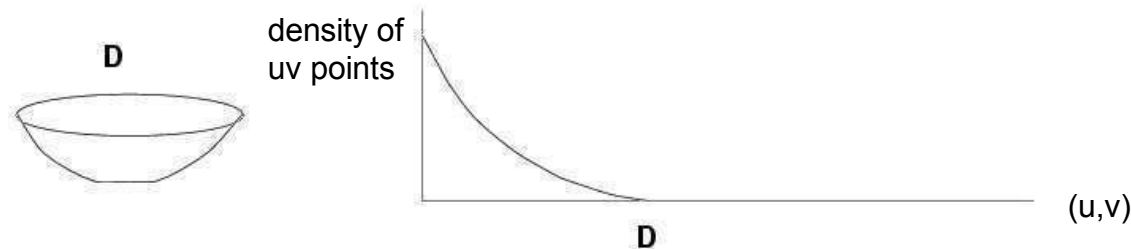
Yes... but only on baselines shorter than $\sim 100 \text{ k}\lambda$.

Missing Short Spacings: Demonstration



Low Spatial Frequencies (I)

- Large Single Telescope
 - make an image by scanning across the sky
 - all Fourier components from 0 to D sampled, where D is the telescope diameter (weighting depends on illumination)



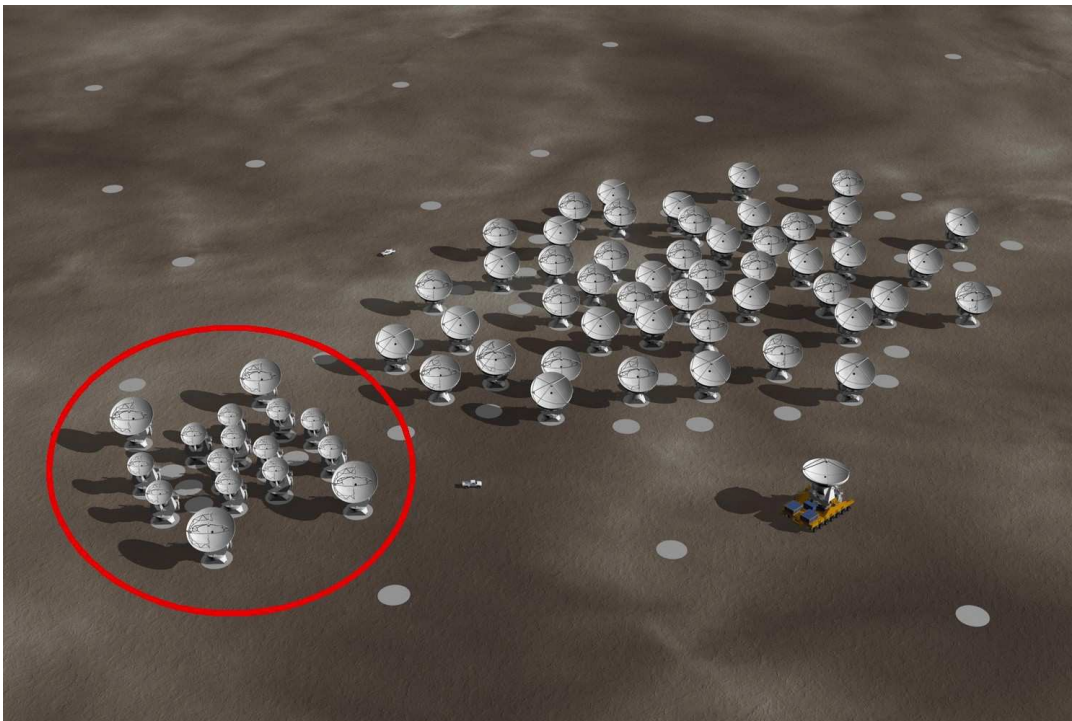
- Fourier transform single dish map = $T(x,y) \otimes A(x,y)$, then divide by $a(x,y) = \text{FT}\{A(x,y)\}$, to estimate $V(u,v)$

$$\hat{V}(u, v) = \frac{[V(u, v)a(u, v)]}{\hat{a}(u, v)}$$

- choose D large enough to overlap interferometer samples of $V(u,v)$ and avoid using data where $a(x,y)$ becomes small

Low Spatial Frequencies (II)

- separate array of smaller telescopes
 - use smaller telescopes observe short baselines not accessible to larger telescopes
 - shortest baselines from larger telescopes total power maps



ALMA with ACA

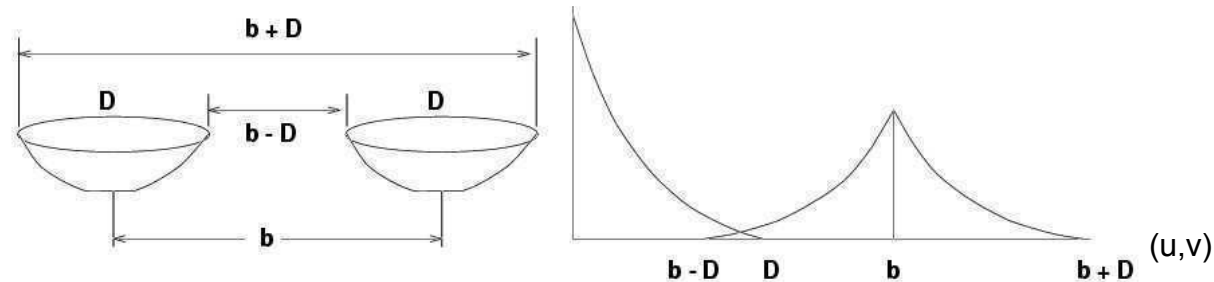
50 x 12 m: 12 m to 14 km

+12 x 7 m: fills 7 to 12 m

+ 4 x 12 m: fills 0 to 7 m

Low Spatial Frequencies (III)

- mosaic with a homogeneous array
 - recover a range of spatial frequencies around the nominal baseline b using knowledge of $A(x,y)$ (Ekers and Rots 1979) (and get shortest baselines from total power maps)



- $V(u,v)$ is linear combination of baselines from $b-D$ to $b+D$
- depends on pointing direction (x_o, y_o) as well as (u,v)

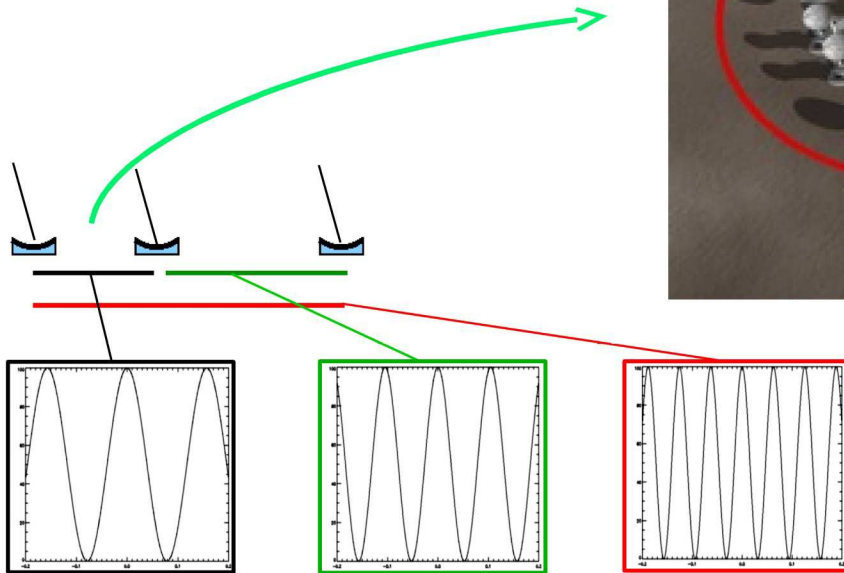
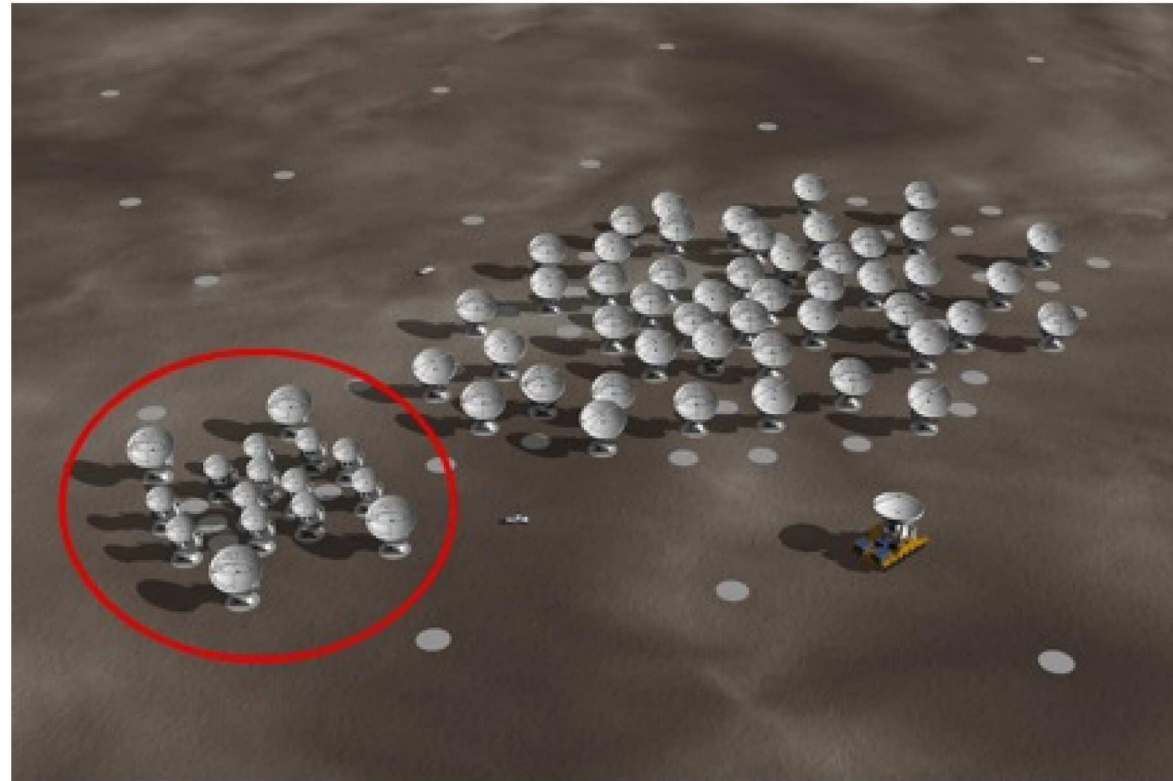
$$V(u, v; x_o, y_o) = \int \int T(x, y) A(x - x_o, y - y_o) e^{2\pi i(ux + vy)} dx dy$$
- Fourier transform with respect to pointing direction (x_o, y_o)

$$V(u - u_o, v - v_o) = \frac{\int \int V(u, v; x_o, y_o) e^{2\pi i(u_o x_o + v_o y_o)} dx_o dy_o}{a(u_o, v_o)}$$

How does ALMA work?

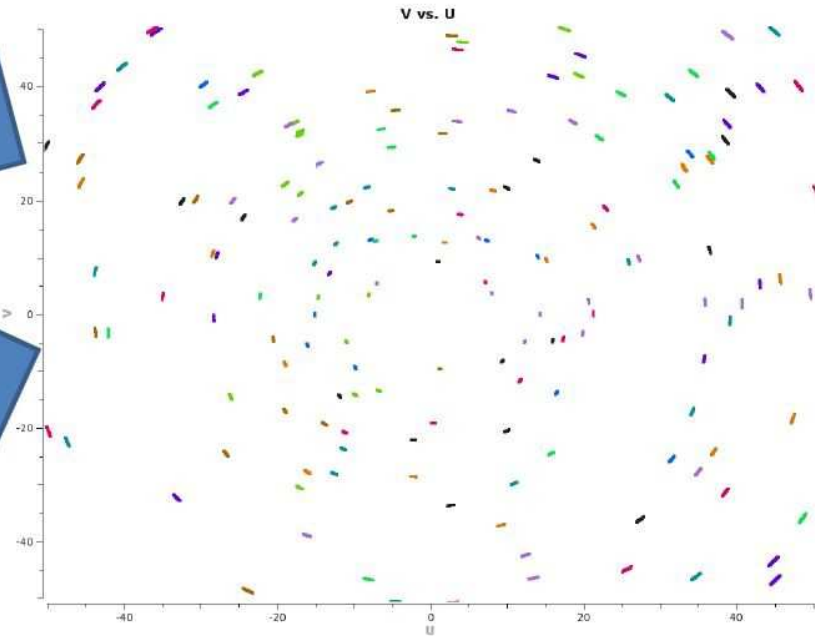
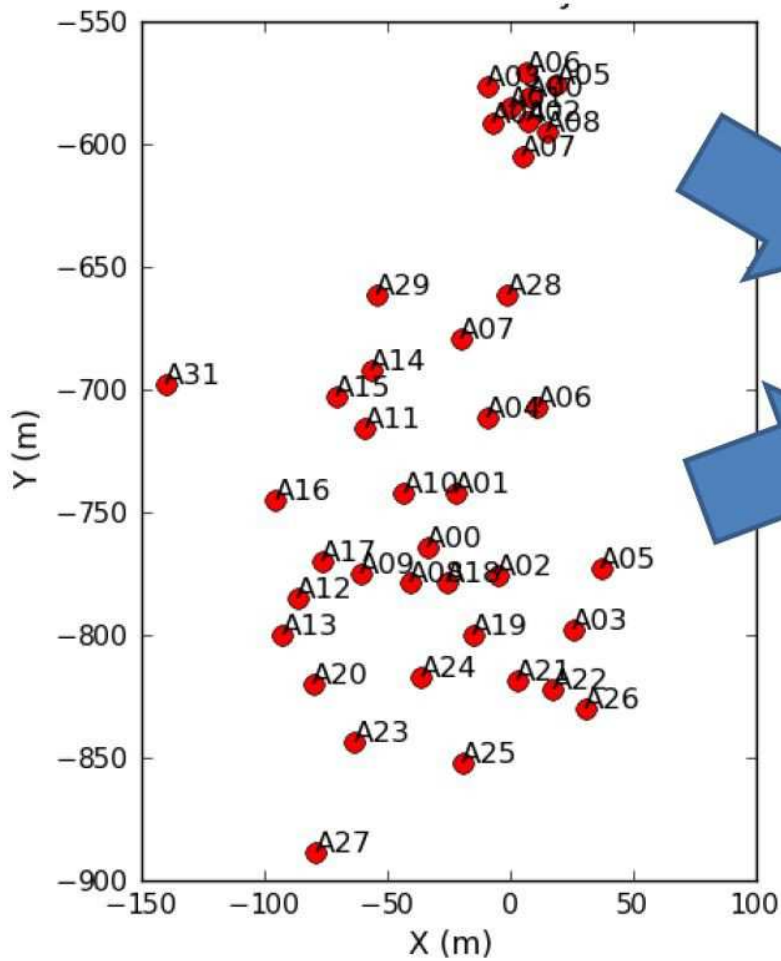
Radio interferometry / aperture synthesis

ACA = Atacama Compact Array – twelve 7-m antennas

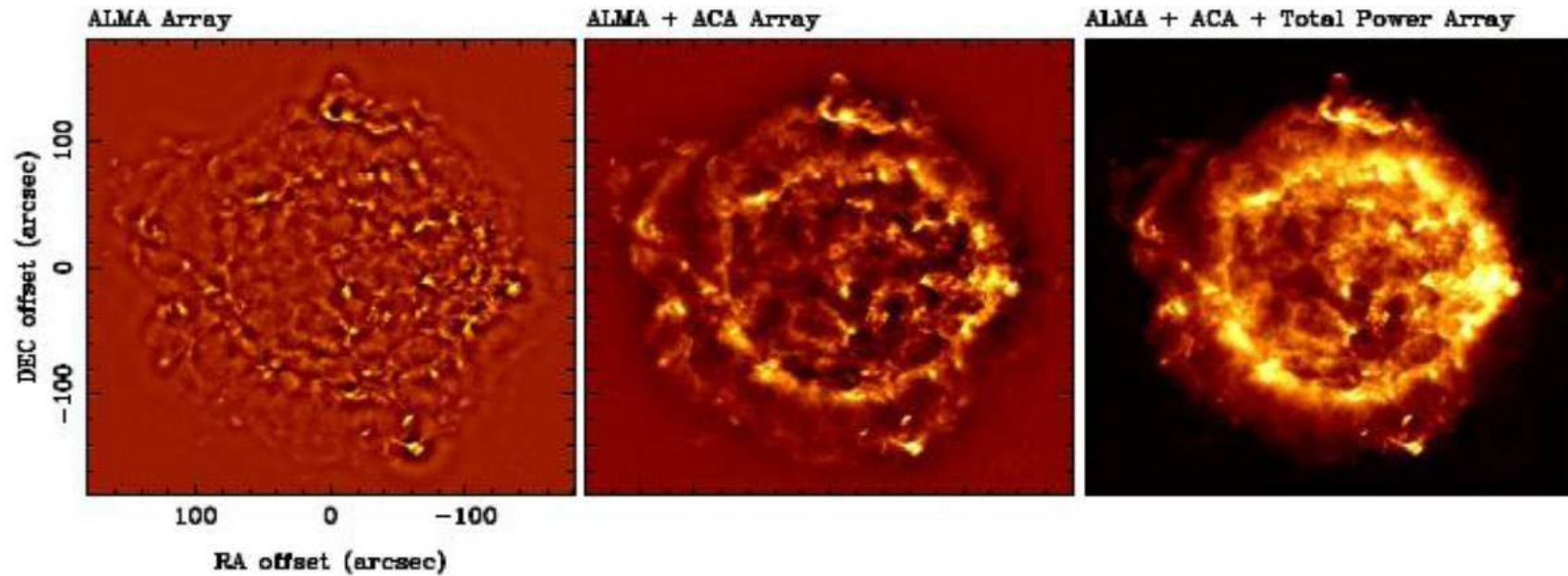


How does ALMA work?

Radio interferometry / aperture synthesis



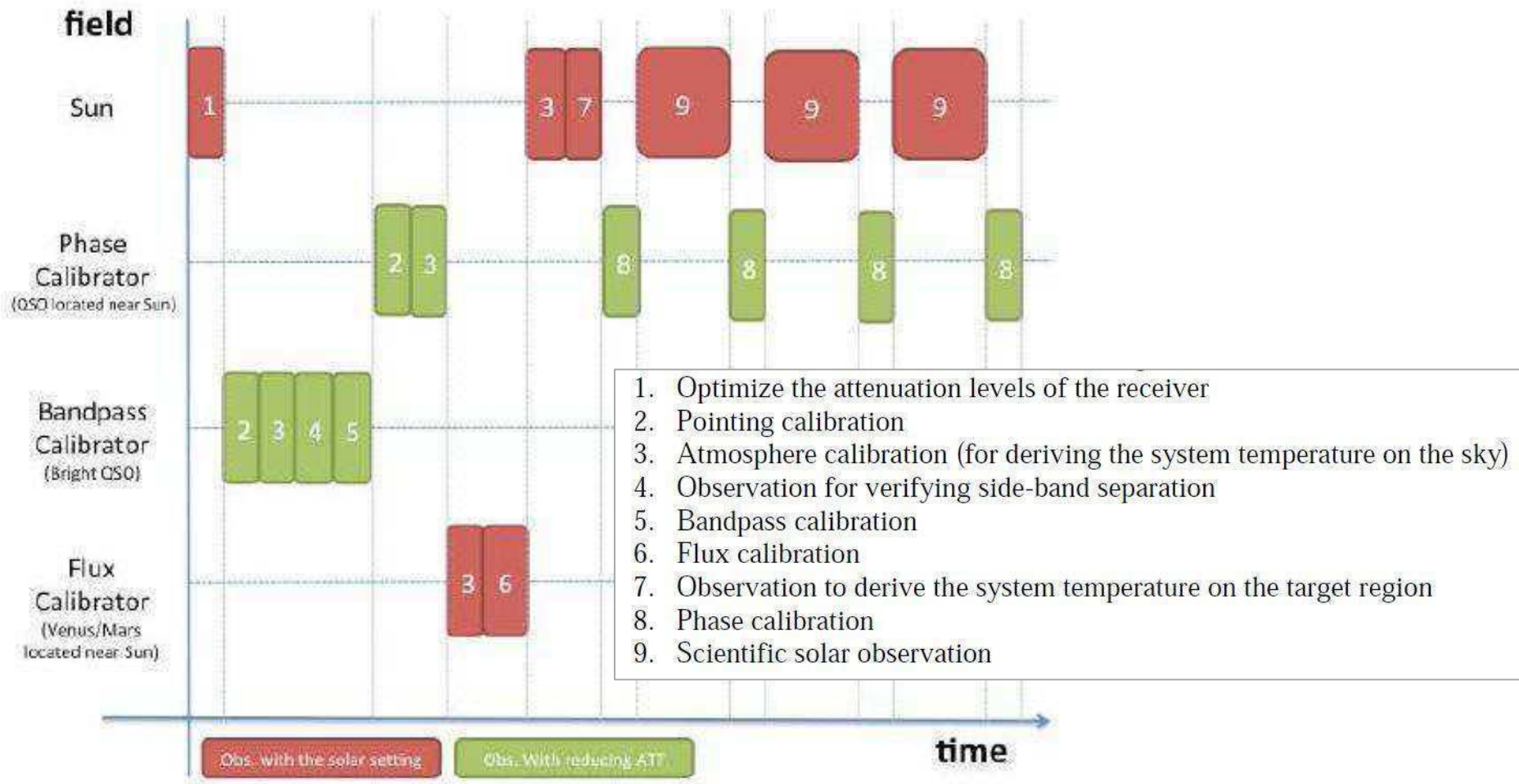
Extended sources with fine structures: Combined approach



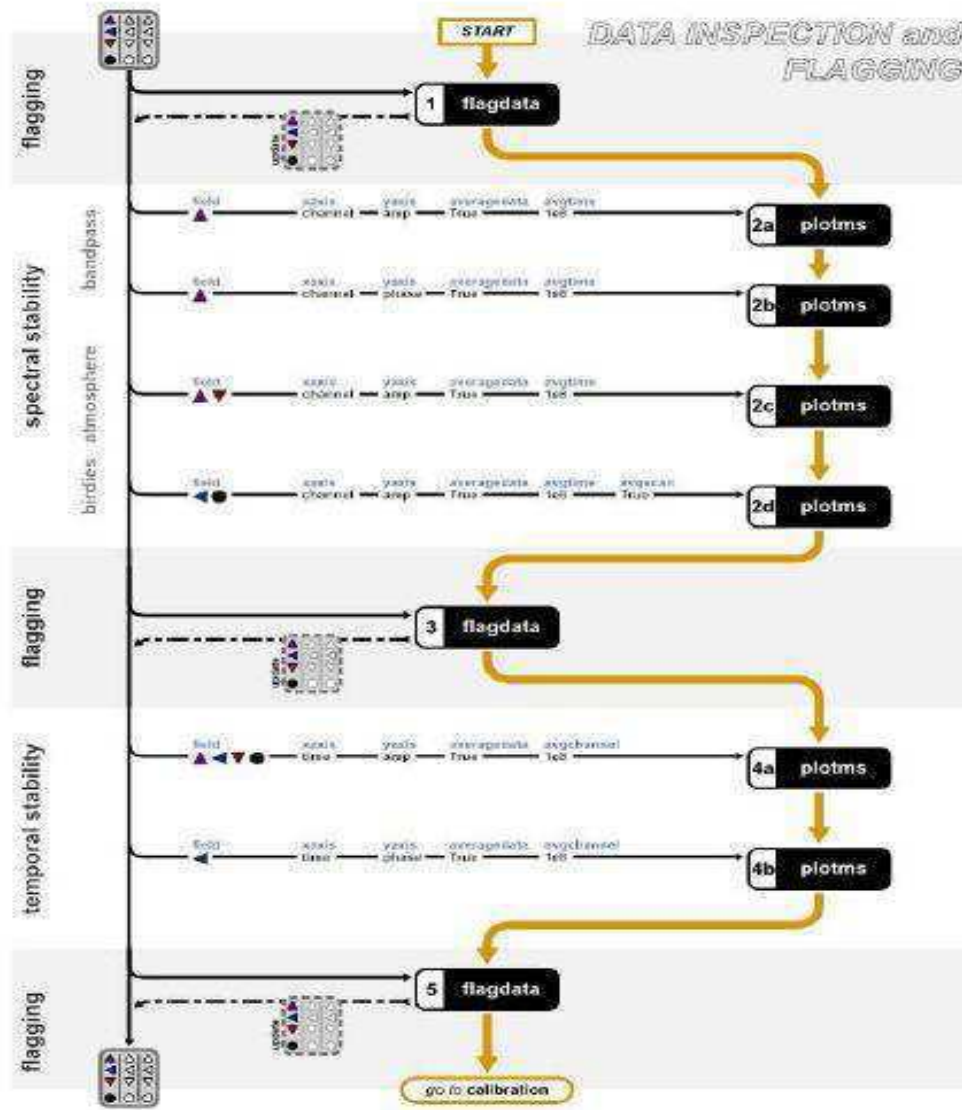
simple simulation of ALMA observation by Y.Kurono

Calibration of interferometric data

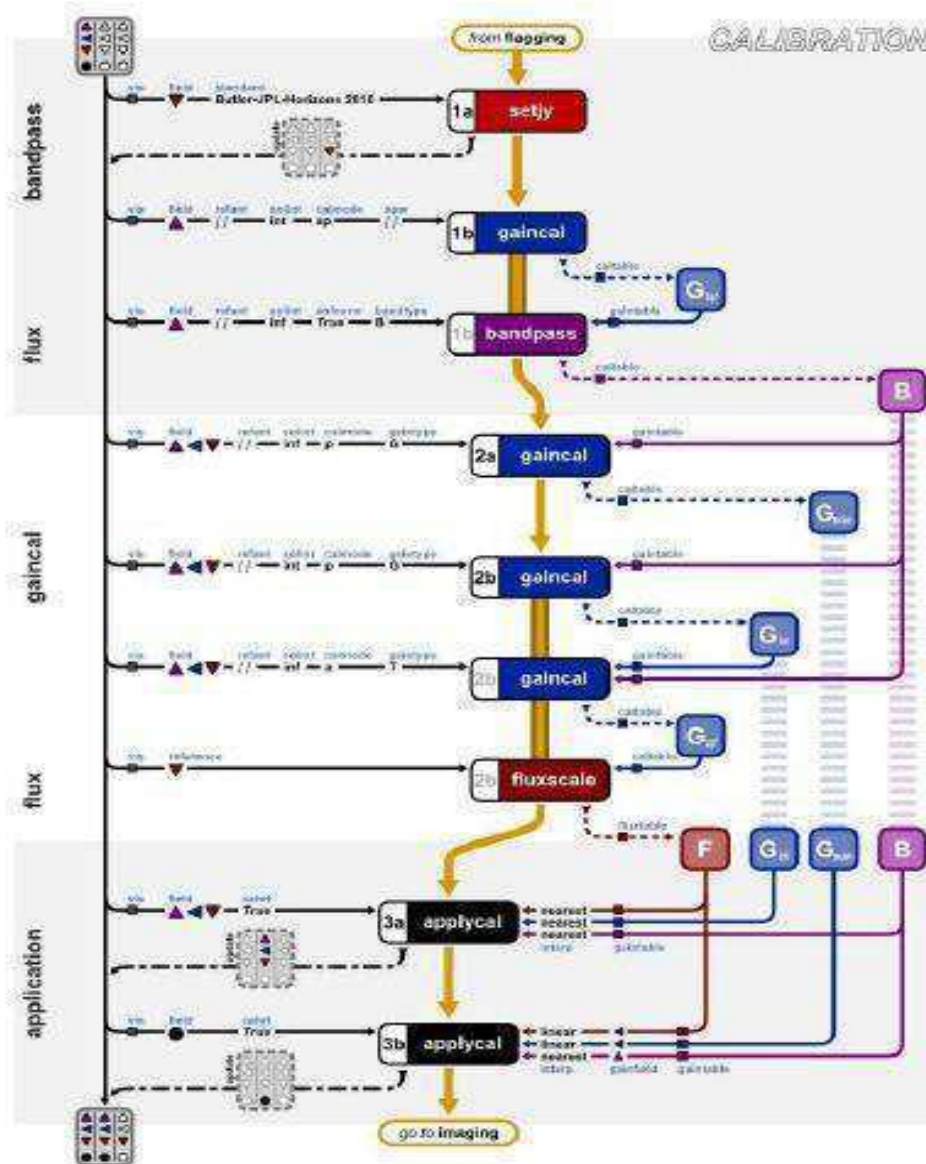
$$\langle P_{AB} \rangle = G_A G_B \iint_{-\infty}^{\infty} I(l, m) \cdot \exp(-2\pi i (ul + vm)) dl dm + P_{sys}$$



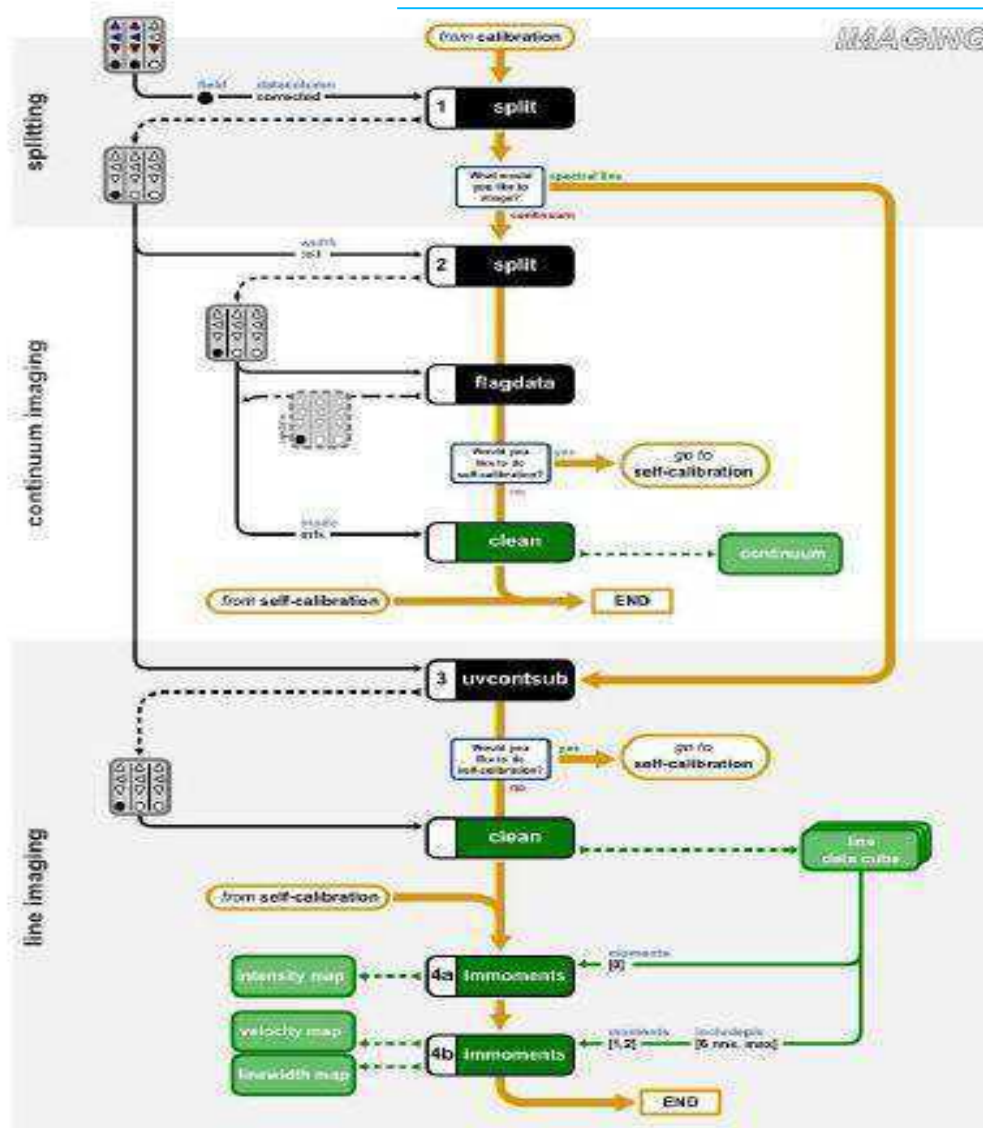
Postprocessing – calibration and imaging in CASA



Postprocessing – calibration and imaging in CASA



Postprocessing – calibration and imaging in CASA



Current and planned large facilities



SSRT



MUSER



LOFAR



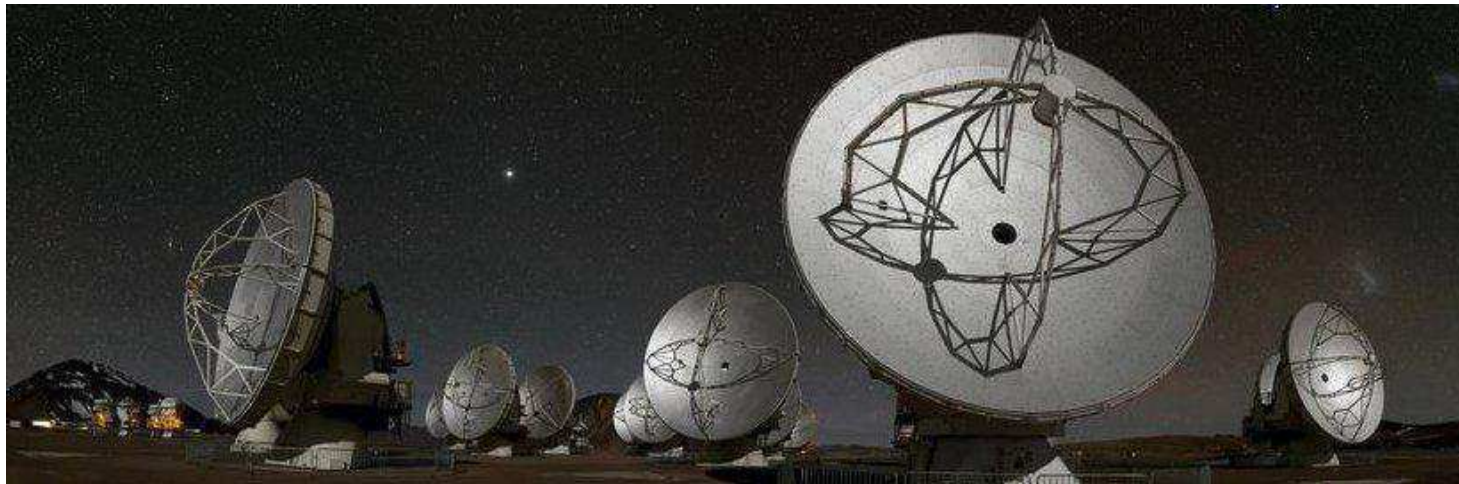
ALMA



SKA

What is ALMA?

- ▶ ALMA = **A**taacama **L**arge **M**illimeter/submillimeter **A**rray
The largest project of contemporary ground-based observational facility in astronomy built in a world-wide international cooperation in Chile
- ▶ The key partners are **ESO**, NRAO and NAOJ
- ▶ System of fifty 12m high-precision antennas + twelve 7m (ACA) phased as an interferometer, + four 12m single-dish (TP)

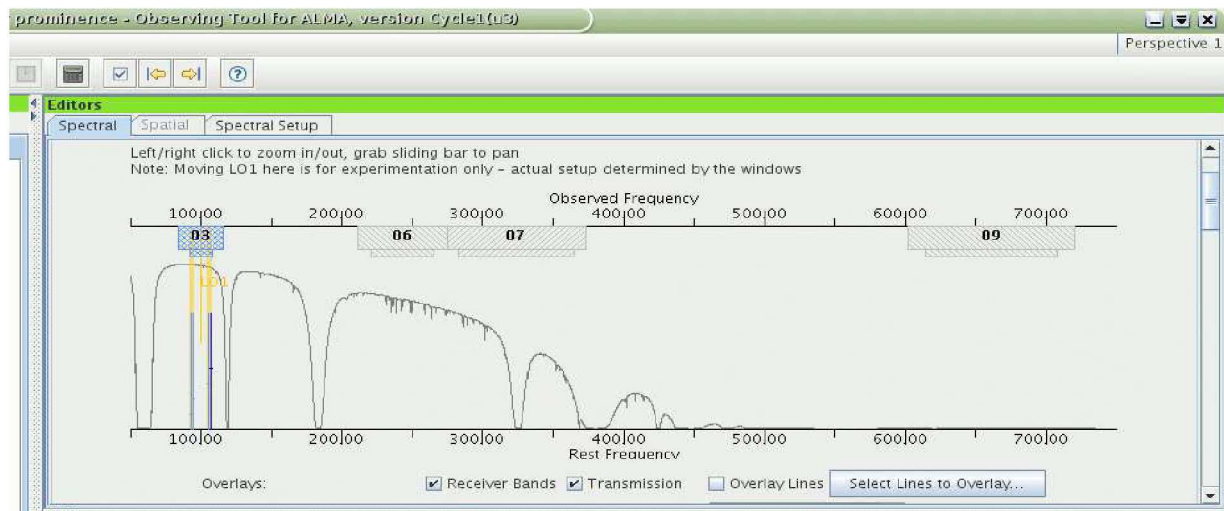
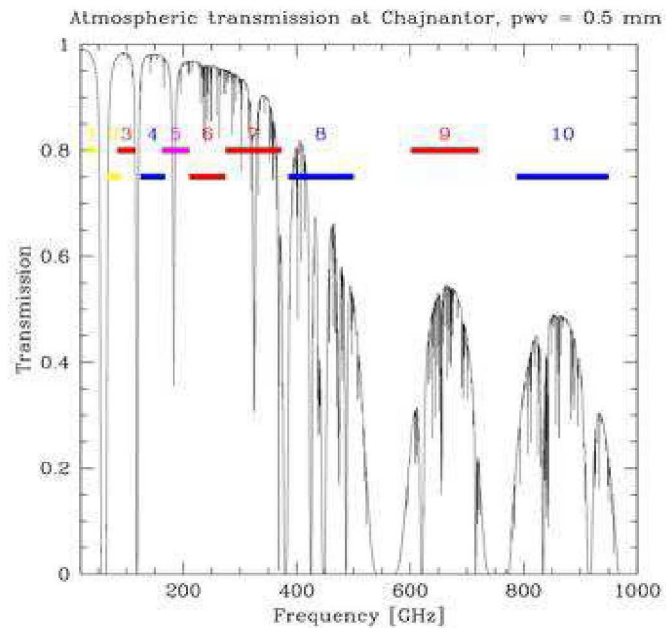


What is ALMA?

For the first time we (will) have

- ▶ Very high spatial resolution (up to 0.005" in extended configuration @ 1THz)
- ▶ Extremely high spectral resolution – up to 30kHz
- ▶ Temporal resolution for very bright sources (e.g. the Sun) ~ 1s
- ▶ Very high sensitivity

at the same moment in a broad range of frequencies from 30GHz up to more than 1 THz



Science with ALMA

1. Cosmology and the high redshift universe
2. Galaxies and galactic nuclei
3. ISM, star formation and astrochemistry
4. Circumstellar disks, exoplanets and the solar system
5. Stellar evolution and the Sun

<http://almascience.eso.org>



Atacama Large Millimeter/submillimeter Array
In search of our Cosmic Origins

Search Site

ESO NRAO NAOJ Log in | Register | Reset Password | Forgot Account

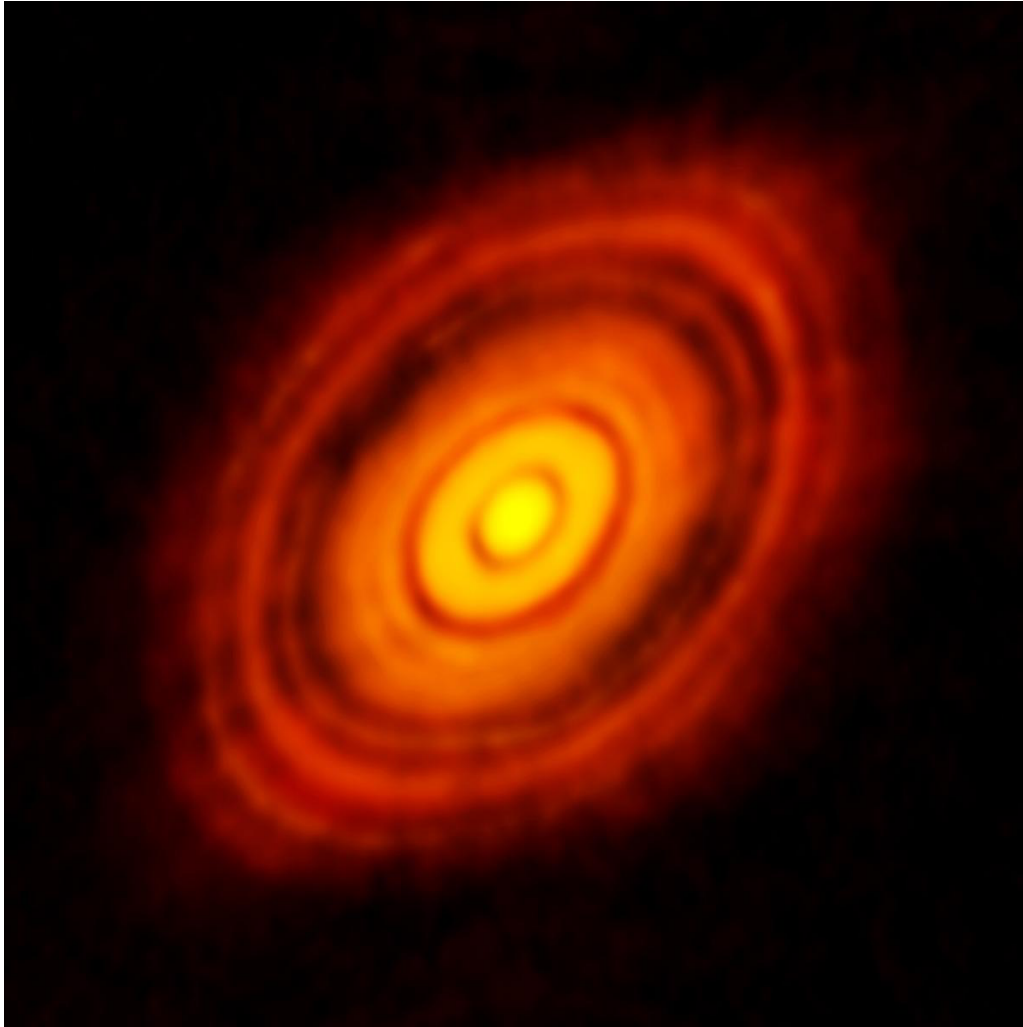
You are here: Home

Welcome to the Science Portal at ESO

Atacama Large Millimeter/submillimeter Array

General News

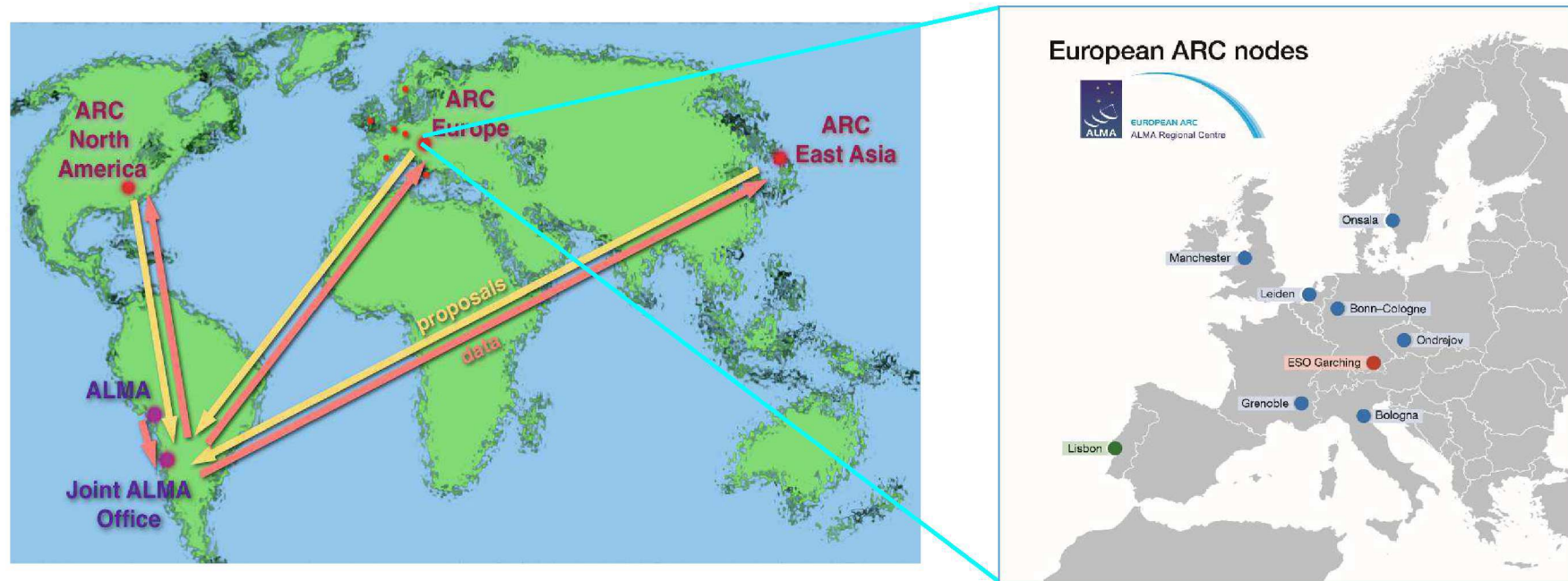
- ALMA Status Report: March 2014
Mar 12, 2014
- ALMA Cycle 2 Call for Proposals closure
Dec 19, 2013
- Urgent: Cycle 2 Observing Tool Update
Nov 15, 2013
- ALMA Cycle 2 Call for



HL Tau

- Formation of a new planetary system
- 450 ly away from Earth
- Resolution better than 5 AU !

ALMA Regional Centers / ARCs and the ARC nodes



ALMA Regional Centers – ARCs:

Supporting infrastructure – interface between ALMA observatory and user community

Structure of the European ARC:

- ❑ Head in ESO Garching
- ❑ Seven nodes across Europe
 - ▶ **One in Ondřejov (Prague), Czech republic**





EUROPEAN ARC
ALMA Regional Centre || Czech

Status

- ▶ Hosted by the Astronomical Institute ASCR
- ▶ Negotiations with ESO started in 2007, **node accepted into EU ARC network in 2009**
- ▶ Since 2016 **Research Infrastructure** (support till 2022, listed in *CZ Roadmap*, one of the 42 in CR)
- ▶ Expertise areas: Galactic & extragalactic physics, stars & ISM, **solar physics**, laboratory mw spectroscopy

Mission

- ▶ User support, community building & training, help with ALMA development
- ▶ Serves the community in CR and entire CE Europe in all its expertise areas
- ▶ In **solar physics** it supports community on the **European-wide scale**

Role of the ARC nodes

Towards user community:

- ▶ Face-to-face (F2F) support of users in all stages of their ALMA-oriented projects.
- ▶ ALMA-system knowledge dissemination
- ▶ Spreading awareness of ALMA among scientific community

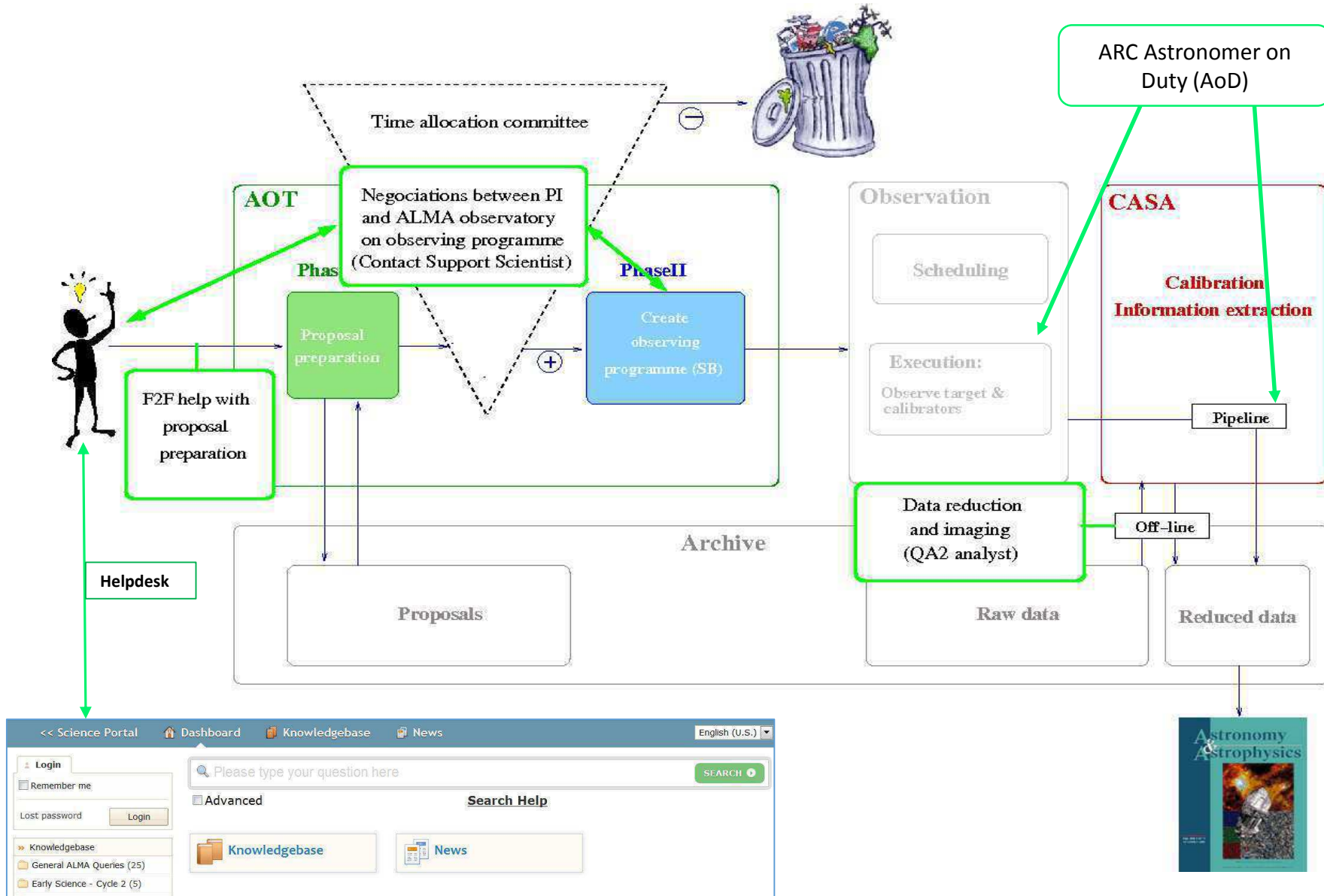
Towards ALMA observatory and ALMA-system developers:

- ▶ Help to the developers of ALMA user software:
- ▶ testing of CASA, ALMA OT, ALMA Helpdesk system,
- ▶ suggestions for improvement

Connecting users ↔ ALMA developers:

- ▶ Definition of new modes of observation – based on scientific community requests:
 - use-case studies, simulations, test observations (CSV/**EOC**),
assembling requirements for system update => suggestions
to ALMA observatory and developers, testing of suggested procedures

User support



Role of the ARC nodes

Towards user community:

- ▶ Face-to-face (F2F) support of users in all stages of their ALMA-oriented projects.
- ▶ ALMA-system knowledge dissemination
- ▶ Spreading awareness of ALMA among scientific community

Towards ALMA observatory and ALMA-system developers:

- ▶ Help to the developers of ALMA user software:
- ▶ testing of CASA, ALMA OT, ALMA Helpdesk system,
- ▶ suggestions for improvement

Connecting users ↔ ALMA developers:

- ▶ Definition of new modes of observation – based on scientific community requests:
 - use-case studies, simulations, test observations (CSV/**EOC**),
 - assembling requirements for system update => suggestions to ALMA observatory and developers.

The ARC node in Ondrejov is developing the solar ALMA observing mode for entire Europe – mandated by ESO: **EOC Project *Solar Research with ALMA***

Specifics of solar ALMA observations: Solutions for project preparation (WP3)

(I. Skokic)

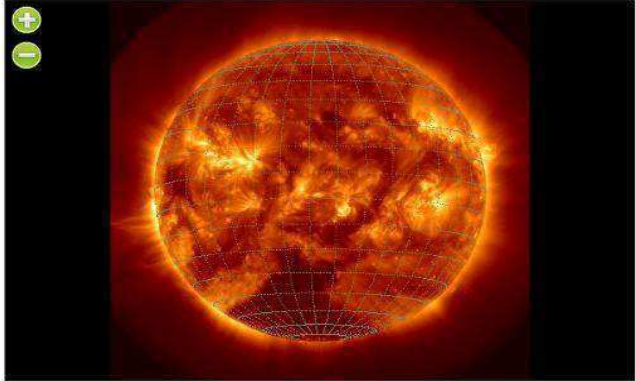
Proper motion of solar sources: Ephemeris/pointings

ALMA OT + *Ephemeris Generator Tool*

ALMA Ephemeris Generator Tool

Input FITS file
File: AIA image (test) Procházet... Soubor novýbrán.
Date: 2015-02-27T13:54:42.8 Size: 1024x1024 Format: 32 View header

Visualization
Scaling function: cuberoot Color: heat Frame: < 0 > of 1.
move=(184,194)=0.7219536304473877



Pointing
pixel (x, y) -
helioprojective (x, y in arcsec) -
heliographic (L, B in deg) -

Observation
Start of observation (UT): 2015-08-27T18:10:47
End of observation (UT): 2015-08-28T18:10:47
Step size (minutes): 20
Differential rotation profile: No rotation
A: 0 B: 0 C: 0
Height above photosphere (km): 0
Generate ephemeris file Original JPL file

Author: **Ivica Skokic**

Project development webpage:

<http://celestialszenes.com/alma/coords/CoordTool.html>

Mirrored at ALMA Science Portal

<https://almascience.eso.org/documents-and-tools>

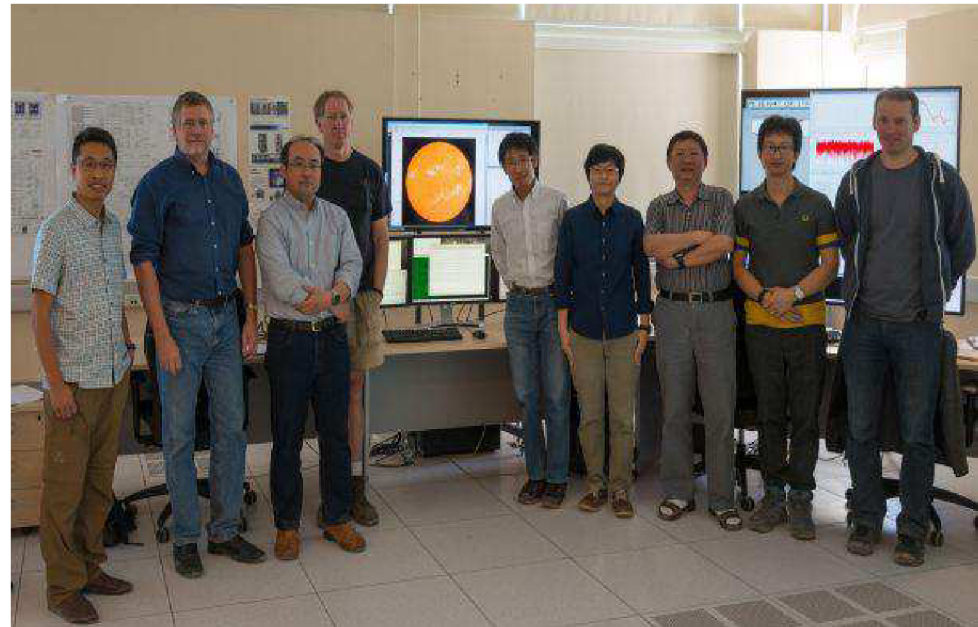
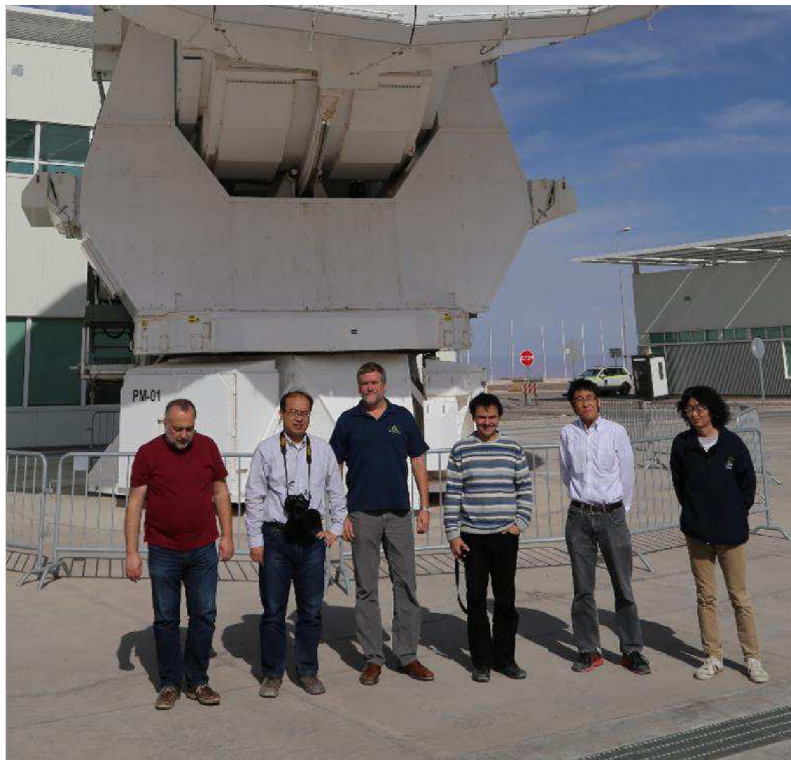
Solar proposal preparation:

**Use ALMA Ephemeris Generator Tool as
an input to ALMA Observing Tool**

Testing of suggested procedures: Solar CSV campaigns 2014/15

Team

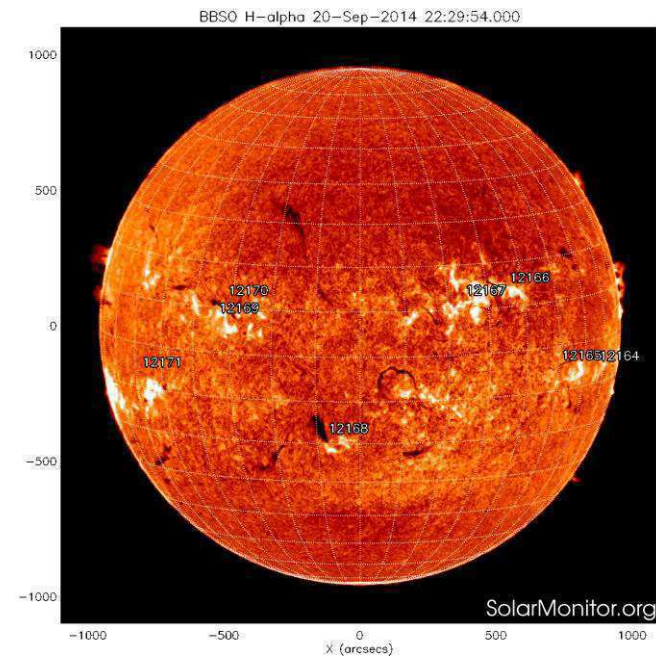
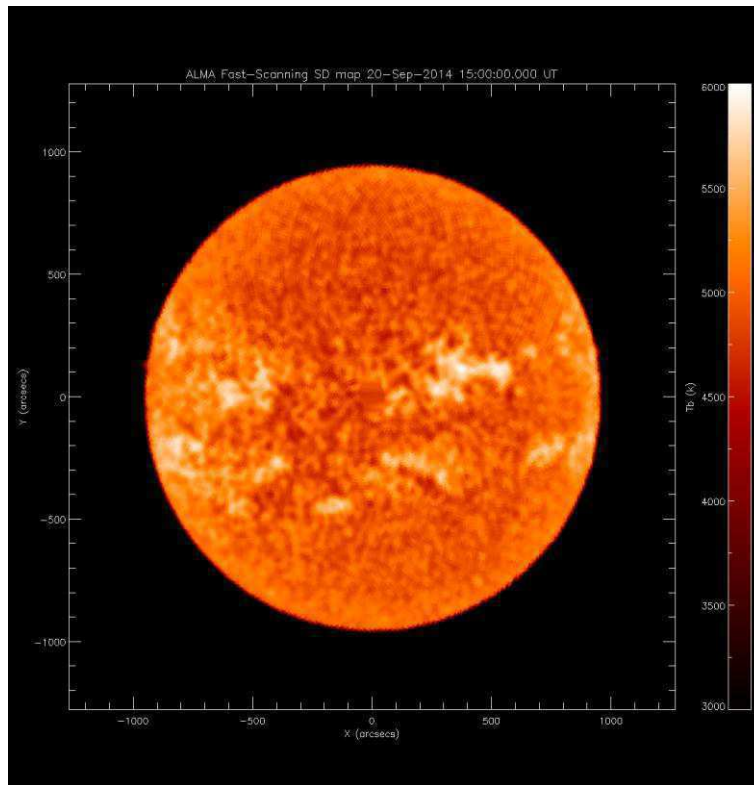
- ❑ EU ARC: M. Bárta (CZ node, Ondrejov), R. Brajša (CZ node, Zagreb), I. Skokic (CZ node Ondrejov)
- ❑ NA ARC: T. Bastian (NRAO), S. White (US Air Force Research Lab)
- ❑ EA ARC: M. Shimojo (NAOJ), S. Kazamusa (NAOJ/Nobeyama)
+ strong JAO support (T. Remijan, A. Hales, A. Hirota,...)



Testing of suggested procedures: Solar CSV campaigns 2014/15

Results

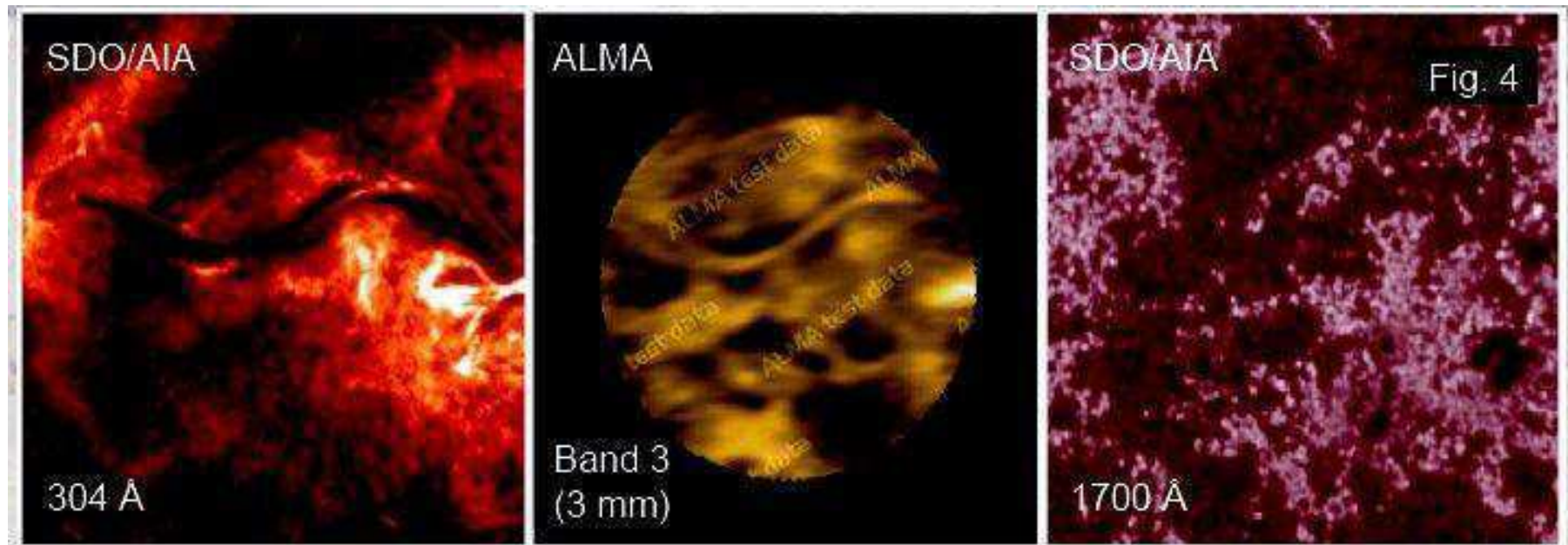
Whole-disc SD scan in ALMA continuum @240GHz (Band 6, left panel) as compared do H α image from BBSO (Dec. 2014)



Testing of suggested procedures: Solar CSV campaigns 2014/15

Results

Filament in ALMA continuum @100GHz (Band 3 – middle panel), compared with AIA observations at 304Å (left) and 1700Å (right). IF image – main array (BL correlator only; Dec 2014)



Testing of suggested procedures: Solar CSV campaigns 2014/15

Results

The sunspot (NOAA 12470) in ALMA continuum Band 3 @100GHz (left), Band 6 @240GHz (middle) and AIA 1700A (right) – **IF images combined with TP scans.**

